MONTANA DEPARTMENT OF TRANSPORTATION (MDT)
Investigation of Bridge Decks

Final Report
April 21, 2017
WJE No. 2016.3598

Prepared for:
Mr. Mike S. DalSoglio, P.E.
Consultant Design Bureau
Montana Department of Transportation (MDT)
2701 Prospect Avenue
Helena, MT 59620-10001

Prepared by:
Wiss, Janney, Elstner Associates, Inc.
330 Pfingsten Road
Northbrook, Illinois 60062
847.272.7400 tel | 847.291.5189 fax

MONTANA DEPARTMENT OF TRANSPORTATION (MDT)
Investigation of Bridge Decks

Elizabeth Nadelman
Project Associate

Paul Krauss, P.E.
Principal and Project Advisor

Todd Nelson
Associate Principal and Project Manager

Final Report
April 21 2017
WJE No. 2016.3598

Prepared for:
Mr. Mike S. DalSoglio, P.E.
Consultant Design Bureau
Montana Department of Transportation (MDT)
2701 Prospect Avenue
Helena, MT 59620-10001

Prepared by:
Wiss, Janney, Elstner Associates, Inc.
330 Pfingsten Road
Northbrook, Illinois 60062
847.272.7400 tel | 847.291.5189 fax

WJE ENGINEERS ARCHITECTS MATERIALS SCIENTISTS

TABLE OF CONTENTS

Introduction and General Background 1
Concrete Bridge Deck Cracking 4
- Random (Map) Cracking 4
- Transverse Cracking 4
- Longitudinal Cracking 6
- Typical Causes of Cracking 6
  - Plastic Shrinkage Cracking 6
  - Craze Cracking 6
  - Materials Related Cracking 7
  - Autogenous Shrinkage 7
  - Drying Shrinkage 7
  - Thermal Movement 8
  - Subsidence Cracks 8
  - Importance of Restraint 9

Investigation and Results 10
- Document Review 11
  - Bridge Design 11
  - Concrete Mixtures 12
  - Deck Condition 13
- Field Investigation 15
  - Crack Mapping 18
  - Core Extraction 19
  - Delamination Survey 21
  - Impulse Response (IR) Survey 21
  - Ground Penetrating Radar (GPR) Scan 22
  - Infrared Imaging 22
  - Efflorescence 22
- Laboratory Studies 22
  - Physical Testing 23
  - Petrographic Analyses 24
  - Chemical Analyses 25
- Modeling 26
  - ConcreteWorks Thermal Model 26
  - Stress Model 27

Discussion 29
- Plastic Shrinkage Cracking 30
- Materials Related Distress 30
- Subsidence 32
- *Corrosion* 33
- *Overlay Bridge Decks* 34
- Transverse Cracking 35

Primary Recommendations for Future Bridge decks 40
- Construction Practices 40
  - Curing 40
  - Placement Times 42
  - Plastic Concrete Temperatures 42

Design Considerations 43
Deck Thickness 43
Secondary Recommendations 43
Design Considerations 43
Top and Bottom Mat Placement 43
Materials and Quality Control 43
Cementitious Content 43
Cementitious Materials 44
Water to Cementitious Ratio 44
Aggregate Optimization 44
Repair Concepts 45
Risk Category 3 45
Risk Category 2 46
Risk Category 1 46

Appendix A - Bridge Information
Appendix B - Investigation Report
Appendix C - Petrography
Appendix D - Modeling
Appendix E - References

WJE ENGINEERS ARCHITECTS MATERIALS SCIENTISTS

MONTANA DEPARTMENT OF TRANSPORTATION (MDT)
Investigation of Concrete Bridge Decks

INTRODUCTION AND GENERAL BACKGROUND

Wiss, Janney, Elstner Associates, Inc. (WJE) has completed the investigation of concrete bridge deck cracking of numerous bridges located in western Montana. The scope of work for this investigation was presented in WJE's proposal dated July 1, 2016 and completed under Montana Department of Transportation (MDT) contract No. 920700, MDT project number STBD STWD (471). The objectives of this investigation were to assist MDT in determination of possible cause(s) of cracking and to provide recommendations to mitigate the potential for future cracking.

In June of 2016, MDT noted severe cracking on two bridge decks, Superior Area Structures - MP 49.397 EB and Lozeau-Tarkio Structures - MP 57.472. For both of these bridges, the cracking led to holes in the decks after small sections of concrete deck fell (Figure 2 through Figure 4). The decks for these two bridges were replaced in 2010 and 2011, respectively. Further review of additional bridge decks in western Montana by MDT revealed widespread deck cracking with potential of future deck penetrations. MDT noted that the widespread cracking was occurring on bridge decks at relatively early ages. Similar deck penetrations were also found in the westbound lane of Keyser Creek, MP 407.862, and east bound lane of Hensley Creek, MP 414.235 (both in the Billings district). These two bridge decks were cast with experimental mixes that included silica fume, fibers, and a shrinkage reducing admixture and may not be representative of the decks investigated and reported herein. WJE did perform brief petrography on concrete cores provided from these two bridges and reported the results in July of 2016; however, this report does not discuss these two bridges.

WJE was commissioned in August of 2016 to assist MDT with the investigation of the deck cracking problem. Based on initial conversations with MDT, most subject bridge decks were in the western part of Montana, primarily west of Missoula and on I-90. The bridge decks in question are 1 to 9 years old and typically represent replacement bridge decks over existing sub-structures. The deck replacements were done on bridges built between 1960 and 1980. The concrete decks are composite with prestressed concrete beams or wide flange steel plate girders. Construction included short- and long-span bridges, and deck thickness varied, generally ranging from 6 ½ to 9 inches. Curing of the decks reportedly included 14 days of wet cure applied shortly after placement followed by an application of a curing compound. Cementitious materials varied from straight portland cement, cement/fly ash blends, and cement/fly ash/silica fume blends with total cementitious contents from 525 to 658 pounds per cubic yard.

Figure 1. Example of typical bridge deck cracking noted by MDT. Superior Area Structures MP 49.3

Figure 2. Hole in bridge deck. Superior Area Structures MP 49.3

Figure 3. Bridge deck cracking that has led to holes in the concrete deck and subsequent concrete falling. Lozeau - Tarkio MP 57.4

Figure 4. Underside of bridge deck in Figure 3 showing hole in bridge deck. Lozeau - Tarkio MP 57.4

The investigation performed by WJE and reported herein was developed to provide a practical approach to investigate the cause(s) of cracking and develop realistic approaches to mitigate the future potential of bridge deck cracking. The scope of work included the following activities:

- **Document Review -** Background documentation of numerous bridge decks in western Montana were provided by MDT and reviewed by WJE. This included plan drawings, specifications, concrete mixture proportions, quality control results, and field photographs.

- **Field Investigation -** Based on the document review and consultation with MDT, WJE selected four (4) bridges for in-depth field investigations and eight (8) bridge decks for cursory, comparative investigations. Field studies included: representative visual inspection, crack surveys, delamination

surveys, impulse response testing, still photography and video, infrared photography and video, ground penetrating radar and concrete core extraction. The four bridges selected for the in-depth survey are presented below. These bridges were selected to represent a range of cracking severity, age, and cementitious materials:

- Florence-East, Bridge over Bitterroot River, MP 10.640
- Lozeau-Tarkio, East-Bound bridge over the Montana Rail Link, MP 57.472
- Henderson-West, Henderson Interchange, MP 22.013
- Superior Area Structures, East-Bound bridge over Clark Fork, MP 49.397

Cursory inspections were performed on the following bridges:

- Lozeau-Tarkio, East bound, MP 58.550
- Lozeau-Tarkio, West bound, MP 58.550
- Lozeau-Tarkio, West bound, MP 57.472
- Henderson-East, MP 25.393
- Henderson-East, MP 24.603
- Henderson-East, MP 23.325
- Superior Area Structures, West-Bound, MP 49.397
- Thompson River, MP 55 to 56

- **Laboratory Evaluations** - Concrete cores were extracted from each in-depth investigation and from selected cursory investigations. These cores were shipped by MDT to WJE's laboratory in Northbrook, Illinois. Laboratory evaluations included the following activities:

  - Petrography - Performed on extracted cores per ASTM C856, *Standard Practice for Petrographic Examination of Hardened Concrete*, and air void analysis per ASTM C457, *Standard Test Method for Microscopical Determination of Parameters of the Air-Void System in Hardened Concrete*.
  - Compressive Strength - Performed on extracted cores per ASTM C42, *Standard Test Method for Obtaining and Testing Drilled Cores and Sawed Beams*
  - Concrete Splitting Tensile Strength - Performed on extracted cores per ASTM C496, *Standard Test Method for Splitting Tensile Strength of Concrete*
  - Coefficient of Thermal Expansion - Performed on extracted cores per In-House method
  - Chloride Ion Content - Performed on ground samples of extracted cores per ASTM C1152, *Standard Test Method for Acid-Soluble Chloride in Mortar and Concrete*
  - X-Ray Diffraction - Performed on samples of the collected field efflorescence from underside of the bridges.

- **Analytical Studies** - WJE simulated the concrete temperature histories for three of the bridge decks in order to assess the effect of placement times and ambient conditions. WJE also studied the effects of various parameters of the bridge decks in order to assess sensitivity to cracking. Parameters consisted of compressive strength, deck thickness, uniform and linear thermal gradients, shrinkage characteristics, and substructure geometry. A model was developed in order to quickly change and assess the effect of these variables.

- **Discussion and Recommendations** - WJE concludes this report with discussions on common causes of bridge deck cracking, which leads into discussion on likely causes of cracking for the investigated

bridges. Based on research performed by WJE and experience with similar cracking, recommendations for future bridge decks are then presented.

CONCRETE BRIDGE DECK CRACKING

Bridge deck cracking continues to be a common occurrence on concrete bridge decks throughout the United States even though numerous researchers have investigated causes and provided recommendations[1-4, 6,7,8.] Cracking of bridge deck concrete is a nation-wide problem that was researched by WJE in NCHRP Report 380 "Transverse Cracking in Newly Constructed Bridge Decks" published in 1996.[4] This cracking usually occurs within the first 6 to 12 months after construction but can continue for several years. Cracking commonly leads to a compromise in service life and increased maintenance costs, primarily due to accelerated corrosion of reinforcing steel in the deck and substructure but occasionally due to structural failure of the deck. Identifying the causes of bridge deck cracking and providing prevention can be complex and challenging, but is very important for maintaining longevity of the bridge deck. The types of bridge deck cracking can be generally divided up into three categories: random (map) cracking, transverse cracking, and longitudinal cracking. Transverse deck cracking is the generally the most prevalent and primary type of deck cracking. A general introduction to these types of cracking are presented in the following.

Random (Map) Cracking

Random cracking is a general term used to describe closely-spaced, intersecting cracks that form an irregular or "random" pattern on the concrete surface. Random cracks may vary in width and depth of penetration beneath the concrete surface, depending on their cause, but most random cracks are fine, with shallow penetration beneath the concrete surface. The most common cause of random deck cracking (Figure 5) is plastic shrinkage. Random cracks may also be caused by crazing or materials-related distress, such as freezing and thawing, D-cracking (cracks near joints caused by freezing and thawing distress of aggregates), and alkali silica reactivity (ASR); however, these material-related occurrences are much less frequent than plastic shrinkage cracking.

Transverse Cracking

Transverse cracking (Figure 6) is cracking that occurs along the transverse dimension of a concrete bridge deck, roughly perpendicular to its length. Transverse cracks are predominately caused by restraint of volumetric movement of bridge deck concrete. Nationally, most bridge decks develop transverse cracks. Some develop at very early ages (within the first couple days), and some develop much later after exposure to traffic. Transverse cracks are typically full depth cracks and often span the entire width of the bridge deck. They most commonly occur directly over transverse reinforcing steel and are typically 10 to 20 mils in width. Transverse crack spacing is typically between 5 and 10 feet. Volumetric movement that leads to transverse cracking occurs because of autogenous/chemical shrinkage, drying shrinkage, and thermal changes/gradients. All three of these volumetric influences can be additive and should be considered when assessing volume change and effect on transverse cracking.

Figure 5. Typical plastic shrinkage cracks. Surface was wetted to accentuate the cracking pattern

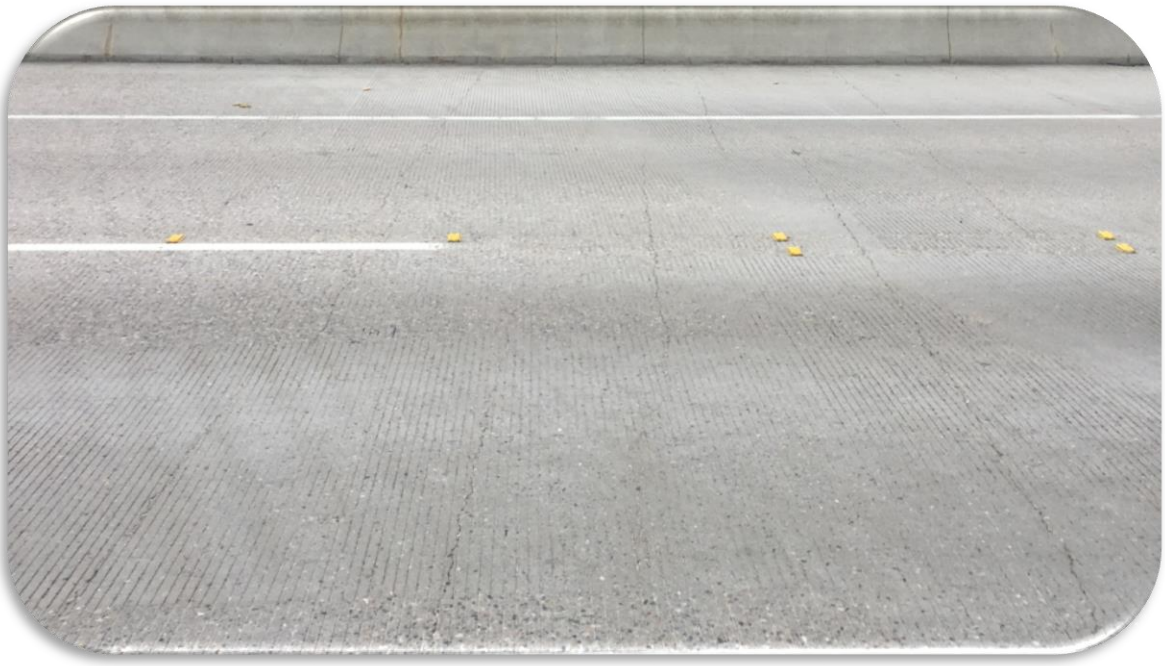

Figure 6. Typical transverse cracking, spacing varies from 5 to 10 feet.

Longitudinal Cracking

Longitudinal cracking is occurs parallel to the length of the concrete bridge deck, along the direction of traffic. In concrete bridge decks, longitudinal cracks typically develop directly over longitudinal reinforcing bars. The most common cause of longitudinal cracking, similar to transverse cracking, is restraint of volumetric movement; however, other factors such as subsidence or corrosion of reinforcing steel may also contribute to longitudinal cracking.

Typical Causes of Cracking

Plastic Shrinkage Cracking

Natural settlement of aggregate and cement particles in fresh-placed concrete causes water to bleed to the surface. Plastic shrinkage cracks form at early ages when water evaporates from a concrete surface faster than it can be replenished during the natural bleeding process. This creates rapid drying of the surface and results in contraction. When the concrete is at an early age, it has little strength, making it susceptible to cracking because of the local surface contraction. This results in plastic shrinkage cracks.

Individual plastic cracks are typically wider at the surface and tighten with depth, but are not typically longer than a couple feet. The depth of plastic shrinkage cracks is typically less than 2 inches. The cracking pattern is generally random (Figure 5), but can be oriented perpendicular to wind direction, if present. Plastic shrinkage cracks are aesthetically undesirable but rarely structurally significant. However, they will allow aggressive chemicals to penetrate the concrete faster and can also become worse with drying shrinkage, thermal movement, and loading.

The possibility of plastic shrinkage cracking is increased by high ambient temperatures, low humidity, and high winds. All of these conditions increase the evaporation rate near the concrete surface. Slow concrete setting increases the risk of plastic cracking. ACI 305R-10, “Guide to Hot Weather Concreting”, provides guidelines for assessing and preventing early age plastic cracking, which includes calculating surface evaporation rate as a function of ambient temperature, wind velocity, and concrete temperature. Mixes with little bleed water are also more susceptible. For example, mixes with low water-cementitious ratios (w/cm), air entrainment, silica fume, and superplasticizers are commonly more prone to plastic shrinkage cracks. Low w/cm mixes will have less bleed water available in the system. The fineness of silica fume and use of air entrainment both lower the rate of bleeding. Superplasticizers are often used to increase the slump of concrete but can also reduce the amount of bleed. Plastic shrinkage cracks can be reduced by limiting the amount of surface evaporation. Construction procedures can be implemented to reduce surface evaporation such as: fogging during placement, night placements, and early application of curing compounds or evaporation retarders, and protection from direct sunlight. Increasing the amount of mix bleed water in the mix is not practical and would lead to other undesirable effects.

Craze Cracking

Craze cracks are typically very tight (less than 1 mil) and shallow map cracks that form at early ages. Craze cracks are induced by restrained shrinkage of the near surface opposed by less shrinkage below. The pattern of cracking is typically random and is often called “map cracking”. Some amount of crazing is expected on all bridge decks, with the frequency and magnitude affected by construction practices, carbonation, richness of the mix, and drying conditions. “Blessing” the concrete with water to aid finishing of stiff concrete often results in magnified craze cracking. Craze cracks typically have no negative impacts on structural integrity or service life. These cracks can be mitigated with proper early age curing, finishing procedures, and mix proportioning; similar to method used to prevent plastic shrinkage cracks.

Materials Related Cracking

Materials related distresses such as freeze-thaw and alkali-silica reactivity (ASR) can cause random cracking of bridge decks although reports of ASR cracking in decks are rare. Conditions have to be present for these distress mechanism to exist. For freeze-thaw distress, the concrete must be critically saturated (typically understood to be at least 92 percent of full saturation) and undergo freeze/thaw cycles. Freeze/thaw resistance is gained by adequate w/cm, air entrainment, and durable aggregates. With bridge decks, this distress is most often noted near and below joints. For ASR to occur, the concrete must have moisture present; contain aggregates that are reactive; and have sufficient alkalis available. ASR risk is reduced by using durable aggregates that have been tested for potential reactivity. This is typically assessed for reactivity in accordance with ASTM C1260, "Standard Test Method for Potential Alkali Reactivity of Aggregates (Mortar-Bar Method)" and ASTM C1293, "Standard Test Method for Determination of Length Change of Concrete Due to Alkali-Silica Reaction." If potentially reactive aggregates are used, the reactivity can be mitigated by use of low alkali cements, less cement, and use supplementary cementitious materials (Class F fly ash, slag cement, and metakaolin). Guidance for mitigation is provided in ASTM C1778, "Standard Guide for Reducing the Risk of Deleterious Alkali-Aggregate Reaction in Concrete." The cracking patterns associated with these distress mechanisms can often mimic other random cracking, and internal cracking of the concrete is always apparent with these mechanisms. Therefore, concrete petrography is required to verify mechanisms of materials related distress. Many years, typically 10 years or more, are often needed for manifestation of materials related distress.

Autogenous Shrinkage

Autogenous shrinkage is volumetric movement caused by the consumption of water from the capillary pores during cement hydration. Autogenous shrinkage occurs during normal cement hydration and manifests itself at very early ages during initial strength gain. When sufficient water is present in the paste, concrete will generally swell. However, if the amount of water is limited in the cement paste (very low w/cm), the concrete will contract. This is sometimes called self-desiccation because of the limited moisture available for hydration, and results in shrinkage of the paste. Autogenous shrinkage increases with lowering w/cm; rapid setting cements; high replacement rates of slag cement; fine mineral admixtures (like silica fume), and higher concrete temperatures. A w/cm in the range of 0.38 to 0.42 is generally considered the maximum for autogenous shrinkage to occur, and it more commonly results from w/cm ratios less than 0.35. Although autogenous shrinkage is three dimensional, it is usually expressed as a linear strain. Typical autogenous shrinkage values range from 40 to 100 microstrain[5]. Autogenous shrinkage can be mitigated in the design phase by proper selection of cementitious materials and mixture proportioning.

Drying Shrinkage

Drying shrinkage is a natural process as the concrete losses moisture to the environment. The loss of moisture in concrete is a two phase process. The first phase consists of loss of free water, which causes little volumetric movement. The second phase consists of losing adsorbed water from the concrete, which results in volume change essentially equal to the volume of water lost. This drying will continue until it reaches equilibrium with the surroundings. The drying shrinkage of concrete mixes is usually assessed by measurement per ASTM C157, "Standard Test Method for Length Change of Hardened Hydraulic-Cement Mortar and Concrete". The ultimate drying shrinkage of bridge deck concrete when tested in accordance with ASTM C157 is typically in the range of 500 to 1000 microstrain[4]. In this test method, concrete test samples are cured at 50 percent relative humidity. The amount of drying shrinkage will vary depending on the relative humidity of the exposure conditions.

When considering drying shrinkage of bridge decks, not only does the bulk volume change have to be considered, but also the volume change caused by differential drying. The top surface of the bridge decks will dry faster than the center of the deck or the bottom (especially with stay in place forms); thus, creating a differential drying gradient throughout the deck thickness. The top surface will shrink more than central regions. The stresses developed because of the differential drying can be very large and are additive with the bulk volumetric movement. Furthermore, because of the large surface area to volume ratio, bridge decks are susceptible to rapid drying rates and significant moisture differentials, and most bridge deck drying and associated stresses will occur in the first year. The amount of drying shrinkage can be reduced by: reducing paste and cement content, optimized aggregate gradation, optimizing w/cm, and use of quality aggregate. Reducing the rate of drying and moisture differentials reduces the risk of cracking; but practical considerations limit implementation.

Thermal Movement

Bridge decks can develop large stresses at early ages because of rapid temperature changes. While drying is slow, allowing creep to dissipate stresses, thermal changes can be very rapid.

Cement hydration is a primary contributor to the first temperature changes in a new bridge deck. The process of cement hydration is exothermic, so concrete temperatures will increase with hydration and strength gain. Stresses will develop as the concrete cools from the peak temperatures of hydration while gaining minimal strength levels. Reducing the peak temperature and slowing the cooling rate will reduce these early-age stresses allowing dissipation of stresses by creep. This can be done by reducing plastic concrete temperatures (chilling the concrete); using low heat of hydration cements (avoid Type III cement); reducing cement contents; placing concrete at cooler temperatures; early moist curing; and adding timely insulation to slow the rate of heat loss.

The coefficient of thermal expansion (CTE) of the deck concrete influences the amount of volume change (strain) of the deck concrete for a given temperature change. Higher CTE concretes will expand and contract more; lower CTE concretes will expand and contract less. The primary determinant of the CTE of concrete is the aggregate type. Therefore, aggregate selection is important in controlling the volume movement created by thermal changes. CTE values can also be controlled by maximizing aggregate size and volume and by reducing cement content. The CTE will also vary with moisture content and concrete age. Fully saturated and dry concrete have been found to have similar CTE values. In between saturated and dry conditions, the CTE will be higher with the maximum CTE around 50 to 60 percent relative humidity[5]. Typical CTE values for saturated or fully dry concrete range from 4.0 to 7.5 x 10^{-6} / °F. The actual CTE will be typically higher than these values because bridge deck concrete is rarely completely saturated and never completely dry.

Temperature differentials are created through the deck thickness because of daily ambient temperature changes. Daily fluctuations in ambient temperatures force the top surface of bridge decks to cool or heat quicker creating non-linear temperature gradients. These gradients are important because of the strains created are above and beyond the bulk thermal change. Nonlinear shrinkage and temperature changes cause stress, even without restraint. Thus, it is important to consider strains developed by both bulk volume change and deck temperature differentials.

Subsidence Cracks

Cracks can be caused by subsidence (settlement over reinforcing steel). Subsidence or settlement cracks occur when settlement of concrete occurs at some obstruction, like reinforcing steel (Figure 7). Reinforcing

steel is typically supported by chairs or bolsters. When concrete is in a plastic state, natural settlement occurs as dense constituents (aggregate and cement) sink to the bottom. The supported reinforcing steel stops this natural settlement process and can cause tensile stress and cracking directly above the reinforcing steel. These types of cracks can significantly compromise the service life, because the cracks directly expose lengths of the reinforcing steel and allow aggressive agents to easily penetrate the concrete directly to the steel. These types of cracks are more common with high slump mixes, mixes with poor aggregate gradation, large placement (lift) depths, low concrete cover, and large bar diameters and can be typically prevented with proper mixture proportioning, design, and construction practices.

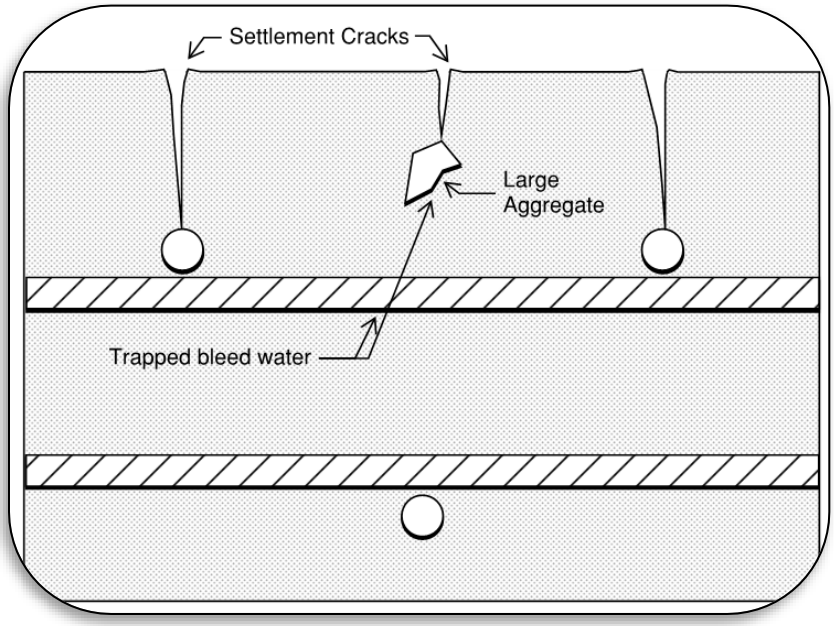

Figure 7. Diagram showing subsidence cracking at the location of reinforcing steel and a large aggregate.

Importance of Restraint

If concrete is unrestrained during any of the volumetric movement noted above, the concrete will move freely and remain crack-free. This movement, as stated above, is measured in strain or microstrain, a unit-less measurement which is calculated by dividing the amount of linear movement by the length of the element. Strain by itself does not cause stresses to develop. However, if the concrete is restrained, which is the case for all bridge decks, stresses will develop in the concrete. Restraint of bridge decks is primarily provided by the composite action of girders, somewhat by the internal reinforcing steel, and by self-bending due to non-uniform strain. The composite action is developed primarily by the use of shear studs or stirrups and bond of the deck concrete to the concrete girders. The restraint provided by the girders will develop tensile stress in the bridge deck and when the tensile stresses exceed the tensile strength of concrete, transverse cracking will occur. This can be most important at early ages when the concrete has developed little tensile strength. Tensile strength lags compressive strength and modulus development at early ages. Therefore, minimizing early-age temperature and drying/autogenous shrinkage effects is important for avoiding early-age crack development.

Because of the restraint provided by the girders, additional stresses can also develop in the bridge decks because of the differences in thermal expansion and temperatures of the girders. The coefficient of thermal expansion (CTE) of the deck concrete influences the amount of stresses that will develop and are typically linearly proportional. Higher CTE concretes will develop higher stresses, lower CTE concretes will develop lower stresses. However, when restraint is provided by the girders, these stresses can be exacerbated by difference in CTE of the deck and supporting girders and differences in girder/deck temperatures. Even with the same temperature changes in the deck and girders, stresses can be developed by the differences in CTE.

There is a difference between the tendency of concrete to shrink and its tendency to crack, since the tensile stress is the product of three terms: free shrinkage, effective modulus of elasticity, and degree of restraint. Effective modulus is also called sustained modulus in that it includes the plastic flow or creep. A concrete with a low modulus and high creep, typical of a low strength mix, will develop less stress for a given strain (temperature or moisture change) and has been found to have a lower risk of cracking. The degree of restraint is the percentage of the free shrinkage that is prevented. This restraint can be due to the external conditions (beams, girders or piers) or due to non-uniform thermal or moisture changes.

For example, if the concrete has a free shrinkage of 500 microstrain, but it is restrained and allowed to shorten only 250 microstrain, the restraint is 50 percent. Tensile creep induced by drying stresses is directly proportional to the free shrinkage strain. The tensile creep-shrinkage ratio at cracking is around 0.5 regardless of the mixtures w/cm[9]. Therefore, a concrete with a modulus of elasticity of 4×10^6 psi might have an effective modulus of only 2×10^6 psi, because of creep. The resultant tensile stress would be the product of the strain (500 microstrain) times the restraint (50 percent) times the effective modulus of elasticity 2×10^6 psi for a resultant tensile stress of 500 psi. If the actual, sustained tensile strength of the concrete is greater than 500 psi, cracking will not occur. Note that the actual tensile strength of the concrete in service is expected to be less than the laboratory measured strength by 0.6 (split tensile) to 0.8 (direct tensile) due to the effects of sustained loading (static fatigue) and cumulative microdamage.[9] Further, additional tensile stresses from thermal gradients or loading could crack such a concrete. Therefore, effects of shrinkage and temperature changes, effective concrete modulus, restraint conditions, tensile strength, and loading conditions must be considered.

A combination of shrinkage and thermal stresses causes most early-age cracking. However, the history of cumulative stresses as well as “notch” effects caused by settlement (subsidence) of high slump concretes that result in voids below transverse reinforcing bars and fine cracks above these bars can significantly reduce the cracking resistance of bridge decks. Concrete settlement voids and cracks at reinforcing bars, plastic shrinkage due to surface evaporation, falsework settlement, rapid cooling of the concrete as hydration temperatures dissipate, daily temperature changes, and long-term drying shrinkage combine to create stresses that cause micro-cracking and transverse deck cracking. Careful attention to the concrete mix design and to placing, finishing, and curing practices can help minimize these cracks. However, some cracking may be unavoidable in reinforced structures having high restraint conditions.

INVESTIGATION AND RESULTS

The investigation of the bridge deck distress consisted of a document review, field investigation, laboratory studies, and computer modeling and simulation. A summary of the investigation and results is presented in the following paragraphs, and a detailed presentation can be found in Appendix B.

Document Review

Prior to WJE's field investigation and laboratory studies, MDT personnel provided WJE with project documentation to better understand the design, construction, materials, and distress patterns exhibited by the Missoula-area bridge decks. Documentation was provided for the following projects:

- Florence - East, STPS-STPB 203-1(12)10
- Henderson - East, IM 90-1(175)23
- Henderson - West, IM 90-1(142)2
- Lozeau-Tarkio Structures, IM 90-1(168)29

Plan drawings were also provided for the bridge over the Thompson River in Thompson Falls, MT, although the bridge was not included in the original document review. In total, documentation was received for 22 bridges in the Missoula area and three (3) additional bridges in the Billings area showing similar types of distress. Subsequent investigations by WJE focused primarily on the 22 Missoula-area bridge decks; the Billings-area bridges are not discussed in this report.

Bridge Design

The 22 Missoula-area bridge decks under investigation were all placed between 2007 and 2015, with many decks being replacements for bridges built between 1960 and 1980. At least three deck rehabilitations between 2007 and 2015 consisted only of overlays applied to the original decks from the 1960s to 1980s, while the remaining projects were full deck replacements. The two bridges at Florence-East and Thompson River were new construction.

The bridges varied in terms of the number of spans, total length, and structural type, but most of the superstructures consisted of either prestressed concrete beams or welded plate girders. Deck thicknesses varied between 6 1/2" and 9" but were most commonly specified between 7 1/4" and 8". Epoxy-coated steel reinforcing bar was specified for the transverse (No. 5 bar) and longitudinal (No. 4 bar) reinforcement in all new construction and replacement deck slabs. Transverse reinforcement was specified at the same spacing in the top and bottom mats for most of the bridges, and ranged between 5" and 10 1/2", with a typical spacing of 6" to 7". Longitudinal reinforcement for each deck was specified at 1'-6" on center in the top mat, and ranged between 3 1/2" and 9" in the bottom mat, with a typical spacing of 6" to 7 1/2". Top cover to the transverse bars was specified at 2 3/8" for all new bridge decks, and bottom cover to the lower bars was specified at 1". Representative cross-sections cut parallel to the longitudinal and transverse reinforcement are shown in Appendix B.

Table 1. Specified Deck Thicknesses and Reinforcement Bar Spacing for Selected Bridge Decks

Bridge Location	Year of Construction (Reconstruction)	Specified Deck Thickness	Transverse Bar Spacing: Top and Bottom Mats	Longitudinal Bar Spacing: Top Mat	Longitudinal Bar Spacing: Bottom Mat
Florence-East, MP 10.640	2014	8”	7 1/4”	1’-6”	7 3/8”
Lozeau-Tarkio, MP 57.472 EB	1967 (2011 - redeck)	7 1/4” to 8”	7” or 7 1/2”	1’-6”	7 1/2”
Lozeau-Tarkio, MP 58.550 EB	1967 (2011 - overlay)	7 1/4” to 8” (+)	6” or 10 1/2”	1’-3” or 1’-8”	5” or 6”
Lozeau-Tarkio, MP 58.550 WB	1967 (2011 - redeck)	7 1/2” to 8 1/4”	7” or 7 3/4”	1’-6”	7” or 7 1/2”
Lozeau-Tarkio, MP 57.472 WB	1967 (2011 - redeck)	7 1/4” to 8”	7” or 7 1/2”	1’-6”	7 1/2”
Henderson-West, MP 22.013	1980 (2007 - redeck)	7 1/2”	5 3/4”	1’-5 3/4”	6 1/8”
Henderson-East, MP 25.393	1980 (2008 - overlay)	7” to 7 3/4”	5”, 5 3/4”, or 6 1/4”	1’-6”	5”, 6”, or 7”
Henderson-East, MP 24.603	1980 (2008 - redeck)	6 5/8”	6 1/8”	1’-5 3/4”	6”
Henderson-East, MP 23.325, WB	1979 (2009 - overlay)	8 1/4”	5”	1’-5 3/4”	3 1/2”
Superior Area, MP 49.397 EB	1966 (2010 - redeck)	7 1/2” to 8 1/4”	6 1/4” or 7”	1’-6”	6 7/16” or 7 11/16”
Superior Area, MP 49.397 WB	1960 (2011 - redeck)	6 3/4” to 7”	6” or 6 1/2”	1’-6”	4 1/4” or 7 1/8”
Thompson River, MP 55-56	2015	9”	6 1/4” (top) 9 3/4” (bottom)	1’-6”	9”

(+) Includes 1/2” added from overlay.
Note: In-depth investigations were performed on highlighted bridges (see “Field Investigation” below).

Concrete Mixtures

The concrete used for each bridge deck was typically Class SD “special deck” concrete. Class SD concrete, as specified in Section 551 of the MDT *Standard Specifications for Road and Bridge Construction, 2006 Edition*, has a maximum water-cementitious materials ratio (w/cm) of 0.40, a target slump of 1 1/2 to 3 in. (prior to HRWR), a required air content of 5-7%, and a minimum 28-day compressive strength of 4500 psi. Special provisions modifying the requirements for Class SD concrete were issued for the Florence-East project, but all other projects adhered to the then-current 2006 MDT requirements. Class SD-L “low-permeability” deck concrete was also specified for one bridge deck in the Superior Area Structures project, and Class SF silica fume deck overlay concrete was specified for the Lozeau-Tarkio project.

The concrete mixtures and raw materials (cement, aggregates, admixtures, etc.) used for each project were provided by different suppliers, although similar mix designs were typically used for each bridge (see Table 2 and Table 3). A detailed review of the concrete mix designs, QC data, and batch ticket reports is included in Appendix A for 12 of the 22 Missoula-area bridge decks included in this investigation.

Table 2. Mix Designs, Class SD Concrete

Material	Florence-East (Class SD)	Henderson-East (Class SD)	Henderson-West (Class SD)	Lozeau-Tarkio and Superior Area (Class SD)
Water, pcy	217	242	258	214
Cement, pcy	345	611	658	600
Fly ash, pcy	146	-	-	-
Silica fume, pcy	30	-	-	-
Stone, pcy	1821	1850	1875	1779
Sand, pcy	1299	1205	1100	1334
Air entrainer, fl. oz./cwt	2	4.6	6	8
Mid-range water reducer, fl. oz./cwt	12	31	33	22
High-range water reducer, fl. oz./cwt	4	-	-	-
Set retarder, fl. oz./cwt	4	-	-	32
w/cm (nominal)	0.42	0.40	0.39	0.36
w/cm (including admixtures)	0.43	0.42	0.41	0.39

Table 3. Mix Designs, Class SF and SD-L Concrete

Material	Lozeau-Tarkio (Class SF)	Superior Area (Class SD-L)
Water, pcy	243	205
Cement, pcy	570	500
Fly ash, pcy	-	-
Silica fume, pcy	43	25
Stone, pcy	1749	1844
Sand, pcy	1260	1328
Air entrainer, fl. oz./cwt	8	9
Mid-range water reducer, fl. oz./cwt	22	30
High-range water reducer, fl. oz./cwt	-	-
Set retarder, fl. oz./cwt	32	30
w/cm (nominal)	0.40	0.39
w/cm (including admixtures)	0.43	0.43

Deck Condition

Photographs were provided by MDT personnel for most of the bridges included in the investigation. The photographs showed varying levels of distress in each of the decks. Most of the decks showed transverse cracking on the underside, often highlighted by white or gray-white efflorescence that appeared in the older decks to leach out of the cracks and onto the underside of the deck. Some - but not all - of the bridge decks that received only an overlay (e.g., the east-bound Superior Area bridge at MP 45.180) also exhibited this type of distress, but there were generally fewer and less frequent cracks observed in the undersides of those decks. Transverse cracks were estimated to be spaced less than 1 ft. apart in the most severely distressed decks, and more widely spaced (~6 ft.) in the less severely distressed decks. The cracks generally appeared parallel to one another, but occasional longitudinal cracks (perpendicular to the predominant transverse cracks) were also observed in a few of the MDT photos. Some decks exhibited a darkening discoloration of the concrete surrounding the efflorescence-filled cracks that suggested the presence of moisture in or near the crack opening at the time of the photograph.

The top surfaces of the bridge decks showed wide-spread abrasion in decks both with SCMs (fly ash or silica fume) and without SCMs. Spalls in both the concrete and the asphalt could be seen at pavement and expansion joints in several of the photographs. Transverse and map cracks were also observed on the top surfaces of several of the decks, with the most severely distressed decks showing large transverse cracks throughout the top surfaces.

Two of the Missoula-area bridge decks exhibited severe cracking that broke the concrete free from the reinforcing steel. The Lozeau-Tarkio Bridge over the Montana Rail Link (MP 57.472) developed a full-depth crack that dropped a "chunk" (approximately 4 in. by 4 in.) of the deck concrete onto the ground below. A portion of this "chunk" was retrieved for laboratory study prior WJE's field investigation. The Superior Area Bridge over the Clark Fork River (MP 49.397) also developed a deep crack that dislodged a "chunk" of concrete from the top of the deck, but not through the full depth of the deck. Photographs of the two holes were similar, with the cracks appearing directly above (or below) the reinforcing bars along their lengths. The coatings of the bars in all photographs appeared to be in satisfactory condition, and no corrosion products were visible within the cracks.

Figure 8. Through-hole in east-bound Lozeau-Tarkio bridge at MP 57.472 (photo provided by MDT).

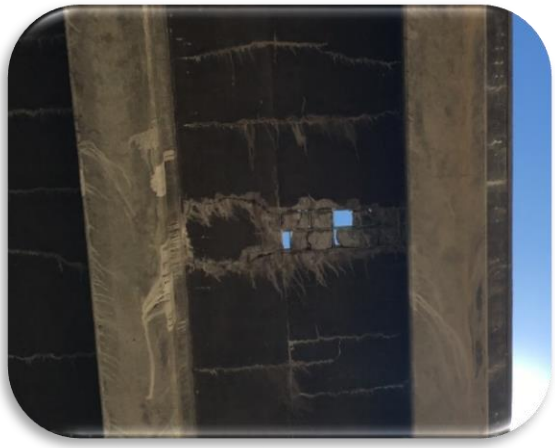

Figure 9. Through-hole in east-bound Lozeau-Tarkio bridge at MP 57.472, as seen from the underside of deck (photo provided by MDT).

Figure 10. Delaminated "chunk" in deck of east-bound Superior Area bridge at MP 49.397 (photo provided by MDT).

Figure 11. Delaminated "chunks" along expansion joint of east-bound Superior Area bridge at MP 49.397 (photo provided by MDT).

Field Investigation

Based on findings of the document review, four bridges were identified by WJE in consultation with MDT personnel for further in-depth field investigation. These bridges include:

- **Florence-East, Bridge over the Bitterroot River, MP 10.640**: A two-year old new construction bridge deck showing initial signs of distress. Extensive map cracking and deep transverse cracks were visible in MDT photographs of the top surface of the deck. Light efflorescence-filled cracks were also observed by MDT personnel on the underside of the deck. This bridge was selected for in-depth investigation due to its young age and the use of fly ash and silica fume in its mix design.

- **Lozeau-Tarkio, East-bound Bridge over the Montana Rail Link, MP 57.472**: A five-year old bridge deck replacement showing severe signs of distress, including deep cracks, spalls, and through-holes. The bridge was selected for in-depth investigation due primarily to the severity of its distress. MDT had completed repairs on the bridge by the time of the field investigation, but part of the "chunk" of concrete that had fallen through the deck was submitted to WJE for laboratory study.

- **Henderson-West, Henderson Interchange, MP 22.013**: A nine-year old bridge deck replacement showing distress representative of other area bridge decks. Frequent transverse cracks were visible in MDT-provided photographs of both the topside and underside of the bridge deck. This bridge was selected for in-depth investigation due to its older age, representative distress pattern, and straight cement mix design.

- **Superior Area Structures, East-bound Bridge over Clark Fork, MP 49.397**: A six-year old bridge deck replacement showing severe signs of distress, including deep cracks and large spalls. The severity of distress observed in the MDT photographs was comparable to that of the east-bound Lozeau-Tarkio Bridge at MP 57.472, but no through-holes had yet been formed. This bridge was selected for in-depth investigation due to the severity of its distress and its silica fume (Class SD-L) mix design. The adjacent west-bound bridge deck, which did not contain silica fume (Class SD mix) and did not show as severe distress in MDT photographs, was also investigated for comparison in a cursory investigation.

An additional eight bridges were also selected for cursory inspection, to provide supplemental information regarding the type and severity of distress exhibited by the area bridge decks. A total of twelve bridges were investigated, as described in Appendix A. Bridges were numbered 1 through 12 for easier identification.

The field investigations were performed between August 22 and 25, 2016. Field investigations consisted of crack mapping, core extraction, delamination surveys, impulse response (IR) surveys, ground penetrating radar (GPR) scans, and infrared imaging. The field investigation also included visual observation of the undersides of each deck, periodic measurements of deck surface temperatures, and sampling of efflorescence from the underside of the bridge decks for further laboratory analysis. A table summarizing the methods used on each bridge deck is provided in Table 4. Plan drawings showing the locations of the cores, crack maps, and delaminations identified during the four in-depth investigations (Bridges 1, 2, 6, and 10) are provided in Appendix B.

Table 4. Description of Bridges Investigated

Bridge #	Bridge Location	Date of Field Investigation	Year Constructed (Re-constructed)	Superstructure	Concrete Mixture	Notes
1	Florence-East, MP 10.640	Aug. 22, 2016	2014	Prestressed concrete beam, 378 ft.	Fly ash (28%) and silica fume (6%)	Two years old at time of investigation; early stages of distress documented by MDT personnel
2	Lozeau-Tarkio, MP 57.472 EB	Aug. 23, 2016	1967 (2011)	Prestressed concrete beam, 296 ft.	No SCMs	Deep cracks and through-holes documented by MDT personnel
3	Lozeau-Tarkio, MP 58.550 EB	Aug. 23, 2016	1967 (2011)	Welded plate girder, 826 ft.	Silica fume (7%)	2 1/2" overlay applied in 2011
4	Lozeau-Tarkio, MP 58.550 WB	Aug. 23, 2016	1967 (2011)	Welded plate girder, 826 ft.	No SCMs	Companion to Bridge 3, but full deck replacement used different concrete mixture than Bridge 3 overlay
5	Lozeau-Tarkio, MP 57.472 WB	Aug. 23, 2016	1967 (2011)	Prestressed concrete beam, 311 ft.	No SCMs	Companion to Bridge 2
6	Henderson-West, MP 22.013	Aug. 24, 2016	1980 (2007)	Prestressed concrete beam, 138 ft.	No SCMs	Oldest bridge deck
7	Henderson-East, MP 25.393	Aug. 24, 2016	1980 (2008)	Prestressed concrete beam, 122 ft.	No information provided	2 1/2" overlay applied in 2008
8	Henderson-East, MP 24.603	Aug. 24, 2016	1980 (2008)	Prestressed concrete beam, 402 ft.	No SCMs	Under two-way traffic at time of investigation; investigation only performed on underside
9	Henderson-East, MP 23.325	Aug. 24, 2016	1979 (2009)	Welded plate girder, 658 ft.	No SCMs	EB lanes under two-way traffic at time of investigation; investigation only performed on WB lanes
10	Superior Area, MP 49.397 EB	Aug. 25, 2016	1966 (2010)	Welded plate girder, 800 ft.	Silica fume (6%)	Deep cracks and spalls documented by MDT personnel
11	Superior Area, MP 49.397 WB	Aug. 25, 2016	1960 (2011)	Welded plate girder, 800 ft.	No SCMs	Companion to Bridge 10, but used different concrete mixture
12	Thompson River, MP 55-56	Aug. 25, 2016	2015	Prestressed concrete beam, 446 ft.	No information provided	Approximately one year old at time of investigation; early cracking observed by MDT personnel

Note: In-depth investigations were performed on highlighted bridges

Crack Mapping

Transverse, longitudinal, and random cracks were sketched on plan drawings for 20-foot wide sections of each bridge deck. Multiple areas of Bridges 1, 2, 6, and 10 were mapped during the in-depth investigations, and individual areas of Bridges 3, 5, 11, and 12 were mapped during the cursory investigations. Crack map details can be found in Appendix B. Cumulative crack widths were also measured over 50-foot lengths of Bridges 1, 2, and 6 to estimate the volume change of the decks.

All 12 bridge decks exhibited some degree of transverse and longitudinal cracking. The transverse cracks were more frequent and generally wider than the longitudinal cracks for all 12 of the bridges investigated. The transverse cracks typically extended from the girders or ran along the piers, while the longitudinal cracks typically formed over the girders and occasionally half-way between adjacent girders. The transverse cracks were spaced at 2 to 4 feet in most bridges, and ranged in top surface width from 5 to 35 mils (0.005 to 0.035 inches). Some decks also exhibited random map cracking, but these were not always visible on older decks. Map cracking was most pronounced for Bridge 1, which contained silica fume.

The frequency of wider cracks generally increased with the age of the bridge deck. The widest average crack widths were measured on the deck placed nine years ago (Bridge 6), while the finest cracks were measured on the deck placed one year ago (Bridge 12). Despite the finer cracks, however, the younger decks still showed similar crack patterns to the older decks, suggesting that the cracks initiate early in the life of the concrete and propagate and widen over time under environmental and live loads.

Based on the progression of the crack patterns from the youngest decks to the oldest decks, it is hypothesized that the transverse cracks initiate near the girders, where the restraint is the greatest, and propagate away from the girders with time. When the transverse cracks propagate past one another in close proximity (typically, within 6 to 18 inches), the crack tips bend toward one another, eventually "jumping" from one crack to another. Such "jump" crack patterns were observed in Bridges 2, 6, and 10, and were reflected on the top and bottom surfaces of the deck in Bridge 6 (see Figure 12 and Figure 13). It is hypothesized that the holes previously observed in Bridges 2 and 10 may have initiated at such "jump" crack locations.

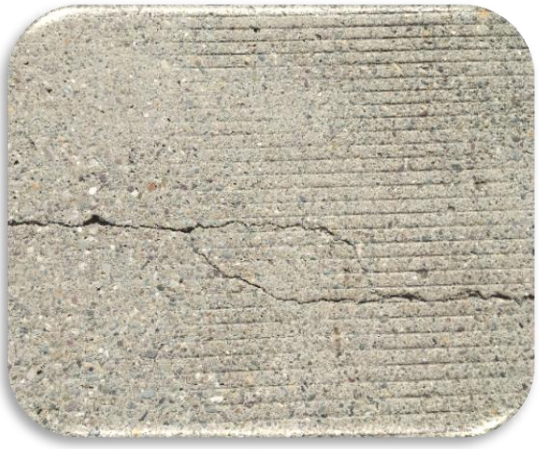

Figure 12. "Jump" cracks in top side of Bridge 6. Transverse cracks are spaced approximately 6 inches apart.

Figure 13. "Jump" cracks from Figure 12, as reflected in the underside of the deck of Bridge 6.

Core Extraction

A total of 43 four-inch nominal diameter cores were extracted from the bridge decks for further laboratory study at WJE's Janney Technical Center (JTC) in Northbrook, IL. Cores were extracted in both cracked and uncracked areas of the deck and over reinforcing bars to for subsequent visual observation, physical testing, and chemical and petrographic analysis. The number and location of cores extracted from each bridge is summarized in Table 5, and the description of the cracks and reinforcing bar present in each core is summarized in Appendix B. A complete description of the laboratory tests performed on each core is described in the "Laboratory Analysis" section of this report.

Table 5. Core Location Summary

Bridge #	# of Cores	Core Location(s)		Notes
1	11	Cores 1A, 1B: Cores 1C, 1D: Cores 1E, 1F: Cores 1G, 1H: Cores 1I, 1J, IK:	Span 2, EB lane, 220’ station marking, above Girder G3 Span 2, EB lane, 180’ station marking, C.L. of structure Span 3, EB lane, 10’ station marking, above Girder G3 Span 1, WB lane, 320’ station marking, 5’ from edge of deck Span 2, WB lane, 180’ station marking, 10’ from edge of deck	Core 1K fell through deck and was not retrieved
2	8	Cores 2A, 2B: Cores 2C, 2D-I/II, 2E: Cores 2F, 2G:	Pier 5, driving lane, 250’ station marking, 7’ from edge of deck Span 3, driving lane, 125’ station marking, 7’ from edge of deck Span 1, driving lane, 50’ station marking, 5’ from edge of deck	Core 2D-I fell through deck and was not retrieved; replaced by Core 2D-II from same location
3	3	Cores 3A, 3B: Core 3C:	Span 3, driving lane, 280’ station marking, 5’ from edge of deck Span 5, driving lane, 575’ station marking, 10’ from edge of deck	Cores taken through overlay
4	-	-		-
5	1	Core 5A:	Span 2, driving lane, 65’ station marking, 7’ from edge of deck	-
6	9	Cores 6A, 6B, 6C: Cores 6D, 6E, 6F: Cores 6G, 6H, 6I:	Span 3, passing lane, 125’ station marking, 15’ from C.L. barrier Span 1, driving lane, 35’ station marking, 15’ from edge of deck Span 2, driving lane, 65’ station marking, 10’ from edge of deck	Crack in core 6G was reflected through underside of deck
7	-	-		-
8	-	-		-
9	-	-		-
10	5	Cores 10A, 10B: Cores 10C, 10D, 10E:	Span 2, driving lane, 165’ station marking, 7’ from edge of deck Span 3, driving lane, 325’ station marking, 10’ from edge of deck	-
11	3	Cores 11A, 11B, 11C:	Span 4, driving lane, 330’ station marking, 10’ from edge of deck	Core 11A taken over crack with sealant
12	3	Cores 12A, 12B: Cores 12C:	Span 2, EB lane, 275’ station marking, 15’ from edge of deck Span 2, EB lane, 280’ station marking, 15’ from edge of deck	Core 12A taken over “jump” crack; Core 12C taken over crack with sealant

Note: In-depth investigations are highlighted. C.L. = center line.

Delamination Survey

Near-surface delaminations were identified by mechanical sounding of the bridge decks using chain dragging and hammering methods. The locations of the delaminations were identified, and their approximate areas were recorded. The total delaminated area was estimated for each deck. Delamination surveys were not performed on Bridges 4 and 8. Delaminations were detected on Bridges 1, 3, 6, and 7. Most delaminations measured less than 1-foot by 1-foot, and in all cases, the total delaminated area was less than 0.5% of the deck area surveyed. Bridge decks 3 and 7, which had the largest delaminated fractions of the 12 bridge decks, both consisted of a 2 1/2-inch overlay applied to an existing concrete deck; the small fraction of delaminated areas in these decks suggests that the overlays are well-bonded to the concrete substrate. The delamination surveys are detailed in Appendix B.

Table 6. Delaminations Detected

Bridge	Estimated Total Area of Delaminations (ft^2)	Estimated Fraction of Surveyed Area (%)
1	3	0.03
2	None detected	0
3	10	0.08
4	*Not surveyed*	
5	None detected	0
6	1	0.02
7	13	0.26
8	*Not surveyed*	
9	None detected	0
10	None detected	0
11	None detected	0
12	None detected	0

Impulse Response (IR) Survey

Impulse response (IR) surveys were conducted using a Germann Instruments s'MASH unit on Bridges 1, 2, 6, and 10 to compare the relative modal response of the bridge decks and to identify areas potentially containing initiation of structural distress. Impulse response is a non-destructive test method in which a hammer is used to impact an element, and the nearby vibration response is collected and analyzed to obtain the mobility spectrum of the element. The mobility spectrum provides an indication of the relative flexibility (stiffness) of the element at the test location and can also be used to identify locations of poor consolidation (e.g., honeycombing), distress, or delamination within a concrete element. Contour plots of the average mobility and dynamic stiffness determined by IR for each bridge are presented in Appendix B.

The mobility and stiffness plots both indicate that the deck is less flexible (i.e., has a lower average mobility or a higher dynamic stiffness) over the piers and girders than it is away from them. The higher mobility between the girders helps explain the occurrence of "jump" cracks and that through-deck failures are most likely to occur mid-way between girders. Overall, these baseline mobilities and stiffnesses are generally small (less than 20 units), compared to the mobilities and stiffnesses in areas that are affected by delaminations, voids, or other effects. The deck repairs to Bridge 2 appear to have only a small effect on the mobility and stiffness measured.

Two scanned areas of the Bridge 1 deck had significantly higher average mobilities than the surrounding bridge deck. Average mobilities in excess of 50 units were detected near the 285' and 195' station markings. Although delaminations or voids were not detected by chain drag at these locations, other delaminations of

similar size were detected in the vicinity of these high-mobility regions, suggesting that intense cracking, delaminations, or voids may be present in the concrete at these additional locations. No other areas of high average mobility were identified for the other three bridge decks, which had infrequent incidence of delaminations and voids detected by chain drag. Due to the locality of the characteristic cracking that causes the deck penetrations, a general survey of the deck mobility may not pick up incipient areas of distress. Although IR testing was informative, identification of incipient deck distress is more easily done by visual inspection and recognition of tell-tale indicators rather than by measuring deck mobility.

Ground Penetrating Radar (GPR) Scan

A Geophysical Survey Systems, Inc. (GSSI) StructureScan Mini ground penetrating radar (GPR) unit was used to estimate the thickness of the deck slab and to identify the location and depth of the reinforcing bars. GPR was also used during core extraction to determine the location of the reinforcing bar relative to the core extraction site. The GPR scanning data is summarized in Appendix B, which includes details of bar locations and deck thicknesses.

Infrared Imaging

Infrared videos of the deck surfaces were recorded for Bridges 1, 2, and 12 using a drone equipped with an infrared camera. Infrared images can be used to identify cracks, delaminations, areas of poor consolidation, and other features of the bridge decks where defects cause sharp, minute differences in surface temperature. Overhead videos without infrared imaging were also recorded for Bridges 1, 2, 10, and 12. All drone-recorded footage was provided to MDT personnel separate from this report.

In general, there were very few delaminated or poorly consolidated areas identified by the infrared camera, which was consistent with the low frequency of delaminated areas identified by chain drag, GPR, and impulse response surveys. The delaminated areas identified by the infrared camera tended to be on the order of 1 square foot in area, which is also similar in size to the areas identified by the other techniques.

Efflorescence

Efflorescence samples were collected from the undersides of Bridges 2 and 6 for further laboratory study. The sample from Bridge 2 was primarily white in color, while the sample from Bridge 6 contained both white and gray components.

Laboratory Studies

The cores and efflorescence samples taken during the field investigation were delivered to WJE's laboratories in Northbrook, IL for further study. A preliminary visual assessment was performed on each core to document the size of the core, the approximate depth of crack penetration, and the types and locations of the reinforcing bars. Based on the preliminary observations, specific cores were selected for physical testing, petrographic analysis, and chemical analysis. Each method is described briefly below. A list of samples used for each study is provided in Table 7.

Table 7. Summary of Laboratory Analyses Performed on Cores

Bridge #	Compressive Strength	Splitting Tensile Strength	Modulus of Elasticity	Coefficient of Thermal Expansion	Petrographic Analyses[1]	Air Void Analysis	Chloride Profiles
1	1E, 1J	1C	1A	1A	1D, 1I	1D	-
2	2D-II, 2E	2F	2A	2A	2C	2C	-
3	-	-	-	-	3A - overlay 3B - overlay	-	-
4	*No cores taken*						
5	-	-	-	-	-	-	-
6	6E, 6H	6I	6B	6B	6G	-	6A
7	*No cores taken*						
8	*No cores taken*						
9	*No cores taken*						
10	-	-	-	-	10B	-	10E
11	-	-	-	-	11A - sealant	-	-
12	-	-	-	-	12A	-	-

[1] Full petrographic analyses, including thin-section analyses, were performed on cores from Bridges 1, 2, 6, 10, and 12.

Physical Testing

The following physical properties of the concrete were determined from cores containing no cracks or reinforcing bar:

- **Compressive and Splitting Tensile Strength** were measured in accordance with ASTM C42, *Standard Test Method for Obtaining and Testing Drilled Cores and Sawed Beams of Concrete*. The ends of the compressive strength specimens were cut and capped prior to testing, and the edges of the tensile strength specimens were lapped free of any chatter as needed to provide a smooth testing surface. All cores were tested in the as-received moisture condition.

- **Modulus of Elasticity** was measured in accordance with ASTM C469, *Standard Test Method for Static Modulus of Elasticity and Poisson's Ratio of Concrete in Compression*. The ends of the specimen were cut and capped prior to testing. Three wire strain gauges, located at approximately third points around the circumference, having an effective length of 2 inches were bonded to the surfaces of each specimen to measure strains under the applied load. The modulus of elasticity was calculated from the stress-strain data averaged over two runs for each test specimen.

- **Coefficient of Thermal Expansion** was measured according to an in-house testing procedure. Three sides of each core, located at approximately third points around the circumference, were made plane by grinding. Two Whittemore strain buttons were installed on each planed surface at a 4 inch gauge length. The specimens were submerged in a water bath at room temperature (72 °F) for a minimum of 48 hours, and an initial reading was made with the Whittemore gauge. The temperature of the bath was cycled twice between 140 °F and 40 °F, holding each temperature for at least 48 hours prior to subsequent length change measurements. The coefficient of thermal expansion was determined after each temperature change as the average temperature-induced strain in the specimen divided by the change in temperature. The specimen's saturated coefficient of thermal expansion was taken as the average of the four individual measurements.

Table 8 gives a summary of the average physical properties measured on cores taken from Bridges 1, 2, and 6. Bridge 1 had the greatest compressive and tensile strengths and the stiffest modulus of elasticity of the three bridges examined, which is consistent with the use of fly ash and silica fume in its mixture. Bridges 2 and 6 had similar straight-cement concrete mixtures, and both consequently had similar compressive strengths and elastic moduli that were less than those measured for Bridge 1. All three bridges measured similar coefficients of thermal expansion between 3.6 and 5.0 × 10^{-6}/°F; typical thermal expansion coefficients for concrete reported in the literature range between 4 and 7 × 10^{-6}/°F.[10]

Table 8. Summary of Measured Physical Properties

Bridge	Compressive Strength (psi)	Splitting Tensile Strength (psi)	Modulus of Elasticity (ksi)	Coefficient of Thermal Expansion (/ °F)
1	7,370	770	4,450	4.8 × 10^{-6}
2	5,090	600	3,300	3.6 × 10^{-6}
6	6,090	605	3,950	5.0 × 10^{-6}

Petrographic Analyses

Petrographic analyses were conducted to examine the general quality of the concrete, the progression of the cracks within the concrete, the bond quality at the overlay/substrate interfaces, and the presence of any internal distress mechanisms. Petrographic examinations were conducted in accordance with the applicable methods of ASTM C856, *Standard Practice for Petrographic Examination of Hardened Concrete*. Water-cementitious (w/cm) ratio and total air contents were estimated by visual observation, and complete air void analyses were conducted according to ASTM C457, *Standard Test Method for Microscopical Determination of Parameters of the Air-Void System in Hardened Concrete*, on three cores (1D, 1I, and 2C) selected for additional follow-up study. Detailed petrographic observations are reported in Appendix C.

The petrographic studies revealed no materials-related cause for the cracking. Proportions of constituents appeared normal, except for variations in air content. Evidence of internal distress mechanisms that could produce bulk volumetric instability was not observed. Pertinent observations include:

- The volume of fly ash in the concrete did not appear excessive.
- Water-cementitious materials ratio were variable and occasionally higher than designed.
- Aggregates were sound and had performed adequately in service. The coarse aggregate included substantial amounts of high-absorption sedimentary rocks that could contribute to high shrinkage; however, evidence of adverse aggregate behavior was not observed.
- Measured air contents were high for cores 1D, and 2C, and estimated air contents were high for cores 1I, 3B, 6G, and 10B (at least locally – up to 12%). Despite the high air contents and local variations within the cores, the air void systems generally appeared adequate to protect the concrete against distress caused by cyclic freezing and thawing.
- Cracks adjacent to steel reinforcement were common. Cracks predominantly passed around aggregate particles and appeared to be wider at the top of the concrete. Cracking through aggregate particles was less commonly observed and only seen in the bottom region of the concrete. Crack observations indicate that cracking was initiated early at the top of the concrete (before the concrete had gained strength and while paste-to-aggregate bond was weak). The cracks progressed deeper in the concrete after the concrete had gained appreciable strength.
- The frequency of paste microcracking was not excessive (generally infrequent except near the main cracks). Movement of the cracked sections of concrete probably caused these secondary cracks.

- White glaze that was observed on some crack surfaces was analyzed using SEM/EDX. The glaze mostly contained calcium, silicon, oxygen, and carbon. Smaller amounts of aluminum, potassium, sodium, magnesium, and iron were routinely detected. The composition of the glaze is consistent with precipitation from water saturated with elements leached from the cementitious paste.

Chemical Analyses

Chloride Contents

Acid-soluble chloride analyses were performed according to ASTM C1152, *Method for Acid Soluble Chloride in Mortar and Concrete* on a total of twelve slices sampled from cores 6A and 10E. Samples for analysis were taken at three different depths along the cracks in each core, and from three identical depths away from the cracks in each core. The chloride contents of the twelve slices are listed in (Table 9).

Table 9. Chloride Contents

Sample	Location	Acid-Soluble Chloride, percent by mass of sample
Core 6A Crack	Top Middle Bottom	0.359 0.196 0.171
Core 6A Non-Crack	Top Middle Bottom	0.332 0.210 0.205
Core 10E Crack	Top Middle Bottom	0.159 0.096 0.070
Core 10E Non-Crack	Top Middle Bottom	0.187 0.093 0.045
Bridge 6 Efflorescence White Portion	---	0.091

The chloride concentrations were similar in both the cracked and non-cracked areas of both cores. Studies have shown that chloride contents above 0.02 to 0.03 percent by mass of concrete, depending on the cement content, can promote corrosion of embedded carbon steel in non-carbonated normal weight concrete. The chloride contents of all the samples analyzed were well above this threshold level, and therefore, may promote the corrosion of embedded black steel in the presence of sufficient moisture and oxygen. However, no evidence of corrosion was noted on any of reinforcing steel in the cores or observed in the field.

Efflorescence

Two efflorescence samples from Bridges 2 and 6 were analyzed for crystalline components by x-ray diffraction (XRD). The efflorescence sample from Bridge 2 was separated into grey and white portions prior to analysis. The efflorescence sample from Bridge 6 was mostly white and was analyzed as received.

During x-ray diffraction analysis, radiation produced from an x-ray source is diffracted off the sample at various angles. A detector measures the intensity of the diffracted energy, and the location (angle) and intensity are recorded as a graph. This graph, which displays a pattern of peaks, can be interpreted to identify the crystalline components of the sample. The peaks are compared to a library of diffraction patterns of known components to identify the crystalline materials present. The results are listed in Table 10.

Table 10. X-ray Diffraction Analysis

Sample	Crystalline Components Detected
Bridge 6	Major--Calcite ($CaCO_3$)
Bridge 2 White Portion	Major--Calcite
Bridge 2 Grey Portion	Major--Quartz (SiO_2), calcite, Minor--Feldspar Possibly--Clay
Bridge 2 Spall Residue From Water Extraction	Major--Calcite Minor--Halite (NaCl), sylvite (KCl)

Calcite was the only crystalline component detected in the white portions of the efflorescence samples. The crystalline components detected in the grey portion of the Bridge 2 efflorescence sample were typical of crystalline components normally found in concrete or dirt.

Acid-soluble chloride analysis was also performed essentially according to ASTM C1152 on the efflorescence sample from Bridge 6. The sample contained 0.091 percent chloride contradicts the chloride testing performed on the concrete, near and away from cracks. If moisture migrating through the cracks contains chlorides and effloresces on the underside, it would be assumed that the chloride levels would be higher near the cracks. The measured chloride levels do not support this assumption. Further investigation is necessary to understand the chloride levels and ingress.

Modeling

Petrographic observations of the cracked cores indicate that the transverse cracks initiated early at the top of the concrete deck and progressed deeper after the concrete had gained appreciable strength. Early transverse cracking may develop due to restrained autogenous/drying shrinkage of the deck concrete or to thermal changes or gradients in the deck and supporting beams. Because there is no information available regarding the early-age temperature in the bridge decks under investigation, two models were used to simulate the conditions under which early cracks may have developed in the bridge decks.

ConcreteWorks Thermal Model

Temperature histories were simulated for the decks of Bridges 1, 2, and 6 using ConcreteWorks[11]. To simulate the temperature history of a bridge deck element, the ConcreteWorks software uses user-defined mixture proportions and cement compositions to approximate the heat of hydration of the concrete (an internal source of heat), and historical or user-defined environmental conditions to generate air temperature, wind velocity, and solar radiation histories (external sources of heat). The thermal properties of the concrete - thermal conductivity and specific heat capacity - are assumed by the software based on the materials and mix proportions. The deck thickness and the thermal properties of the formwork and insulation (if used) are entered as additional inputs. The model combines these parameters with fundamental models for heat transfer to generate an approximate temperature profile history for the bridge deck element.

Temperature histories were simulated for the decks of Bridges 1, 2, and 6, assuming placement times as indicated on the batch tickets. Three additional simulations were performed for placement times of 6:00 a.m., 12:00 p.m. (noon), and 6:00 p.m. to demonstrate how temperatures develop in the bridge decks as at different deck placement times. Appendix B summarizes the ConcreteWorks input parameters and the values assumed for each model. Figure 14 shows an example of the maximum simulated deck temperatures for Bridge 1 at each assumed placement time. Additional plots are provided in Appendix B for other bridges. A constant plastic concrete temperature of 65 °F was assumed for all models.

The simulation results demonstrate that temperatures develop in the concrete deck at different rates depending on the placement time. In every case, the deck experiences the greatest temperature increase due to its internal heat of hydration. When the concrete is placed in the morning (e.g., 12:00 am. - 12:00 p.m.), the peak hydration temperatures occur at approximately the same time as the peak ambient temperatures and solar radiation. This rapidly warms the deck, so that the concrete reaches its peak temperature approximately 18 hours after placement, or at about the time that the air is the coolest, creating the largest temperature differential. When the concrete is placed in the late afternoon or early evening, the hydration temperatures build while the air temperatures and solar radiation are lower. This restricts the rate at which the deck heats up, so that the peak concrete temperature is reduced and does not occur until approximately 24 to 30 hours after placement, when the daytime air and solar radiation are near or just past their peak. These different rates of heat development could have potentially significant effects on the stresses that are generated in the decks.

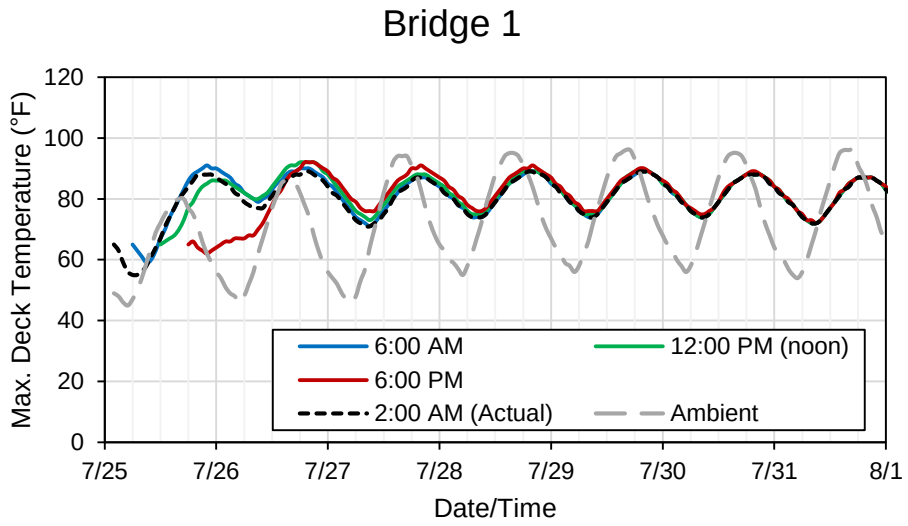

Figure 14. Example of temperature simulations. Maximum deck temperature simulated for Bridge 1 in ConcreteWorks for various placement times.

Stress Model

To simulate the stresses generated in the bridge decks under various thermal and shrinkage strains, a basic stress analysis model was developed in Mathcad, based on the analysis of W. Zuk.[13] The model first separates the deck into three horizontal sections (Figure 15) and calculates the free (unrestrained) strain in the girder and in each section of the deck due to a specified linear temperature or shrinkage profile over the section. For thermal strains, the free strains are calculated from the temperature profiles as:

$$\begin{pmatrix}\epsilon_{top}\\ \epsilon_{bot}\end{pmatrix}=\alpha\begin{pmatrix}\Delta T_{top}\\ \Delta T_{bot}\end{pmatrix}$$

where $\varepsilon_{top,\ bot}$ are the free strains at the top and bottom of the section, respectively, α is the coefficient of thermal expansion for the material, and $\Delta T_{top,\ bot}$ are the temperature change in the top and bottom of the section, respectively, relative to an initial, strain-free temperature T_0.

After calculating free strains in each section, the model then applies compatibility requirements to force equal strains and curvatures at all deck/deck and deck/girder interfaces. The shear forces and moments required to maintain this compatibility are calculated and then used to determine the overall stresses developed at the top and bottom surfaces of the deck under the applied thermal and shrinkage profiles.

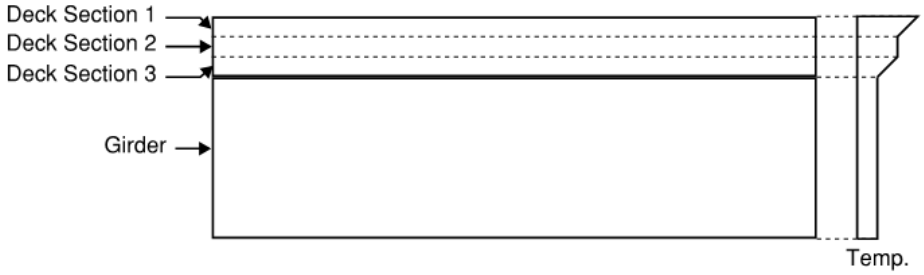

Figure 15. Sketch of sections used in stress model. A possible temperature profile is shown to the right.

Three models were developed to simulate the thermal and shrinkage stresses generated in Bridges 1, 2, and 6. A parameter sensitivity study was conducted using the Bridge 1 model to determine which factors most influence the development of tensile stresses in the decks. Additional simulations were performed on all three bridge decks to investigate early-age and long-term stress development under various temperature and shrinkage profiles.

Appendix B presents the parameters included in each model and defines the values assumed for each simulation. The thermal and mechanical properties used in the simulations were either obtained by physical testing on cores or assumed based on prior experience. Creep of the deck concrete is implicitly included in the model by reducing the elastic modulus of the young concrete by one-half and the mature concrete by one-third. The creep adjustment factor reduces the stresses estimated for the bridge deck to account for stress recovery under sustained loads.

For early-age concrete, the tensile strength was assumed to be approximately 10 percent of the assumed compressive strength; for mature concrete, the tensile strength was assumed to be approximately the value measured for the laboratory cores. In both cases, the concrete was considered “at risk” for cracking if the tensile stresses in the deck exceeded 80% of the tensile strength, due to the effect of fatigue.

Sensitivity Analysis

A parameter sensitivity study was initially performed using the model for Bridge 1. Factors investigated include the compressive strength of the deck concrete, the thickness of the deck, the spacing of the girders, the magnitude of autogenous and drying shrinkage, a uniform temperature change in the deck and beam, and a linear temperature change through the deck. Each factor was varied independently, and the resulting stresses in the top and bottom of the deck were evaluated. A complete summary of the sensitivity analysis is provided in Appendix D. The key findings are summarized below:

- The compressive strength (elastic modulus) of the deck concrete has a small effect on the stresses that are developed. While doubling the compressive strength of the deck concrete approximately doubles its tensile strength, it only increases the thermal stresses in the deck by an estimated 20-25%. This implies that the risk of thermal cracking is the greatest at early ages, when the magnitude of the thermal stress is large relative to the tensile strength of the concrete.

- Thermal and shrinkage stresses are larger in thin decks than in thicker decks. A 2-inch increase in the thickness of the deck (e.g., from 6 inches to 8 inches) can reduce the magnitude of thermal and shrinkage stresses generated in the deck by 10 to 25%.

- Thermal and shrinkage stresses are larger in bridge decks with more closely spaced girders, influencing deck stresses by about 10 to 20%.

- The initial temperature rise caused by the heat of hydration generates compressive stresses in the deck. Tensile stresses are generated only after the deck has cooled below its strain-free temperature, T_0. Larger stresses are generated in the deck by temperature gradients than by uniform temperature changes, increasing stresses by about 30%. This highlights the importance of early age cooling and temperature gradients.

- Autogenous shrinkage is a potentially significant contributor of tensile stresses in young concrete. An autogenous shrinkage of 40 microstrain generates tensile stresses of approximately 30 psi in the deck of Bridge 1, or about 20% of the assumed early-age tensile strength of the deck concrete.

- Drying shrinkage is the largest contributor of tensile stresses in mature concrete but would not be expected until after wet curing is complete. A uniform shrinkage of 500 microstrain generates tensile stresses of 413 and 477 psi in the top and bottom of the Bridge 1 deck, respectively, or approximately 60% of the measured splitting tensile strength of the deck concrete.

DISCUSSION

This investigation was developed and implemented in order to provide a focused, practical approach to determining the cause(s) of bridge deck distress and to provide reasonable recommendations. Hands-on field observations; laboratory evaluations of concrete cores; and analytical modeling of the bridge decks provided a comprehensive understanding of the distress. Each, on an individual basis, may or may not provide a complete understanding of the observed distress and subsequent resolution to the cause(s). The following discussion presents the observed conditions of the investigated bridge decks, and how it relates, or doesn't relate, to the observed penetrations in the bridge decks. Where appropriate, specific field conditions are presented along with any field, laboratory, and analytic supporting evidence of any opinions on the observed conditions. This discussion concludes with a narrative on the likely crack progression that

leads to penetrations in the deck along with the likely cause(s). In this discussion, characteristic transverse cracks are defined as cracks similar to the cracking that has led to deck penetrations.

Plastic Shrinkage Cracking

Plastic shrinkage cracking was observed on all of the inspected bridges, with varying degrees of severity. The primary cracking pattern on Florence East (Bridge 1) was related to plastic shrinkage cracking (Figure 16). This bridge likely has the highest density of plastic cracks. Core 1D was extracted over a plastic crack, and petrography showed this plastic crack extended to a depth of 3 inches mostly propagating around aggregate particles. Crack width was estimated to be less than 15 mils. Core 2B, 2G, and 3A, were also extracted over plastic cracks, and crack depths varied from 1 to 2 1/2 inches with tight crack widths (less than 15 mils). The plastic cracking in Florence East is likely more pronounced because of the inclusion of silica fume (6 % replacement rate); fly ash (25 % replacement rate); and low as-placed w/cm (estimated to be 0.38 to 0.43); thereby reducing the bleeding rate and quantity of available bleed water. In addition, the fly ash will slow the setting characteristics, prolonging the period of time the concrete is in a plastic state.

Even though plastic shrinkage cracking was noted on all of the bridge decks, it is not a major contributing factor to the observed penetrations in the bridge deck. Plastic cracks were not observed at the locations deemed potential susceptible to future deck penetrations. Early-age placement and concrete surface protection procedures and adjustments to mixture proportions, as discussed in the recommendation section of this report, will aid in the mitigation of plastic shrinkage cracks.

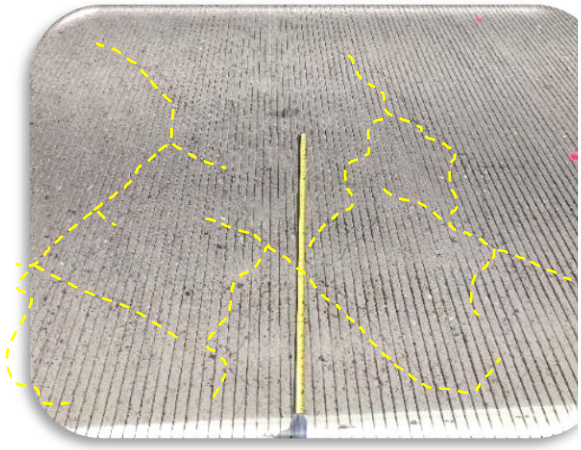

Figure 16. Plastic shrinkage cracks noted on Bridge 1 (Florence East). Note random, "map cracking."

Figure 17. Plastic cracking observed on Bridge 2 (Lozeau Tarkio, MP 57.412 EB).

Materials Related Distress

No evidence of any materials related distress was noted in any of the cores examined petrographically. This eliminates freeze/thaw, alkali silica reactive (ASR), D-Cracking, or poor aggregate durability as contributing causes. Freeze-thaw distress would include micro-cracking in the cement paste and/or aggregates. This was not noted near or away from any of cracked cores extracted from the bridge decks. In general, the w/cm, air void characteristics, and aggregates were found to be consistent with good freeze/thaw durability. For the exposure conditions of these Montana bridge decks, a w/cm less than 0.45

and air contents from 5.5 to 8.0 percent would typically be adequate for freeze/thaw resistance in a saturated condition. ASR distress initiates with the formation of silica gel around aggregate particles. This gel absorbs water and expands, which may result in aggregate and paste cracking. These ASR distress mechanisms were not noted in any of the cores. For ASR distress to occur, the following three components have to be present: a reactive aggregate, moisture, and sufficient alkalis. For the Montana bridge deck concrete, based on the petrography performed by WJE, the majority of the aggregate particles are likely non-reactive. A few reactive particles were noted in concrete from Bridge 6, Henderson West MP 22.013, but these only represent a very small number of particles and are deemed insignificant to manifest ASR distress.

Prior to the WJE's field investigation, some discussion was made about the possibility of magnesium chloride contributing to the observed distress. Based on discussions with MDT, the deicer most commonly used on the investigated bridges is magnesium chloride. Magnesium chloride can cause a chemical degradation of the cement paste by attacking the hydration products (CSH). Under certain conditions, this chemical attack can be quite severe. As noted in the investigation portion of this report, petrography and scanning electron microscopy (SEM) were performed on sections of fell concrete from Bridge 2 (Lozeau - Tarkio MP 57.421). The goals of these initial studies were to aid in the development of WJE's subsequent investigation and to assess any potential materials related distress. Studies found the concrete to be sound; free of internal distress; free of secondary deposits; and sound aggregates. The concrete had an estimated w/cm of 0.46 to 0.51 (specified 0.36) with an air content ranging from 9 to 12 percent. Even with the higher w/cm and air contents, no materials related distress was noted. Further, SEM studies were performed on a white glaze that was observed coating the reinforcing steel imprints and on fractured surfaces (Figure 18). SEM revealed the glaze was likely leachate from the cement paste, a common occurrence from water migration through concrete and not an indicator of any distress mechanisms. No evidence of chemical attack from the use of magnesium chlorides was noted in the petrography or SEM studies. The use of magnesium chloride is not contributing to the observed bridge deck distress that leads to deck penetrations.

Figure 18. Arrows showing white glaze in the imprint of the reinforcing steel, 6 times magnification.

WJE did observe variable air content and w/cm in most of the examined cores (Table 11). The air contents range from 4 to 12 percent for the cores analyzed. Since the air content is variable on the high end, the

primary compromise would be to the strength of the concrete and some reduction in bleeding. Based on the strength data received from MDT (Appendix B), the measured 28 day strength generally exceeds the specified strength of 4,500 psi. The estimated w/cm ranged from 0.38 to 0.51, commonly higher than designed. The high and variable w/cm could have an impact on the observed cracking. An increase in water content (increase w/cm) will increase the drying shrinkage potential of the mix; therefore, increase the potential for transverse cracking. With a higher drying shrinkage, the strains associated with natural drying would be higher, creating higher tensile stresses in the deck concrete. The high water content and the high air content will reduce the concrete tensile strength needed to resist the stresses. Tighter quality control policies are likely needed to limit this variability. This would include more frequent checks of the air content; checking air content at the point of placement; and prohibiting or limiting site-added water.

Table 11. Air Content and Estimated W/CM

Core ID	Air Content (%)	Estimated w/cm	Designed w/cm
1D	11.5	0.38 to 0.43	0.42
1I	9 to 12	0.38 to 0.43	0.42
2C	11.5	0.46 to 0.51	0.36
3A	6 to 9/ 5 to 6*	Not examined	0.40
3B	6 to 8/ 4 to 6*	Not examined	0.40
6G	6 to 9	0.42 to 0.47	0.39
10B	10 to 12/ 4 to 6	0.45 to 0.50	0.39
12A	5 to 8	0.45 to	***
Concrete Fragments - Bridge 2	9 to 12	0.45 to 0.50	0.36

*Top number represents overlay concrete/ bottom number represents substrate concrete
**Some values are measured values per ASTM C457 and some are estimates
***No mix design provided

Subsidence

The following cores were extracted directly over top mat reinforcing steel: 1F, 1I, 2C, 6A, and 12C. Cores 2C, 6A, and 12C were specifically selected because of the characteristic transverse crack that has potential for future distress (deck penetrations). None of the cores show any evidence of settlement related cracking. Typically, a settlement crack would be directly above the reinforcing steel, with characteristics of plastic tearing of the paste. Also, voids underneath the reinforcing steel are very common with plastic settlement cracks. None of these characteristics were noted. The deeper concrete cover (specified 2 3/8 inch) and relatively small reinforcing bars (No. 4s and 5s) were helpful in preventing subsidence cracking. Subsidence is not a primary contributing cause to the potential for deck penetrations.

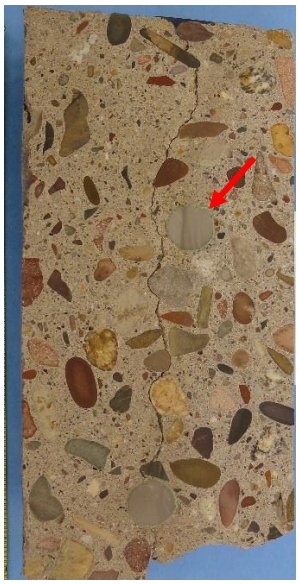

Figure 19. Lapped section of Core 22, extracted on a transverse crack directly over a reinforcing steel bar (red arrow).

Figure 20. As-received condition of Core 1I, extracted on a transverse crack directly over a reinforcing steel bar (red arrow).

Corrosion

No evidence of corrosion was noted on any of the epoxy coated reinforcing steel. All reinforcing bars were in good condition. No corrosion products were observed on any of the bars or imprints in the concrete. Furthermore, corrosion damage typically creates delamination at the level of reinforcing steel. There were very few delaminated areas identified by chain dragging, which was consistent with the low frequency of delaminated areas identified by infrared camera and impulse response surveys. Corrosion staining was noted on the underside of one bridge, Bridge 8, Henderson-East MP 24.603. No cores were extracted from this bridge, and further investigation would be needed to assess the significance. Based on the cores taken over the characteristic transverse cracks, reinforcing steel corrosion is not a contributing factor for the observed deck penetrations.

With this being said, the chloride levels in the concrete at the level of reinforcing steel (approximately 2 3/8 inch) exceed the typical threshold for corrosion initiation of uncoated reinforcing - 0.020 to 0.030 percent by mass of concrete (Table 12). Based on the relatively young age of the bridge decks (nine years for Bridge 6 and six years for Bridge 10), the chloride levels are higher than anticipated. Of interest, the chloride levels near cracks were not appreciably higher than chloride levels away from cracks. Based on the evidence of efflorescence on the underside of these two bridges, significant moisture movement has occurred through the transverse cracks. It is expected that the chloride levels would be higher near the cracks, because the moisture movement through the cracks would likely carry deicer solution. Further investigation is needed to assess the effect of the cracking on deck service life.

Table 12. Chloride Levels at Depth of Reinforcing Steel

Sample	Chloride Levels	Typical Threshold Uncoated Steel
6A - Near Crack	0.171	0.02 to 0.03
6A - Away from Crack	0.205	0.02 to 0.03
10E - Near Crack	0.070	0.02 to 0.03
10E - Away from Crack	0.045	0.02 to 0.03

Overlay Bridge Decks

Instead of full deck replacements, three investigated bridge decks included overlays, Bridges 3, 7, and 9 (WB Lane). These overlays consisted of 2 1/2 inches of latex modified concrete (lmc) or silica fume concrete and were constructed in 2011, 2008, and 2009, respectively. These overlays were applied to existing concrete decks, with the top two (2) inches removed, that were originally constructed in 1967, 1980, and 1979, respectively.

The overlay condition appears to be good for these bridges. The delamination surveys yielded little to no hollow sounding areas, indicating bond between the overlay and substrate still exists. This was further substantiated by the petrography performed on cores 3A and 3B, which revealed the overlay to have adequate adhesion to the substrate. Performance and longevity of overlays are primarily determined by bond to the substrate. Therefore, it is anticipated that these overlays will continue to perform well.

Plastic shrinkage cracks were noted on all overlays; with Bridge 3 having substantially more map cracks (Figure 21). The width of plastic cracks in the overlays appeared to be much tighter than the non-overlay bridges.

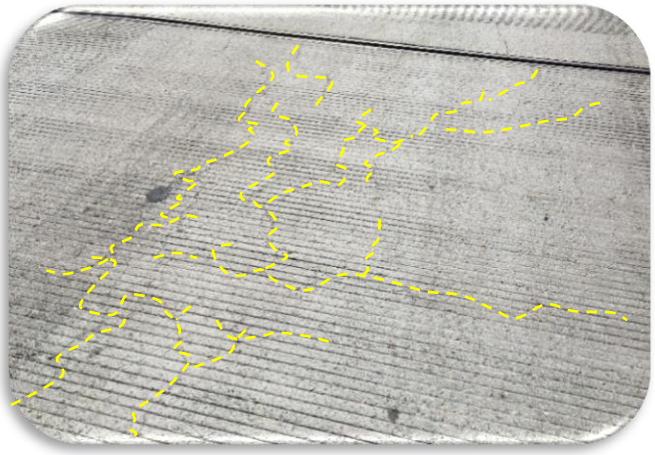

Figure 21. Map cracking noted in the overlay of Bridge 3. Cracks are very tight, but frequent. Dotted yellow lines help identify crack locations

The transverse cracks observed on the overlay bridges were much less pronounced than the non-overlay bridge decks, with less frequency and tighter crack widths. No indication of the characteristic transverse cracks leading to deck penetrations was noted on the overlay bridges. Based on the petrography performed on Cores 3A and 3B, the transverse cracking appears to be unique to the overlay and not reflecting from

the substrate concrete. On the contrary, longitudinal cracking appears to reflect from the substrate concrete. The longitudinal cracking appears most frequently over the girders. The underside decks had little to no observed transverse or other cracking and very little efflorescence compared to the other non-overlay bridges (Figure 22). This would indicate that the transverse cracking is likely much tighter than other bridge decks and/or does not propagate through the entire thickness.

Figure 22. Underside of Bridge 3. Little to no transverse cracking was observed.

Transverse Cracking

The focus of the following discussion will be on the likely cracking pattern and progression that leads to the observed deck penetrations. Prior to discussing the relevant field and laboratory observations, the documentation provided by MDT prior to the investigation yielded useful information. The deck penetrations were occurring on bridges with varying mixture proportions; girder type, design and spacing; contractors; and span lengths. In reviewing photographic documentation of the previous hole penetrations (provided by MDT - Figure 23 and Figure 24), the following important observations were made:

- Each penetration had closely spaced transverse cracks leading up to the penetration and outlining the perimeter.
- The characteristic transverse cracks appeared to have occurred directly over transverse reinforcing bars and have experienced significant raveling. Raveling is described as erosion of the crack edges due to traffic loading.
- A semi-longitudinal crack likely formed and connected the two transverse cracks. This crack is referred to as the "jump" crack.
- The top and bottom mat of transverse reinforcing steel bars appear to be aligned, i.e. in the same vertical plane.

Figure 23. Deck penetration noted by MDT, Lozeau-Tarkio

Figure 24. Deck penetration noted by MDT, Superior Area Structures

Many concrete bridge decks develop transverse cracking, with some transverse cracking occurring at early ages (within 3 days) and some at later ages. Typical spacing of transverse cracks are 5 to 10 ft.[4]. During WJE's field investigations, very closely spaced transverse cracks, 6 to 18 inches, were noted on occasion. WJE observed closely spaced transverse cracks on Bridges 2, 5, 6, 8, 9, 10 and 12, with varying degrees of severity (Figure 25 and Figure 26). These cracks were identified as characteristic transverse cracks that may lead to future deck penetrations.

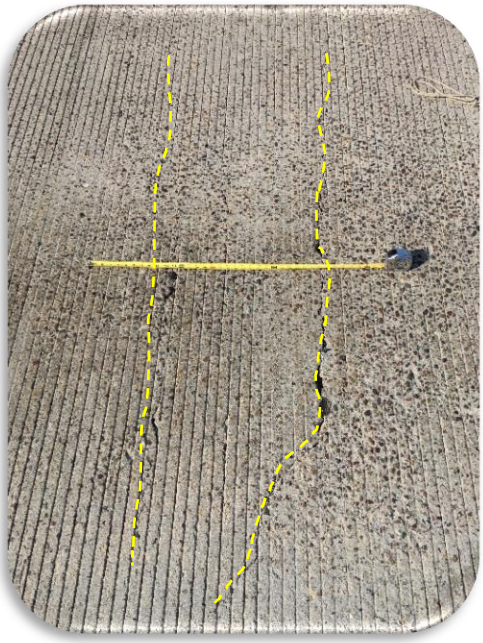

Figure 25. Closely spaced transverse cracks, Bridge 11, transverse cracks running up and down on the photo.

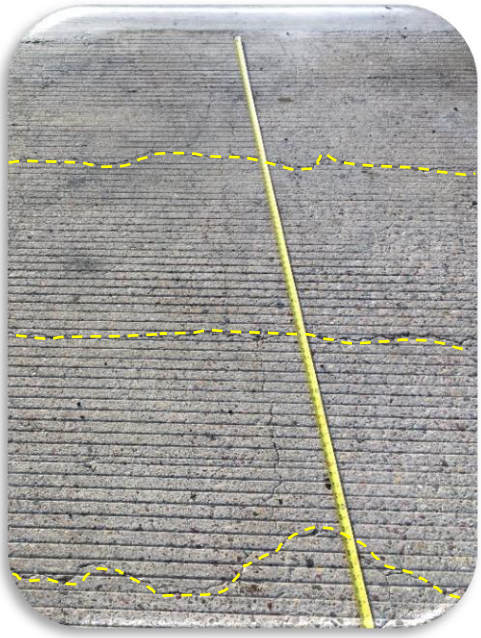

Figure 26. Closely spaced transverse cracks, Bridge 2, transverse cracking running left to right on photo.

Early and late stages of the crack progression were identified and documented. The early stages are characterized by closely spaced early-age transverse cracks that propagate from adjacent girders. Girders provide local restraint to the composite deck, and calculated stresses are highest at the girder location. As the deck concrete shortens due to temperature changes or drying shrinkage, longitudinal movement is restrained by the girders and fine cracks initiate immediately above or adjacent to the girder interface. Cracks align with transverse reinforcing bars since they represent a weakened plane or notched section, especially when top and bottom mat bars are aligned. Global stress conditions typically cause crack initiation over girders to occur in the same area (station) and along a single transverse bar. Fine transverse cracks originate at the girders then propagate transversely to connect in the span between girders. A single transverse crack across the entire deck width results. However, cracks sometimes originate over adjacent girders at slightly different stations along the bridge length and propagate along different adjacent transverse reinforcing bars. As the cracks propagate between girders, these cracks may be offset by only 6 to 18 inches. As these transverse cracks propagate with time (due to temperature cycles and drying shrinkage) to meet between adjacent girders, a "jump" crack from one of reinforcing bars to the other forms connecting the two adjacent transverse cracks. The early stages of this cracking were noted on the Thompson River Bridge (Figure 27). During the early stages of crack progression, the "jump" crack does not extend the total thickness of the deck, based on petrography of Core 12A, from Thompson River Bridge. The crack depth was measured to be 4.5 inches, just over half the deck thickness. Core 12C was taken over the transverse crack adjacent to 12A. The transverse crack was wider on the surface; propagated the entire deck thickness; and was tighter on the bottom. This indicates greater top strain than bottom strain.

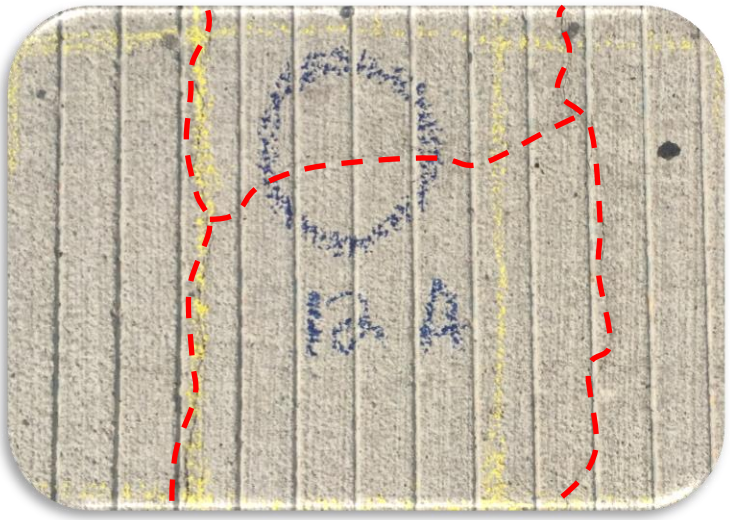

Figure 27. Photograph showing early age development of cracking - Thompson River Bridge. Dotted red lines accentuate the tight transverse and "jump" crack. All cracks were less than 5 mils in width. Core 12A was extracted over the "jump" crack.

With time, the characteristic transverse cracks widen and ravel, as noted on Bridges 2, 6, 8, and 10. The widening of the crack is expected due to continued drying shrinkage and thermal effects. The raveling of the crack likely occurs because of vehicle loading of the edges of the crack, eroding the shoulders. Diurnal temperature changes likely play a role in opening and closing of the cracks and subsequent raveling. The continued movements of the transverse cracks, helps propagate the "jump" cracks through the deck

thickness, which is characteristic of the later age crack progression (Figure 28 through Figure 31). With continued traffic loading and volumetric movement, the section of concrete encompassed by the transverse and "jump" cracks loses aggregate interlock, essentially being unreinforced, and disengages. When the top and bottom mats of steel are aligned, this allows concrete to dislodge and fall. During field investigations, the mobility of the deck was measured using impulse response. The higher measured mobility between the girders helps explain the occurrence of "jump" cracks and that through-deck failures are most likely to occur mid-way between girders.

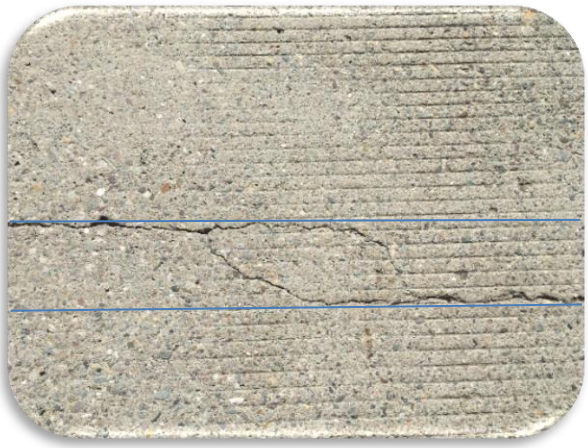

Figure 28. Top side of Bridge 6, showing transverse cracking and "jump" cracks between rows of reinforcing.

Figure 29. Underside of Bridge 6, same location as Figure 28.

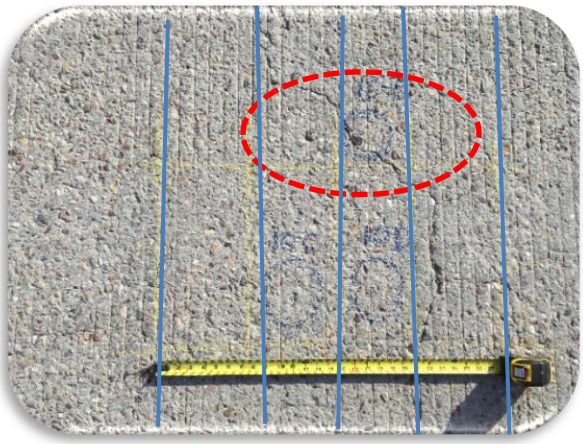

Figure 30. Bridge 10, transverse cracking with "jump" crack, prior to extraction of Core 10 B. Note jump crack crosses two transverse bar lines (blue/yellow lines).

Figure 31. Bridge 10, left side showing early stages of transverse deck cracking (no through thickness "jump" cracks). Right side of photograph showing underside of Figure 30, later stages of "jump" crack between transverse deck cracks.

Based on the field investigation, petrography, and the modeling, tightly spaced transverse cracks are primarily caused by restraint of early-age thermal movement. These early-age transverse cracks are a major contributing factor to the crack progression that leads to deck penetrations. The early-age development of the transverse cracks were identified based on the following:

- Petrography performed on characteristic transverse cracks, Cores 1I and 2C, showed signs of very early age crack initiation. Early crack initiation is characterized by meandering cracks around aggregates without any distinct fractures. The studied cores also show wider cracks at the surface compared to bottom surface. This would imply higher strains on the top surface as opposed to the bottom surfaces, and consistent with early age cooling of the top of the slab. Propagation of the early age cracks likely continued with time due to normal drying shrinkage and thermal movement.
- MDT has noted the presence of some transverse cracks after removal of wet-curing. Wet curing is typically removed after 14 days.
- The sensitivity study performed to determine early age stress on the bridge deck included the following parameters: concrete compressive strength, deck thickness, girder spacing, magnitude of autogenous and drying shrinkage, uniform temperature changes in the deck and beam, and linear temperature changes through the deck. This study showed a high sensitivity to increased stresses based on early-age thermal temperature drops. During early-age strength development, the temperature increases due to heat of hydration and is accompanied by a volume increase, which, if restrained, leads to compressive stresses in the concrete. Since the concrete is only hours old, creep quickly dissipates these stresses. The occurrence of shrinkage (normally autogenous shrinkage due to self-desiccation), which works in opposite direction to the initial thermal expansion, further lowers compressive stresses. Of much significance is the volume reduction that occurs as soon as the concrete temperature decreases after the peak hydration temperature. The volume reduction is then the sum of the autogenous shrinkage and the thermal contraction. With the mixes used for the MDT bridge decks, the thermal contraction is much more prominent than the autogenous shrinkage. Significant tensile stresses will be generated at the deck girder interfaces due to the girder restraint while the concrete is only moderately strong. These initial stresses likely cause the local early-age transverse cracks at the girder interfaces. Continued thermal cycling and drying shrinkage further propagates the cracks between girders.

Of the bridges inspected, four did not exhibit characteristic transverse cracking that would appear to lead to deck penetrations: Bridge 1 is entirely a new structure and exhibits pronounced plastic shrinkage cracks but not the tightly spaced transverse cracks. The transverse cracks on this bridge are spaced more typically at 5 foot intervals. The likely preference to this bridge deck is related to increased deck thickness, new concrete prestressed girders that shorten and creep, and possibly stress relief and redistribution due to high density of plastic cracks. Bridges 3, 7 and 9 are not new bridge decks, but all have latex modified concrete overlays and exhibited much less pronounced transverse cracking. Also, no indication of the closely spaced transverse crack was observed. However, all other bridges that had full deck replacement on older superstructures exhibit closely spaced transverse cracking.

The following table presents the severity of the transverse cracking as it relates to the possibility of future deck penetrations. Late stages of cracking, which would be characterized by full thickness “jump” cracks with efflorescence on the underside, is the primary reason for the most severe ratings. No closely spaced transverse cracks and no signs of the “jump” crack are characteristics of the least severe rating. Although impulse response testing was informative, identification of incipient deck distress and deck penetrations is more easily done by visual inspection and recognition of tell-tale indicators rather than by measuring deck mobility.

Table 13. Bridge Deck Severity Rating

Severity	Bridge No.	Location	Notes
3	6	Henderson West MP 22.013	Late stages of crack progression
3	2	Lozeau-Tarkio MP 57.472	Late stages of crack progression
3	10	Superior Area Structures MP 49.397	Late stages of crack progression
3	8	Henderson East MP 24.603	Late stages of crack progression
2	5	Lozeau - Tarkio MP 57.472	Early stages of crack progression
2	12	Thompson River MP 55 to 56	Very early stages of crack progression
2	4	Lozeau - Tarkio MP 58.550	Transverse cracking less frequent
1	9	Henderson East MP 23.325 WB	Overlay, No characteristic transverse cracking
1	11	Superior Area Structures MP 49.397	Transverse cracking less frequent
1	1	Florence - East MP 10.640	Mostly plastic, no characteristic transverse cracking
1	3	Lozeau - Tarkio MP 58.550	Overlay, no characteristic transverse cracking
1	7	Henderson - East MP 25.393	Overlay, no characteristic transverse cracking

Severity	Description
3	Late stages of characteristic transverse cracking, most likely to see future deck penetrations
2	Early stages of characteristic cracking, future deck penetrations may be avoided
1	No characteristic cracking, future deck penetrations are not likely

PRIMARY RECOMMENDATIONS FOR FUTURE BRIDGE DECKS

The following primary recommendations are presented with the goal of mitigating the potential for future early-age, closely-spaced transverse cracks in new decks. The primary recommendations presented herein are most important and effective on mitigating the early-age transverse cracks. Secondary recommendations are presented after this section as additional considerations that may be less effective but cumulatively can be important. The factors affecting early-age deck cracking are complex and multiple, but the subsequent recommendations have been proven to reduce the risk of early-age cracking by decreasing the early-age thermal volume change potential and shrinkage effects. Generally, this can be done by reducing plastic concrete temperatures; reducing early-age thermal changes and gradients; limiting autogenous shrinkage; increased deck thickness; reduce girder stiffness; increase girder spacing; and limit drying shrinkage. These recommendations have been provided based on WJE's experience with similar cracking and further substantiated by primary publications reviewed by WJE [1, 2, 3, 4, 6, 7, and 8]. The reviewed publications focus on previous DOT-funded efforts to reduce early-age transverse cracks.

Construction Practices

Curing

Characteristic transverse cracking is primarily caused by early-age thermal volume changes. Early-age thermal cracks likely developed in the first few days after placement due to temperature drops (cement hydration and diurnal temperature). Modeling of the bridges revealed a high sensitivity to these cooling effects. Modern cements are prone to high temperature increases during chemical hydration due to high C3S contents and fineness. Small cement particles, especially passing #325 sieve, are responsible for rapid cement reaction and increased heat. Choosing a cement with moderate C3S and coarse grind would be very helpful; however, such cements are no longer readily available. Curing procedures play an important role

in alleviating both early thermal and plastic shrinkage cracks. The current MDT Standard Specification, subsection 551.03.7, *Curing Concrete*, requires a 14 day wet-cure. The water cure consists of placing pre-soaked wet burlap immediately behind the concrete operations, fogging the burlap to maintain moisture until soaker hoses can be placed without marring the surface, then covering the wet burlap and soaker hoses with plastic sheeting, and maintaining a moist surface for 14 calendar days. Continuation of this practice is highly encouraged.

Control of the peak hydration temperatures and rapid temperature drop has been found to help mitigate early-age thermal cracks. Previous research suggests protection of concrete from solar radiation to reduce the temperature due to hydration as well as insulation of the bridge to reduce the rate of cooling[1]. For avoiding excessive loss of bleed water and resulting plastic cracking, researchers have found that the most effective method is the use of fogging during construction followed by rapid placement of wet curing methods[1,7]. The recommendations presented below are targeted to reduce plastic shrinkage (separate but related issue); reduce peak hydration temperatures; and lessen rapid temperature drops after peak hydration.

- ***Recommendation:*** Immediately fog mist concrete placements until wet curing media is in place to minimize surface evaporation and cool the concrete. Contractor should submit a curing plan to reduce evaporation rate. Some projects require the contractor to measure and record evaporation rates once per hour at the job site in accordance with ACI 305. As previously mentioned, ACI 305 provides methods for calculating the evaporation rate (nomograph) based on concrete temperature, ambient temperature, ambient relative humidity, and wind velocity. For field application, this would require measurement of ambient temperature and wind speed. When evaporation rates are in excess of 0.15 lb./sq. ft./hr, extra precautions may be needed such as additional fogging and early application of curing media. Fogging will increase the near surface relative humidity; reduce surface evaporation rate; and mitigate subsequent plastic shrinkage. Also, the fogging of the near surface will help reduce concrete temperatures and reduce peak hydration temperatures. Apply wet-curing as soon as possible after finish. Wet-curing should be either cotton mats or prewetted burlap, do not apply plastic that will trap heat, especially on sunny days. Continuous wetting of the mats and burlap should be performed for the entire length of wet curing. Prior to every concrete placement, pre-construction meetings should be held to discuss the required curing procedures.

- ***Recommendation:*** Apply insulation blankets after peak hydration temperatures and only after the peak hydration temperatures. After peak temperatures are achieved, blankets insulate the deck from the environment, improve strength gain, and slow the rate of cooling. This will help prevent rapid reduction in concrete temperatures and decrease early-age stress development, allowing creep time to dissipate the stresses. This requires concrete temperature monitoring during placement and while curing. Thermocouples should be installed at the beginning and end of each placement, at least 10 feet from any edge. The temperature should be monitored at four depths through the deck thickness: top of slab, top third, middle third, and bottom of slab. Thermocouples should be protected during placement and should read to the nearest 2 °F. Logging equipment should be able to record once every 15 minutes. Continue to monitor temperatures for the entire wet-cure. Within three hours after peak hydration temperatures are reached, apply cold weather insulating blankets. When concrete temperatures are within 5 °F of ambient; vertical temperatures through deck thickness are uniform (within about 10 °F); and concrete is a minimum of 72 hours old (or 96 hours old if concrete contains silica fume), remove all curing and allow deck to dry. After the surface has dried, white-pigmented curing compounds may be applied. The curing compound will slow the initial rate of drying and shrinkage and the white pigment will reduce peak diurnal temperatures of the deck surface by about 10 °F.

Placement Times

The modeling performed by WJE showed that placement times and diurnal temperatures had a significant effect on the potential for early-age transverse cracking. Figure 32 shows simulated deck temperatures for Bridge 6. Concrete placement times were simulated at 6 AM, 12PM (noon), and 6PM. The initial peak hydration temperatures for the 6AM simulation and actual 7AM placement are approximately 15 hours after placement. The initial peak temperatures for the 12 PM and 6 PM placements shift to 30 hours. At this later age, the concrete has developed additional tensile strength and will be more resistant to stresses developed during cooling. For this reason, early-age cracking is expected to be mitigated. In addition, the modeling shows that the concrete peak temperatures and associated cooling are affected by the ambient conditions. The peak ambient temperatures will exacerbate the peak concrete hydration temperatures and thereby accelerate cooling. Other researchers have provided similar recommendations on placement times and maximum diurnal temperature changes such as: avoiding large temperature variation on the day of concrete placement, greater than 50 °F[7]; best results for mitigation of transverse cracks when ambient temperatures varied between 65 to 70 °F (highs) and 45 to 50 °F (lows)[2]; and avoid morning and early afternoon placements and use later afternoon and evening placements[4].

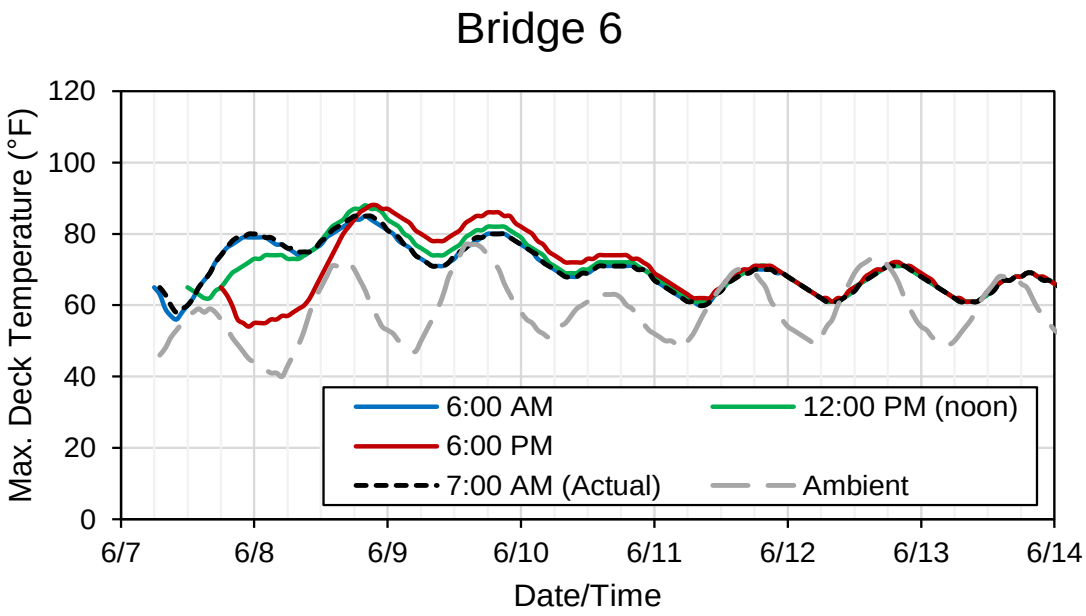

Figure 32. Temperature simulations for Bridge 6.

- ***Recommendation*** - Move concrete placement times to late afternoon or evening; preferably from 4 to 8PM. This recommendation is based on not allowing peak concrete temperatures to coincide with cooling evening ambient temperatures and on increasing the concrete strength prior to the cooling period. This recommendation assumes similar concrete mixes will be used in the future.

Plastic Concrete Temperatures

Reducing concrete temperatures will decrease hydration rates and lower the early hydration temperature cycle; resulting in lower thermal stresses and decreased risk of transverse cracking. The risk is minimized when concrete temperatures are as low as possible. If possible, delivered concrete temperatures should be kept

cooler than ambient air temperature. This may require concrete suppliers to shade stockpiles, sprinkle aggregates, or use chilled water or ice. The following recommendations have been researched by others: use a maximum concrete temperature of 80 °F for bridge deck construction[7], concrete temperatures should be below 85 to 90 °F[2], cast concrete 10 °F cooler than ambient, except when temperatures are below 60 °F, then they should be cast at ambient[4].

- ***Recommendation*:** Limit plastic concrete temperature at the time of placement, ideally to below 75°F when able. The cooler the concrete the better. Discuss with concrete suppliers how to minimize concrete delivery temperature by adding chilled water or ice and/or modifying aggregate storage practices. Aggregate stockpiles can be wetted or shaded to reduce aggregate temperatures and resulting concrete temperatures.

Design Considerations

Deck Thickness

With non-linear temperature and shrinkage gradients, thinner concrete decks will develop higher stresses. From the modeling performed on the MDT bridge decks, thermal and shrinkage stresses are larger in thin decks than thicker decks, especially at early ages. A 2-inch increase in the thickness of the deck (e.g., from 6 inches to 8 inches) can reduce the magnitude of thermal and shrinkage stresses generated in the deck by 10 to 25 percent. In research funded by Michigan DOT, the researchers surveyed 31 DOTs and found the most common bridge deck thickness was 8 inches[1]. Less than 10 % of the states used bridge decks less than 8 inches. Researchers also found 6 1/4 inch thick decks were observed to result in increased transverse cracking[2].

- ***Recommendation:*** Increase design deck thickness to 8 inch minimum.

SECONDARY RECOMMENDATIONS

Design Considerations

Top and Bottom Mat Placement

Often the top and bottom mat of reinforcing steel were found to be aligned at the locations of deck penetrations.

- ***Recommendation***: Modify specifications to require staggering of top and bottom transverse bar mats. Ensure quality control procedures to ensure proper placement.

Materials and Quality Control

Cementitious Content

The amount of cementitious materials will affect the amount of shrinkage and heat of hydration. Higher cementitious contents will shrink more and have a higher heat of hydration. Both of these will increase volume change potential and result in higher risk to transverse cracking. A reduction in cementitious materials can be beneficial assuming workability and cohesiveness are maintained. For the mix designs used for the MDT investigated bridges, the cementitious contents ranged from 525 to 658 lb./yd^3. While not an excessive amount, any practical reduction in total cementitious content will reduce the risk of cracking. Previous recommendations have included a maximum cementitious content of 650 to 660 lb./yd^3 [2]; use a cement content as low as possible[1]; and more strict recommended limits of 470 lb./yd^3.[7]

- ***Recommendation*** - Limit cementitious content to 600 lb./yd^3.

Cementitious Materials

The mixes exhibiting cracking varied widely and supplemental cementitious materials did not appear to be a primary factor. However, caution is needed for mixes containing silica fume, especially at replacement doses above 5 percent.

- ***Recommendation*** - Limit silica fume replacement to 5 %. Work with suppliers to ensure proper batching and mixing of silica fume. Densified silica fume needs be broken down and dispersed during the mixing process in order to be perform effectively. During concrete batching, whether central mixed or truck mixed, the addition of silica fume should be done after the addition of the coarse aggregate and with 25 percent of the water, mixing for 30 seconds prior to the addition of the remaining constituents. This will help break up the densified silica fume and disperse it evenly. At a minimum, total mixing should include 120 revolutions at 15 revolutions per minute, and often mixing times may have to be increase by 10 to 20 percent over the required times in ASTM C94. Trial batches are recommended to ensure proper batching and mixing procedures. The procedures in ASTM C94, Section 12, can be used to verify adequate mixing times, and concrete can be observed petrographically for the presence of any agglomerates of silica fume. ASTM and ACI also recommend not exceeding 63 percent of the mixer capacity for truck mixes and 75% for central mixed concrete when using silica fume.

Water to Cementitious Ratio

For bridge deck concrete, there is a balance of having a too low and too high of w/cm. Too low of w/cm will promote autogenous shrinkage; plastic shrinkage cracking; high modulus, and reduce creep. A w/cm below 0.40 has been found to promote autogenous shrinkage which would increase the tendency for transverse deck cracking. With too high of a w/cm, the long term durability of the concrete will be compromised; reducing freeze/thaw durability and increasing chloride ingress (corrosion). Previous researchers have recommended the following: use a w/cm not lower than 0.40[6]; use of optimum w/cm range of 0.35 to 0.50[1]; and limit w/cm to 0.40 to 0.45[7].

- ***Recommendation*** - Specify the w/cm for deck concrete of 0.42 to 0.45. Ensure ready mix suppliers measured aggregate moisture contents and adjust water weights appropriately. Control water addition at the site to conform to this recommendation.

Aggregate Optimization

Increasing the aggregate volume and optimizing the aggregate gradation beneficially reduces the paste content of concrete mixes. Typically, concrete with higher aggregate contents and lower cement paste contents are less likely to develop cracks. Leaner mixes are also thermally less expensive and develop smaller thermal stress. Optimization programs have been developed at Oklahoma State University, www.optimizedgraded.com and Kansas University (KUMix) among others. However, the local aggregates are very hard, usually rounded, siliceous aggregates. The bond between the cement paste and the aggregates

is weak and slow to develop. This was evident during the splitting tensile strength performed on cores that were greater than 6 year old, the failure plane avoided aggregates more than 50% of the time. Good bond between the aggregates and paste are important for tensile strength of the concrete, especially at early ages.

- ***Recommendation*** - Evaluate the effect of optimizing aggregate grading on the cracking tendency and tensile strength development of local concrete mixes. Evaluate the effect of using part crushed stone on cracking.

REPAIR CONCEPTS

These repair concepts are presented to assist MDT on repair decisions moving forward. Prior to implementation of any repairs, we recommend further chloride analysis be performed on bridges from each severity category. As mentioned in the discussion, chloride levels at the level of top mat steel were higher than the accepted corrosion threshold for *uncoated* reinforcing steel. Even though no corrosion has been noted, these levels would be expected to eventually lead to corrosion of the *epoxy coated* reinforcing steel, especially at the location of cracks. The results of the chloride analyses may significantly weigh MDT's decision to add an overlay or seal the cracks. Overlays may result in the longest service life for the least cost. The repair strategies are presented based on the severity category assigned to each bridge. The assigned bridge ratings should not be considered fixed, but can be used to guide MDT. The exact costs of these options have not been determined by WJE.

Severity	Bridge No.	Notes
3	6	Late stages of crack progression
3	2	Late stages of crack progression
3	10	Late stages of crack progression
3	8	Late stages of crack progression
2	9	Early stages of crack progression
2	5	Early stages of crack progression
2	12	Very early stages of crack progression
2	4	Transverse cracking less frequent
1	11	Transverse cracking less frequent
1	1	Mostly plastic, no characteristic transverse cracking
1	3	Overlay, no characteristic transverse cracking
1	7	Overlay, no characteristic transverse cracking

Risk Category 3

Identify and document all cracks that have late stages of crack progression. Documentation should include photographs, location on plan drawings, and description. Late stages would be defined as full depth "jump" cracks and closely spaced transverse cracks, 6 to 18 inches. Collection of efflorescence on the underside would be an indication of full depth cracks. Raveling of the closely spaced transverse cracks would also be an indication of late stages of crack development. Perform full deck replacement, MDT Class B repairs, of all areas identified as showing signs of late stages of crack progression. Full deck repairs should extend from centerline of girder to girder and at least 1 foot beyond the two characteristic transverse cracks. Remove concrete per MDT Section 562.03.04. Monitor performance of repairs. After completion of full-deck repairs, the following additional crack repair options should be considered:

Additional Crack Remediation - Option 1 - Crack Sealing

For all other cracks, gravity feed all other transverse cracks with high molecular weight methacrylate (HMWM) resins or epoxy resins, or epoxy injection. In order to demonstrate effectiveness of the material and procedures, trial repairs are recommended on all bridge decks. The effectiveness shall be assessed by extracting cores over the cracks. Filling of the cracks shall be assessed by measuring depth of penetration. Generally, a 1 inch penetration or greater indicates reasonable protection. Continue to monitor progression cracks. At least once per year, inspect and document performance of repairs and progression of cracking.

Additional Crack Remediation - Option 2 - Overlay

Bonded overlays can provide good protection to decks with many cracks. They also reduce the permeability and provide a new wear surface. Overlays will normally added structural capacity, but may add dead load. These have to be considered. The top 1 1/2 inches of existing concrete should be milled removing the chloride contaminated concrete. The depth of milling should be at least 1 inch above the concrete cover. A 2 1/2 inch latex modified concrete overlay should be applied. LMC is more prone to plastic shrinkage cracking, so early age curing is imperative.

Risk Category 2

For this category, full deck replacements are not recommended at this time.

Crack Remediation - Option 1 - Crack Sealing

For all other cracks, gravity feed all other transverse cracks with high molecular weight methacrylate (HMWM) resins or epoxy resins, or epoxy injection. In order to demonstrate effectiveness of the material and procedures, trial repairs are recommended on all bridge decks. The effectiveness shall be assessed by extracting cores over the cracks. Filling of the cracks shall be assessed by measuring depth of penetration. Generally, a 1 inch penetration or greater indicates reasonable protection. Continue to monitor progression cracks. At least once per year, inspect and document performance of repairs and progression of cracking.

Crack Remediation - Option 2 - Overlay

Bonded overlays can provide good protection to decks with many cracks. They also reduce the permeability and provide a new wear surface. Overlays will normally add structural capacity, but may add dead load. These have to be considered. The top 1 1/2 inches of existing concrete should be milled removing the chloride contaminated concrete. The depth of milling should be at least 1 inch above the concrete cover. A 2 1/2 inch latex modified concrete overlay, polymer overlay, or other structural overlay should be applied.

Risk Category 1

Perform routine maintenance and continue to monitor.

APPENDIX A - BRIDGE INFORMATION

BRIDGE 1: FLORENCE-EAST, MP 10.640

Bridge ID # S00203010+06401
Date investigated: August 22, 2016
Investigation type: In-depth

Bridge Description

The Florence-East bridge over the Bitterroot River (MP 10.640) is a 378 ft., 3-span bridge with a prestressed concrete beam superstructure. The bridge was constructed in 2014.

The Class SD mixture used for the deck (Table 1) was provided by LS Jensen Ready-Mix Company and was designed with a water-cementitious materials ratio (w/cm) of 0.42. The mixture contained partial substitution of cement with Class C fly ash (28% by wt.) and silica fume (6% by wt.). Air entrainment was used to provide a target air content of 6%. The 28-day compressive strength was designed to be a minimum of 4500 psi.

Table 1. Florence - East, Class SD concrete

Material	Batch weights, per yd^3 at SSD	Source
Water	217 lb (26 gal)	Well
Cement	345 lb	Ash Grove Type I-II-V
Fly Ash, Class C	146 lb	ISG Resources, Inc.
Silica Fume	30 lb	MasterBuilders Rheomac SF 100
Coarse Aggregate	1821 lb	LS Jensen, Mullan Pit
Fine Aggregate	1299 lb	LS Jensen, Mullan Pit
Air Entrainer	8.5 fl. oz.	MasterBuilders AE 90
Water reducer (mid-range)	53 fl. oz.	MasterBuilders Polyheed 1020
Water reducer (high-range)	11 fl. oz.	MasterBuilders Glenium 3030 NS
Retarder	30 fl. oz.	MasterBuilders Delvo Stabilizer

The deck was designed with an 8” depth, 2 3/8” concrete cover to the top mat reinforcing bars, and 1” cover to the bottom mat reinforcing bars. Transverse reinforcement is specified as #5 epoxy-coated steel with 7 1/4” spacing in both the top and bottom mats. Longitudinal reinforcement is specified as #4 epoxy-coated steel with 1’-6” spacing in the top mat and 7 3/8” spacing in the bottom mat.

Six Type MTS-72 prestressed concrete girders support the deck. The girders are spaced at 9’-0 1/2” on center, with a 4’-0” overhang at each side of the deck. A 10’-0” wide pedestrian walkway is located at the north end of the deck, encompassing the overhang and part of the deck area between girders G1 and G2.

Deck Construction

The deck concrete was placed July 25-30, 2014. Batch tickets indicate that the concrete was batched with a w/cm of 0.39. Notes on the batch tickets indicate that additional Glenium 3030 NS high range water reducer was added on site to increase workability and that fresh air contents between 6 and 9.2% were measured, with an average air content of 7.2%. It is not known whether these air contents were measured before or after pumping or conveying. Compressive strength tests on hardened concrete cylinders indicate an average 28-day compressive strength of 6600 psi (minimum reading = 5410 psi). No cylinder tested had a compressive strength less than the 4500 psi design strength.

Field Investigation

An in-depth field investigation was performed on the deck on August 22, 2016. The investigation consisted of visual observation, chain dragging, coring, impulse response (IR), and ground-penetrating radar (GPR) testing.

Visual observations

Widespread, dense cracking was observed over the top surface of the two year old deck (Figure 1). The cracking pattern was similar in the EB and WB lanes, but the EB lane appeared to have more traditional transverse cracking and less random cracking than the WB lane. Most cracks measured 0.010" (10 mil) or less in width, with a small percentage exceeding 0.015" (15 mil). The widest cracks, measuring 0.015" to 0.020", were located over each of the two piers and were oriented at a skew relative to the bridge deck (consistent with the 22° skew of the piers relative to the deck). A cumulative crack width of 0.215" was measured over a 50' length in the EB lane, and a cumulative crack width of 0.280" was measured over a 50' length in the WB lane; these measurements are equivalent to approximately 358 and 467 microstrain, respectively.

Away from the piers, the cracks were generally random, except for between girders G2 and G3 in the WB lane, where primarily transverse cracking was observed; the bay between these two girders has no diaphragms and is immediately adjacent to a pedestrian walkway, which appears to have been cast at a separate time from the rest of the deck. A higher density of longitudinal cracks was observed above the girders and half-way between adjacent girders (Figure 2 and Figure 3).

The underside of the deck showed light transverse cracking with some efflorescence. The transverse cracks appeared to be more closely spaced between girders G1 and G2 (beneath the pedestrian walkway), than between any of the other girders (Figure 4 and Figure 5); the concrete in this section of the deck may have been placed subsequent to the concrete in the rest of the deck. Numerous transverse cracks in the pedestrian walkway are consistent with phased construction placements causing deck restraint of thermal and drying shrinkage.

Chain drag

Three small delaminated or poorly consolidated areas, each measuring less than 1' × 1', were identified by chain drag. These constituted less than 0.02% of the total area of the deck.

Cores

Eleven cores in total were sampled from the deck - six from the EB lane (cores 1A-1F) and five from the WB lane (cores 1G-1K). Six cores were taken over cracks, and three cores were intentionally taken over reinforcing bars:

- Core 1A: No cracks, no rebar
- Core 1B: Taken over transverse crack (< 10 mil)
- Core 1C: No cracks, no rebar
- Core 1D: Taken over longitudinal crack (< 10 mil)
- Core 1E: No cracks, no rebar
- Core 1F: Taken over diagonal crack (< 10 mil) and transverse reinforcing bar
- Core 1G: Taken over diagonal crack (10 mil) and longitudinal reinforcing bar

- Core 1H: Taken over transverse crack (10 mil)
- Core 1I: Taken over transverse crack (15 mil) and transverse reinforcing bar
- Core 1J: No cracks, no rebar
- Core 1K: No cracks, no rebar; core fell through deck and was not retrieved

GPR

The slab depth was estimated from GPR scans to be approximately 7 3/4", and the transverse bar cover was estimated at two locations to be 2 1/8" and 2 7/8". These measurements were within 1/2" of the cover and total depths measured on the cores. Transverse bars were spaced at approximately 7 1/4". All estimated bar depths and spacings were within the MDT-specified tolerances.

Sketches and Photos

Figure 1. Random map cracking, EB lane.

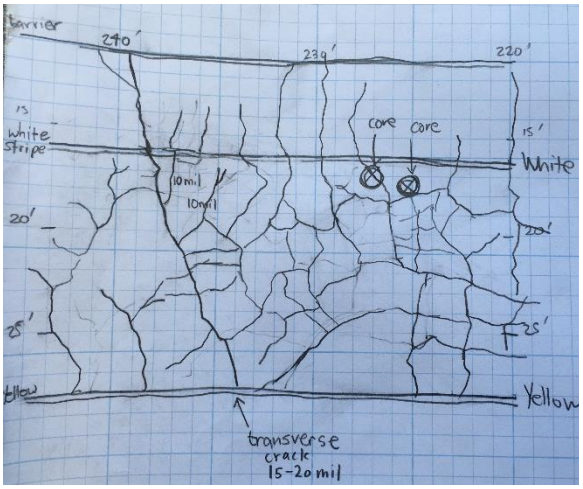

Figure 2. Sketch of cracks, 240' to 220' EB. Cores identified are cores 1A and 1B. Transverse crack at 240' is located over pier.

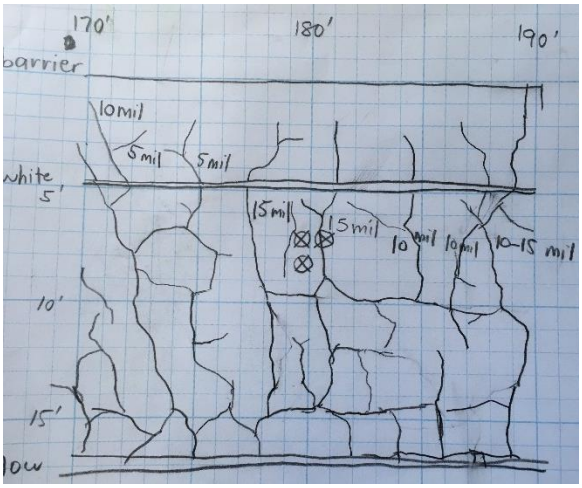

Figure 3. Sketch of cracks, 170' to 190' WB. Cores identified are cores 1I, 1J, and 1K.

Figure 4. Underside cracking between Girders G1 and G2. Cracks between these girders (beneath the pedestrian walkway) were generally more frequent and showed more efflorescence than cracks between the other girders.

Figure 5. Underside cracking between Girders G5 and G6.

BRIDGE 2: LOZEAU-TARKIO, MP 57.472 EB

Bridge ID # I00090057+04721
Date investigated: August 23, 2016
Investigation type: In-depth

Bridge Description

The east-bound Lozeau-Tarkio bridge over the Montana Rail Link (MP 57.472 EB) is a 296 ft., 5-span bridge with a prestressed concrete beam superstructure. The superstructure was originally constructed in 1967 and the deck was replaced in 2011.

The Class SD concrete mixture used for the replacement deck (Table 2) was provided by Knife River and was designed with a water-cement ratio (w/c) of 0.36. Air entrainment was used to provide a target air content of 6%. The 28-day compressive strength was designed to be a minimum of 4500 psi.

Table 2. Lozeau-Tarkio Structures, Class SD deck concrete

Material	Batch weights, per yd^3 at SSD	Source
Water	214 lb (25.6 gal)	-
Cement	600 lb	Ash Grove Type I/II
Coarse Aggregate	1779 lb	Knife River
Fine Aggregate	1334 lb	Knife River
Air Entrainer	8 fl. oz.	MasterBuilders AE 90
Water reducer (mid-range)	22 fl. oz.	MasterBuilders Polyheed 1020
Retarder	32 fl. oz.	MasterBuilders Delvo Stabilizer

In all spans, the transverse deck reinforcement is specified as #5 epoxy-coated steel, and the longitudinal deck reinforcement is specified as #4 epoxy-coated steel. A 2 3/8" cover to the top mat reinforcing bars and a 1" cover to the bottom mat reinforcing bars are specified for the deck in all spans. The superstructure design varies along the length of the bridge.

- In Spans 1 and 2 (0' to 117'-3"), the deck is designed with a 7 1/4" depth. Transverse reinforcing bars are spaced at 7 1/2" on center in both the top and bottom mats, and longitudinal reinforcing bars are spaced at 1'-6" on center in the top mat and 7 1/2" on center in the bottom mat. Five Type A prestressed concrete girders support the deck in this section, spaced at 6'-7 1/2" on center, with a 2'-9 1/2" overhang at each side.

- In Span 3 (117'-3" to 198'-9"), the deck is designed with a 7 3/4" depth. Transverse reinforcing bars are spaced at 7" on center in both the top and bottom mats, and longitudinal reinforcing bars are spaced at 1'-6" on center in the top mat and 7 1/2" on center in the bottom mat. Four Type IV prestressed concrete girders support the deck in this section, spaced at 8'-10" on center, with a 2'-9 1/2" overhang at each side.

- In Spans 4 and 5 (198'-9" to 296'), the deck is designed with an 8" depth. Transverse reinforcing bars are spaced at 7" on center in both the top and bottom mats, and longitudinal reinforcing bars are spaced at 1'-6" on center in the top mat and 7 1/2" on center in the bottom mat. Four Type A prestressed

concrete girders support the deck in this section, spaced at 8'-10" on center, with a 2'-9 1/2" overhang at each side.

Deck Construction

The deck was placed July 7, 2011. Batch tickets indicate that the deck concrete was batched with a w/c of approximately 0.40, which is higher than the nominal 0.36 w/c specified. Further, batch ticket notes indicate that water (typically 5-10 gal for a 12 yd^3 batch) was also added on site to increase workability. It is not known how long after batching the additional water was added. Batch ticket notes also indicate that fresh air contents between 7.2 and 9.3% were measured, with an average air content of 7.9%. It is not known whether these air contents were measured after batching, upon delivery or at point of placement. Compressive strength tests on hardened concrete cylinders indicate an average 28-day compressive strength of 4670 psi (minimum reading = 4240 psi). Two of the six cylinders tested had a compressive strength less than the 4500 psi design strength at 28 days.

Field Investigation

An in-depth field investigation was performed on August 23, 2016. The investigation consisted of visual observation, coring, IR, and GPR. Efflorescence was sampled from the underside of the bridge, at the far west end. The deck surface temperature was measured in the morning and afternoon.

Visual observations

The cracks in the deck of this bridge, Bridge 2, were generally wider and more distinctive than the cracks in the Florence-East Bridge over the Bitterroot River (MP 10.640), Bridge 1. The transverse cracks, on average, measured 0.015" to 0.020" (15 to 20 mil), with a small percentage exceeding 0.030" (30 mil). Transverse cracks were spaced at approximately 2' to 4', with closer spacing observed in localized areas (Figure 6, Figure 7, and Figure 8). The total width of cracks measured over a 50' length in the driving lane was found to be 0.400" (667 microstrain), about 60% greater than the total width of cracks measured over the same length on Bridge 1.

Longitudinal cracks tended to be located above the top flanges of the girders in all five spans of the deck, but were also observed at regular intervals (~1' to 2' spacing) between the girders in Spans 3, 4, and 5. Cracking was generally worse in Spans 3, 4, and 5 in terms of size and quantity. Spans 3, 4, and 5 have one fewer girder than Spans 1 and 2, which results in a 2' increase in girder spacing.

Six areas in the driving lane had been recently repaired. The repaired areas ranged from 15 ft^2 to 180 ft^2, totaling approximately 560 ft^2, or about 6% of the deck area. Based on photographs provided by MDT, the areas receiving repairs had consisted of wide transverse cracks connected to one another by bridging longitudinal cracks. Repair Area 4 also featured a through-hole approximately 6" × 6", within a larger region measuring approximately 1' × 3', where the deck had delaminated. Transverse cracking was observed in the repaired sections of the deck.

Cores

Eight cores in total were sampled from the deck (cores 2A-2G). Two cores were sampled at location 2D (2D-I and 2D-II), after core 2D-I fell through the deck. Five cores were taken over cracks, and one core was intentionally taken over reinforcing bar:

- Core 2A: No cracks, no rebar; taken from a crack-free area in a region with lots of map cracking
- Core 2B: Taken over the end of a fine map crack (hairline)
- Core 2C: Taken over a transverse crack (25 mil) and transverse reinforcing bar
- Core 2D-I: Taken over longitudinal crack (hairline); fell through deck and retrieved
- Core 2D-II: Taken over same longitudinal crack as core 2D-II
- Core 2E: No cracks, no rebar
- Core 2F: No cracks, no rebar
- Core 2G: Taken over a map crack (< 10 mil)

GPR

Slab depth and rebar locations were estimated from GPR data collected between Spans 4 and 5. The slab depth was estimated to be approximately 7 1/8" (compared to 8" specified), and the transverse and longitudinal bar covers were estimated to be 2" and 2 7/8", respectively. Although the bar cover measurements were within the MDT-specified tolerances, the estimated deck thickness was 7/8" less than specified (tolerance = -1/8"). GPR estimates for the entire field investigation were generally within ±1/2" of the cover and total depths measured on cores, so the total thickness of the deck, while likely less than the specified 8", may still have been within the specified tolerances.

Temperature

Deck temperature was measured once in the morning and once in the afternoon (Table 3) during the site visit on August 23, 2016.

Table 3. Deck temperature, Bridge 2

Time	Deck Top Surface	Ambient
Morning	42-45 °F	50-52 °F
Afternoon	86-91 °F	77-78 °F

Sketches and Photos

Figure 6. General crack appearance for Bridge 2. Transverse cracks are regularly spaced at 2 to 4 ft intervals. Longitudinal cracks tend to lie along the girders. The tape measure in the photo is positioned over one of the girders.

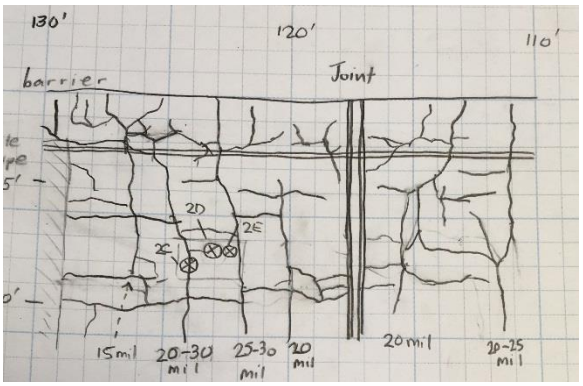

Figure 7. Sketch of cracks, 130' to 110' (Spans 2 and 3), right lane. Longitudinal cracks generally follow girders; location of girders changes between Span 3 (left) and Span 2 (right). Cores identified are cores 2C, 2D, and 2E.

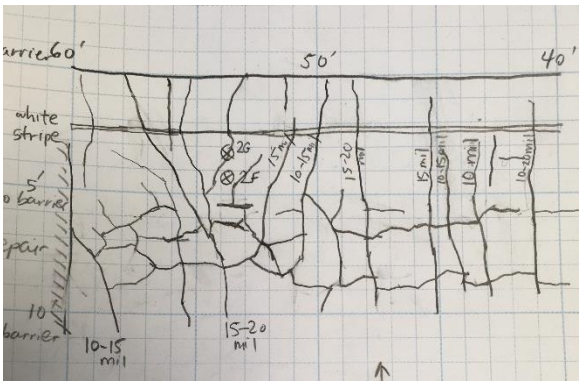

Figure 8. Sketch of cracks, 60' to 40' (Spans 1 and 2), right lane. The long transverse crack near 56' is located over Bent 2. Cores identified are cores 2F and 2G.

Figure 9. General underside appearance for Bridge 2. Transverse cracks are regularly spaced and generally exhibit thick deposits of efflorescence. Longitudinal cracks branch off from some of the transverse cracks.

Figure 10. Thick deposits of efflorescence along cracks on the underside of deck. A longitudinal crack branches between two adjacent transverse cracks.

BRIDGE 3: LOZEAU-TARKIO, MP 58.550 EB

Bridge ID # I00090058+05501
Investigation date: August 23, 2016
Investigation type: Cursory

Bridge Description

The east-bound Lozeau-Tarkio bridge over Clark Fork (MP 58.550 EB) is an 826 ft., 7-span bridge with a welded plate girder superstructure. The superstructure was constructed in 1967, and a 2 1/2" overlay was applied to the existing deck in 2011.

The Class SF deck overlay concrete (Table 4) was provided by Knife River and was designed with a w/cm of 0.40. The mixture contained partial substitution of cement with silica fume (7% by wt.). Air entrainment was used to provide a target air content of 6%.

Table 4. Lozeau-Tarkio Structures, Class SF overlay concrete

Material	Batch weights, per yd^3 at SSD	Source
Water	243 lb (29 gal)	-
Cement	570 lb	Ash Grove Type I/II
Silica Fume	43 lb	MasterBuilders Rheomac SF 100
Coarse Aggregate	1749 lb	Knife River
Fine Aggregate	1260 lb	Knife River
Air Entrainer	8 fl. oz.	MasterBuilders AE 90
Water reducer (mid-range)	22 fl. oz.	MasterBuilders Polyheed 1020
Retarder	32 fl. oz.	MasterBuilders Delvo Stabilizer

The original superstructure design varies along the length of the bridge. In all spans, the transverse reinforcement is specified as #5 black bar steel, and the longitudinal reinforcement is specified as #4 black bar steel. A 1 1/2" cover to the top mat reinforcing bars and a 1" cover to the bottom mat reinforcing bars are specified for all spans.

- In Spans 1, 2, 6, and 7 (0' to 169'-3" and 676'-4" to 825'-9"), the original deck was designed with a 7 1/2" depth. Transverse reinforcing bars are spaced at 10 1/2" on center in both the top and bottom mats, and longitudinal reinforcing bars are spaced at 1'-8" on center in the top mat and 5" on center in the bottom mat. Four welded plate girders support the deck in these sections, spaced at 8'-4" on center, with a 2'-6 1/2" overhang at each side.

- In Spans 3, 4, and 5 (169'-3" to 676'-4"), the deck was designed with a 6 3/4" depth. Transverse reinforcing bars are spaced at 6" on center in both the top and bottom mats, and longitudinal reinforcing bars are spaced at 1'-3" on center in the top mat and 6" on center in the bottom mat. Five welded plate girders support the deck in these sections, spaced at 6'-3" on center, with a 2'-6 1/2" overhang at each side.

The 2011 deck rehabilitation removed the top 2" of the original deck before applying the 2 1/2" overlay. Therefore, the new deck thickness and clear cover to the top reinforcing bars are approximately 1/2" larger than specified in the original design.

Deck Construction

The deck overlay was placed Aug. 9-10, 2011. No concrete batch tickets were provided. Fresh air contents indicated in the MDT-provided QC diary were 5% (Aug. 9) and 5.3% (Aug. 10), but only one measurement was reported for each placement. Compressive strength tests on hardened concrete cylinders indicate an average 28-day compressive strength of 7320 psi (minimum reading = 7060 psi) among four cylinders tested.

Field Investigation

A cursory field investigation was performed on August 23, 2016. The investigation consisted of visual observation, coring, and chain drag.

Visual observations

The bridge deck overlay showed similar random cracking as the other bridge decks (Figure 11). The transverse cracks appeared less distinguishable (tighter) compared to Bridge 2; it was estimated that cracks were, on average, 0.015" (15 mil) or less in width. The underside of the deck (the original deck, Figure 14) showed little transverse or other cracking and very little efflorescence compared to the other bridge decks.

Chain drag

A few small delaminations were detected by chain drag: four delaminations, each measuring 1' × 2' or less, were located along parallel, 0.015' to 0.020" (15 to 20 mil) transverse cracks and the 0.015" (15 mil) longitudinal crack bridging them; and three long, narrow delaminations were located near the expansion joints over piers 6 and 7.

Cores

Three cores were sampled from the deck (cores 3A-3C). All three cores were taken over cracks in the overlay concrete:

- Core 3A: Taken over map crack (< 10 mil); crack does not appear to reflect from the base of the overlay
- Core 3B: Taken over intersecting longitudinal and transverse cracks (< 10 mil); longitudinal crack appears to reflect from the base of the overlay, but the transverse crack does not
- Core 3C: Taken over intersecting map cracks (< 10 mil) close to midspan; crack appears to have reflected from the base into the overlay

Sketches and Photos

Figure 11. General crack appearance, Bridge 3. Cracks are similar in appearance to Bridge 2, but are generally tighter.

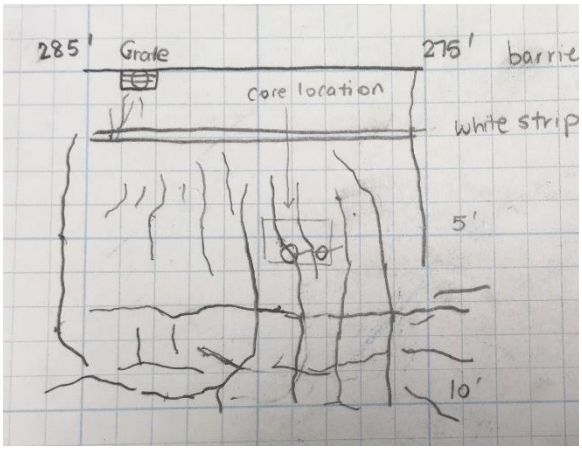

Figure 12. Sketch of cracks 285' to 275'. Cracks are similar in appearance to Bridge 2 cracks.

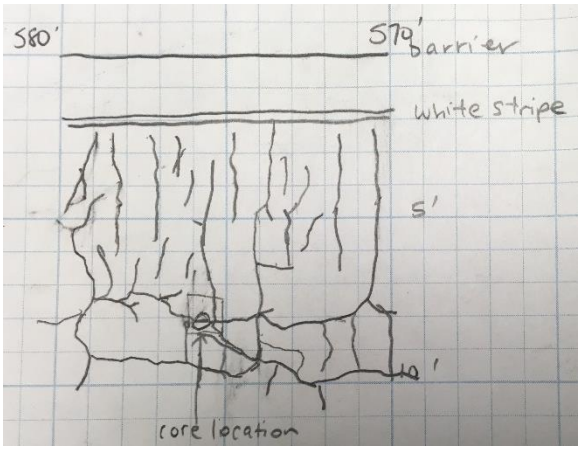

Figure 13. Sketch of cracks 580' to 570'. Cracks are similar in appearance to Bridge 2 cracks.

Figure 14. Bridge 3 shows very little underside cracking and moisture leakage or efflorescence (original deck).

BRIDGE 4: LOZEAU-TARKIO, MP 58.550 WB

Bridge ID # I00090058+05502
Investigation date: August 23, 2016
Investigation type: Cursory

Bridge Description

The west-bound Lozeau-Tarkio bridge over Clark Fork (MP 58.550 WB) is an 826 ft., 7-span bridge with a welded plate girder superstructure. The superstructure was constructed in 1967, and the deck was replaced in 2012.

The same Class SD mixture was used for this deck as for the east-bound Lozeau-Tarkio Bridge over the Montana Rail Link (MP 57.472 EB), Bridge 2 (Table 2). The mix was designed with a w/c of 0.36. Air entrainment was used to provide a target air content of 6%. The 28-day compressive strength was designed to be a minimum of 4500 psi.

Like its sister Bridge 3, the deck and girder superstructure design varies along the length of the bridge. In all spans for the new deck, the transverse reinforcement was specified as #5 epoxy-coated steel, and the longitudinal reinforcement was specified as #4 epoxy-coated steel. A 2 3/8" cover to the top mat reinforcing bars and a 1" cover to the bottom mat reinforcing bars was specified for all spans.

- In Spans 1, 2, 6, and 7 (0' to 169'-3" and 676'-4" to 825'-9"), the deck was designed with an 8 1/4" depth. Transverse reinforcing bars are spaced at 7" on center in both the top and bottom mats, and longitudinal reinforcing bars are spaced at 1'-6" on center in the top mat and 7" on center in the bottom mat. Four welded plate girders support the deck in these sections, spaced at 8'-4" on center, with a 2'-6 1/2" overhang at each side.

- In Spans 3, 4, and 5 (169'-3" to 676'-4"), the deck was designed with a 7 1/2" depth. Transverse reinforcing bars are spaced at 7 3/4" on center in both the top and bottom mats, and longitudinal reinforcing bars are spaced at 1'-6" on center in the top mat and 7 1/2" on center in the bottom mat. Five welded plate girders support the deck in this section, spaced at 6'-3" on center, with a 2'-6 1/2" overhang at each side.

Deck Construction

The deck was placed June 19-22, 2012. Batch tickets indicate that the concrete was batched with a w/c of approximately 0.37. Notes on the batch tickets do not indicate whether additional water or water reducer was added on site to improve workability. Batch ticket notes do indicate that fresh air contents between 5.1 and 6.5% were measured, with an average air content of 5.8%. It is not known whether these air contents were measured after batching, upon delivery, or at point of placement. Compressive strength tests on hardened concrete cylinders indicate an average 28-day compressive strength of 5430 psi (minimum reading = 4750 psi). None of the 16 cylinders tested had a compressive strength less than the 4500 psi design strength at 28 days.

Field Investigation

A cursory field investigation was performed on August 23, 2016. The investigation consisted of visual observation only. No cores were taken.

Visual observations

The bridge deck showed similar random cracking as the other bridge decks, but the random cracks appeared much tighter than on the other decks. Transverse cracks were spaced at approximately 3’ to 5’ (Figure 15), with widths typically between 0.010” and 0.015” (10 to 15 mil). The cracks appeared to be wider at midspan than elsewhere in the deck.

Photos

Figure 15. Transverse cracks on Bridge 4 deck. Cracks are outlined.

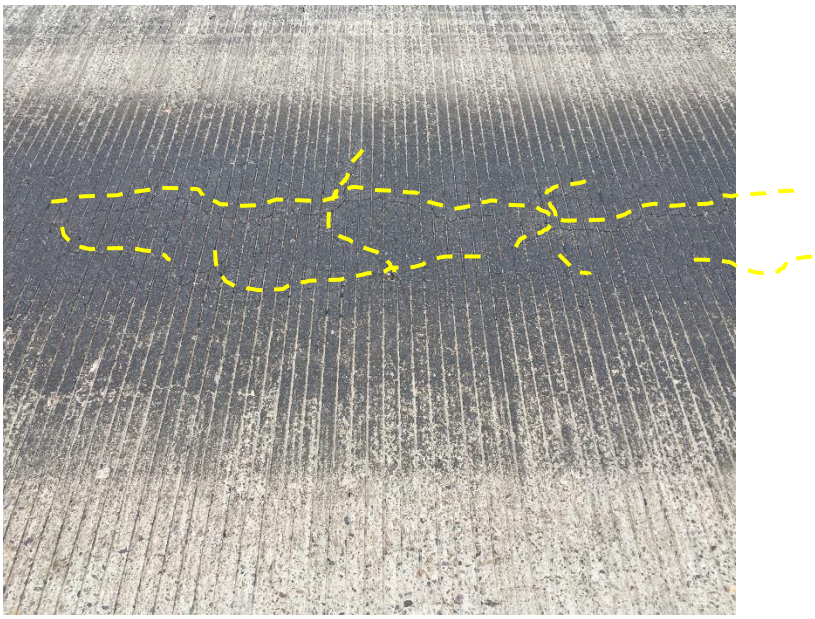

Figure 16. Longitudinal cracks in Bridge 4 deck. Cracks were difficult to photograph due to asphalt residue in wheel paths.

BRIDGE 5: LOZEAU-TARKIO, MP 57.472 WB

Bridge ID # I00090057+04722
Investigation date: August 23, 2016
Investigation type: Cursory

Bridge Description

The west-bound Lozeau-Tarkio bridge over the Montana Rail Link (MP 57.472 WB) is a 311 ft., 5-span bridge with a prestressed concrete beam superstructure. The superstructure was originally constructed in 1967, and the deck was replaced in 2012.

The same Class SD mixture was used for this deck as for Bridge 2 (Table 2). The mix was designed with w/c of 0.36. Air entrainment was used to provide a target air content of 6%. The 28-day compressive strength was designed to be a minimum of 4500 psi.

Like its sister Bridge 2, the superstructure design varies along the length of the bridge. In all spans, the transverse reinforcement is specified as #5 epoxy-coated steel, and the longitudinal reinforcement is specified as #4 epoxy-coated steel. A 2 3/8" cover to the top mat reinforcing bars and a 1" cover to the bottom mat reinforcing bars are specified for all spans.

- In Spans 1, 2, and 4 (0' to 122'-3" and 203'-9" to 260'-3"), the deck is designed with a 7 1/4" depth. Transverse reinforcing bars are spaced at 7 1/2" on center in both the top and bottom mats, and longitudinal reinforcing bars are spaced at 1'-6" on center in the top mat and 7 1/2" on center in the bottom mat. Five Type A prestressed concrete girders support the deck in this section, spaced at 6'-7 1/2" on center, with a 2'-9 1/2" overhang at each side.

- In Span 3 (122'-3" to 203'-9"), the deck is designed with a 7 3/4" depth. Transverse reinforcing bars are spaced at 7" on center in both the top and bottom mats, and longitudinal reinforcing bars are spaced at 1'-6" on center in the top mat and 7 1/2" on center in the bottom mat. Four Type IV prestressed concrete girders support the deck in this section, spaced at 8'-10" on center, with a 2'-9 1/2" overhang at each side.

- In Spans 5 (260'-3" to 311'), the deck is designed with an 8" depth. Transverse reinforcing bars are spaced at 7" on center in both the top and bottom mats, and longitudinal reinforcing bars are spaced at 1'-6" on center in the top mat and 7 1/2" on center in the bottom mat. Four Type A prestressed concrete girders support the deck in this section, spaced at 8'-10" on center, with a 2'-9 1/2" overhang at each side.

Deck Construction

The deck was placed May 15, 2012. Batch tickets indicate that the concrete was batched with a w/c of approximately 0.37. Batch ticket notes indicate that fresh air contents between 5.5 and 6.6% were measured, with an average of 6.2%. It is not known whether these air contents were measured after batching or just prior to placement. Compressive strength tests on hardened concrete cylinders indicate an average 28-day compressive strength of 5590 psi (minimum reading = 5030 psi). None of the eight cylinders tested had a compressive strength less than the 4500 psi design strength at 28 days.

Field Investigation

A cursory field investigation was performed on August 23, 2016. The investigation consisted of visual observation, chain dragging, and coring.

Visual observations

The bridge deck showed similar cracking patterns as its sister eastbound bridge (Bridge 2). Transverse cracks measured approximately 0.010" to 0.015" in width. The underside of the deck had evenly spaced transverse cracking and efflorescence. Deposits of efflorescence were also observed on the ground beneath the bridge.

Chain drag

No delaminations were detected.

Cores

One core was taken (5A). The core was taken over a diagonal crack measuring approximately 15 mil in width. The crack appears to be in the early stages of progression.

Photos

Figure 17. Branching transverse cracks on Bridge 5 (surface grooving is transverse).

Figure 18. Transverse and longitudinal cracks on Bridge 5 (surface grooving is transverse). The transverse cracks shown are spaced 1 ft. apart. Pen points to a hairline longitudinal crack bridging the two transverse cracks.

BRIDGE 6: HENDERSON-WEST, MP 22.013 EB - WB (HENDERSON INTERCHANGE)

Bridge ID # I00090022+00131
Investigation date: August 24, 2016
Investigation type: In-depth

Bridge Description*

The Henderson Interchange (Henderson-West Bridge, MP 22.013) is a 138 ft., 3-span bridge with a prestressed concrete beam superstructure. The bridge was originally constructed in 1980, and the deck was replaced in 2007.

The Class SD mixture used for the deck (Table 5) was provided by Pioneer Concrete and was designed with a w/c of 0.39. The suppliers of the fine aggregate and water reducer admixture were changed in July 2007, but the same mixture proportions were retained. Air entrainment was used to provide a target air content of 5.5%. The 28-day compressive strength was designed to be a minimum of 4500 psi.

Table 5. Henderson - West, Class SD concrete

Material	Batch weights, per yd^3 at SSD	Source
Water	258 lb (31 gal)	-
Cement	658 lb	Lafarge Type I/II
Coarse Aggregate	1875 lb	Thompson Falls S&G
Fine Aggregate	1100 lb	Thompson Falls S&G (before July 2007) JTL, Missoula (after July 2007)
Air Entrainer	6 fl. oz.	Grace Daravair 1000
Water reducer (mid-range)	33 fl. oz.	Grace Mira 92 (before July 2007) MasterBuilders Pozzolith (after July 2007)

The deck was designed with a 190 mm [7 1/2”] depth, a 60 mm [2 3/8”] cover to the top mat reinforcing bars, and a 25 mm [1”] cover to the bottom mat reinforcing bars. Transverse reinforcement is specified as #16 [#5] epoxy-coated steel with 145 mm [5 3/4”] spacing in both the top and bottom mats. Longitudinal reinforcement is specified as #13 [#4] epoxy-coated steel with 450 mm [1’-5 3/4”] spacing in the top mat and 155 mm [6 1/8”] spacing in the bottom mat. Ten prestressed concrete girders support the deck, with variable spacing and overhangs.

** Design is in metric units. Customary unit equivalents are given in brackets.*

Deck Construction

The EB deck was placed June 7, 2007 and the WB deck was placed July 27, 2007; different aggregates and water reducing admixtures were used for each deck. Batch tickets indicate that the concrete was batched with a w/c of approximately 0.34 for both decks. Notes on the batch tickets indicate that additional water (5-10 gal for an 8.25 yd^3 batch) was added on site to increase workability. It is not known how long after batching the additional water was added. Batch ticket notes also indicate that fresh air contents between 6.2 and 6.9% were measured for the EB deck, with an average air content of 6.5%, and between 5.5 and 6.5% with an average of 5.9% for the WB deck. It is not known whether these air contents were measured after batching or just prior to placement. Compressive strength tests on hardened concrete cylinders indicate an average 28-day compressive strength of 4850 psi (minimum reading = 4825 psi) for the EB deck and 5050

psi (minimum reading = 4872 psi) for the WB deck. None of the six cylinders tested had a compressive strength less than the 4500 psi design strength at 28 days.

Field Investigation

An in-depth field investigation was performed on the EB driving and passing lanes on August 24, 2016. The investigation consisted of visual observation, coring, IR, and GPR. The deck temperature was periodically monitored.

Visual observations

The surface of the bridge deck showed significantly more wear than the previous bridge decks, which is consistent with the older age of the bridge. Transverse cracks were observed at 4' to 6' intervals, with average widths between 0.015" to 0.025" (15 to 25 mil) and local widths exceeding 0.035". Substantial raveling was noted around several of the cracks. The total width of cracks measured over a 50' length in the center of the driving lane was found to be 0.240" (400 microstrain), similar to what was measured for Bridge 1. The WB deck appeared to be in a similar condition as the EB deck.

Longitudinal cracks were observed approximately 10' from the south barrier and 8' from the median barrier in the EB lanes. These locations are consistent with the locations of the longitudinal girders noted in the original superstructure drawings. Wide cracks (0.020" to 0.030", on average) were also visible above and along the piers, as had also been observed for the previous bridges.

Map cracks were also present, but were difficult to observe. The cracks were made visible by wetting the deck surface (Figure 19). The widths of the fine map cracks was not measured.

The underside of the deck showed frequent transverse cracks filled with thick deposits of efflorescence (Figure 20). Two areas were identified on the underside of the deck where closely-spaced transverse cracks appeared to "jump" to the adjacent cracks, forming a closed loop. One of the closed-loop areas was reflected in the cracks on the top of the deck (Figure 21 and Figure 22); core 6G was taken over a "progression" (jumping) crack at this location.

Cores

Nine cores in total were sampled from the deck (cores 6A-6I). Three cores were taken over cracks, and one core was intentionally taken over reinforcing bar:

- Core 6A: Taken over transverse crack (15 mil) and transverse reinforcing bar
- Core 6B: No cracks, no reinforcing bar
- Core 6C: No cracks, no reinforcing bar
- Core 6D: Taken over diagonal crack (10 mil)
- Core 6E: No cracks, no reinforcing bar
- Core 6F: No cracks, no reinforcing bar
- Core 6G: Taken over possible "progression" crack (< 10 mil) also visible from underside
- Core 6H: No cracks, no reinforcing bar
- Core 6I: No cracks, no reinforcing bar

GPR

The slab depth was estimated from GPR scans to be approximately 7" on average, but varied locally between 6 1/2" and 7 1/2". The 6 1/2" depth measurement is 1" less than specified and is not within the permitted tolerances of the MDT specifications. The transverse and longitudinal bar covers were estimated to be 2 1/4" and 2 3/4", respectively, which are within the MDT-specified tolerances. Estimated cover depths were within 1/2" of those measured on cores.

Temperature

Deck surface temperatures were measured throughout the morning and early afternoon (Table 6) during the site visit on August 24, 2016.

Table 6. Deck temperatures, Bridge 6

Time	Deck Top Surface	Deck Underside	Ambient
8:00 AM	43 °F		48 °F
9:00 AM	66 °F	58 °F	54 °F
10:00 AM	74 °F		66 °F
12:00 PM (cloudy)	72 °F		71 °F
1:30 PM (sunny)	90 °F		71 °F

Sketches and Photos

Figure 19. General crack appearance, Bridge 6. Wide transverse cracks are accompanied by finer longitudinal cracks and hairline map cracks. Map cracks were only visible after deck surface was wetted.

Figure 20. General underside crack appearance, Bridge 6. Frequent transverse cracks are filled with thick deposits of efflorescence. Efflorescence extends onto the concrete surface several inches past crack opening.

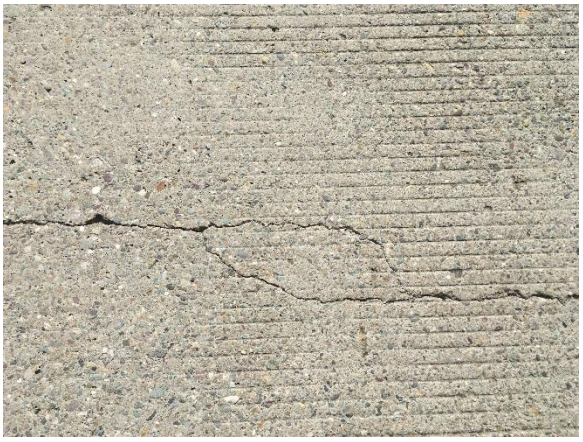

Figure 21. "Jump" crack at location of core 6G, topside of deck.

Figure 22. "Jump" crack at location of core 6G, reflected in underside of deck.

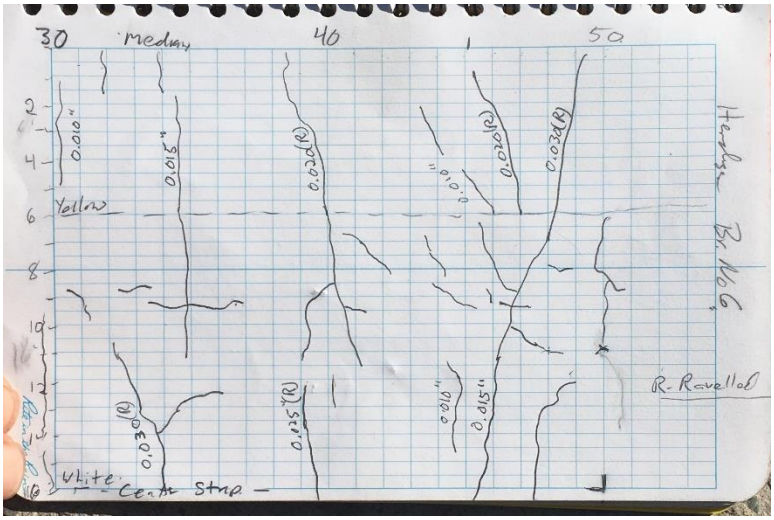

Figure 23. Sketch of cracks, 30' to 50', passing lane. Cracks are primarily transverse, 15-30 mil wide, and raveled ("R"). The long transverse crack between 45' and 50' is located over Pier 2.

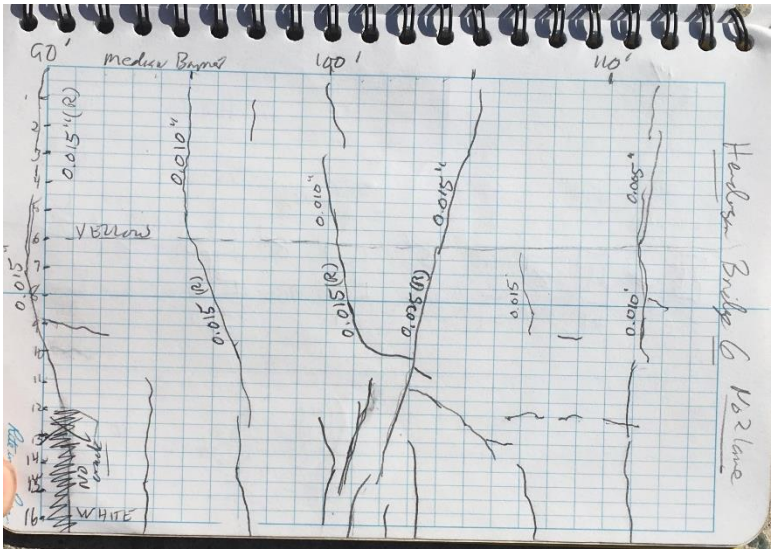

Figure 24. Sketch of cracks, 90' to 110', passing lane. Cracks were typically ~15 mil wide and raveled ("R"). The long transverse crack between 100' and 110' is located over Pier 3.

BRIDGE 7: HENDERSON-EAST, MP 25.393 WB (DREXEL INTERCHANGE)

Bridge ID # I00090025+03932
Investigation date: August 24, 2016
Investigation type: Cursory

Bridge Description

The west-bound Drexel Interchange (Henderson-East, MP 25.393 WB) is a 122 ft., 3-span bridge with a prestressed concrete superstructure. The original superstructure was constructed in 1980, and a latex-modified overlay was applied to the existing deck in 2008. No information was provided regarding the latex-modified concrete mix design used for the overlay.

The original superstructure design varies along the length of the bridge. In all spans, the transverse reinforcement is specified as #5 black, uncoated bars, and the longitudinal reinforcement is specified as #4 black bars. A 2 3/8" cover to the top mat reinforcing bars and a 1" cover to the bottom mat reinforcing bars are specified for all spans. Type I prestressed concrete girders support the deck in all sections, but information about their spacing is not provided on the drawings.

- In Span 1 (0' to 40'-7"), the deck is designed with a 7 1/4" depth. Transverse reinforcing bars are spaced at 5 3/4" on center in both the top and bottom mats, and longitudinal reinforcing bars are spaced at 1'-6" on center in the top mat and 6" on center in the bottom mat.

- In Span 2 (40'-7" to 86'-10"), the deck is designed with a 7" depth. Transverse reinforcing bars are spaced at 6 1/4" on center in both the top and bottom mats, and longitudinal reinforcing bars are spaced at 1'-6" on center in the top mat and 7" on center in the bottom mat.

- In Spans 3 (86'-10" to 122'-6"), the deck is designed with a 7 3/4" depth. Transverse reinforcing bars are spaced at 5" on center in both the top and bottom mats, and longitudinal reinforcing bars are spaced at 1'-6" on center in the top mat and 5" on center in the bottom mat.

The top 2 1/2" of the original WB deck and the top 3" of the original EB deck were removed before the new 2 1/2" and 3" overlays, respectively, were applied. The overlayed bridge decks have the same total deck thickness and bar covers as in the original decks.

Field Investigation

A cursory field investigation was performed on August 24, 2016 in the WB lanes within the traffic closure. The investigation consisted of visual observation and chain drag. No cores were taken.

Visual observations
Overall, the WB bridge deck appeared to be in excellent condition. Transverse cracks were observed over the piers, but only occasional cracking was observed elsewhere in the deck. No efflorescence-filled transverse cracks were observed on the underside of the deck.

The EB bridge deck, which was observed at a distance from the WB dead lanes, showed considerably more distress on the top surface. The passing lane contained several large areas of delaminated and spalled

concrete, where the black bar transverse reinforcement was exposed (Figure 27 and Figure 28). Smaller spalled areas were also visible in the driving lane.

Chain drag

One small delamination, measuring less than 1’ × 1’, was detected in the WB lanes.

Photos

Figure 25. General appearance of the WB bridge deck. Construction debris in the passing lane limited the scope of the cursory investigation, but no significant transverse or random cracks were observed.

Figure 26. Close-up view of the WB bridge deck. A small delamination (1’ × 1’) is outlined, but no significant transverse or random cracks were observed.

Figure 27. Spalled concrete and exposed reinforcing bar, EB deck. No significant distress was observed on the WB deck.

Figure 28. Spalled concrete and exposed reinforcing bar, EB deck. No significant distress was observed on the WB deck.

BRIDGE 8: HENDERSON-EAST, MP 24.603 EB

Bridge ID # I00090024+06031
Investigation date: August 24, 2016
Investigation type: Cursory

Bridge Description*

The Henderson-East bridge over the St. Regis River (MP 24.603 EB) is a 402 ft., 4-span bridge with a prestressed concrete superstructure. The original superstructure was constructed in 1980, and the deck was replaced in 2008.

The Class SD mixture used for the deck (Table 7) was provided by Pioneer Concrete and was designed with a w/c of 0.40. Air entrainment was used to provide a target air content of 5.5%. The 28-day compressive strength was designed to be a minimum of 4500 psi.

Table 7. Henderson - East, Class SD concrete

Material	Batch weights, per yd^3 at SSD	Source
Water	242 lb (29 gal)	-
Cement	611 lb	Lafarge Type I/II
Coarse Aggregate	1850 lb	LS Jensen, Mullan Pit
Fine Aggregate	1205 lb	LS Jensen, Mullan Pit
Air Entrainer	7.4 fl. oz.	Grace Daravair 1000
Water reducer (mid-range)	31 fl. oz.	Grace Mira 92

The deck was designed with a 170 mm [6 5/8”] depth, a 60 mm [2 3/8”] cover to the top mat reinforcing bars, and a 25 mm [1”] cover to the bottom mat reinforcing bars. Transverse spacing is specified as #16 [#5] epoxy-coated steel with 155 mm [6 1/8”] spacing in both the top and bottom mats. Longitudinal reinforcement is specified as #13 [#4] epoxy-coated steel with 450 mm [1’-5 3/4”] spacing in the top mat and 150 mm [6”] spacing in the bottom mat. Six prestressed concrete girders support the deck, with variable spacing along the length (7’-8 3/4” in Span 1; 7’-6 1/2” in Span 2; and 7’-5 5/8” in Spans 3 and 4) and overhangs.

** Design is in metric units. Customary unit equivalents are given in brackets.*

Deck Construction

The current deck was placed August 8 and 12, 2008. Batch tickets indicate that the concrete was batched with a w/c of approximately 0.35. Notes on the batch tickets indicate that additional water (5-15 gal for a 9 yd^3 batch) was added on site to increase workability. It is not known how long after batching the additional water was added. Batch ticket notes also indicate that fresh air contents between 5.4 and 6.1% were measured, with an average air content of 5.8%. It is not known whether these air contents were measured after batching or just prior to placement. Compressive strength tests on hardened concrete cylinders indicate an average 28-day compressive strength of 5230 psi (minimum reading = 4925 psi). None of eight cylinders tested had a compressive strength less than the 4500 psi design strength at 28 days.

Field Investigation

A cursory field investigation was performed on August 24, 2016. The bridge was under two-way traffic at the time of the investigation, so the investigation consisted only of visual observation, primarily from the underside of the deck. No cores were taken.

Visual observations

The top surface of the deck showed very frequent transverse cracking (Figure 29). Visually, it was estimated that the cracks were spaced 2' to 4' apart, with closer spacing in several areas. Some of the transverse cracks could be seen to meander or "jump" to adjacent transverse cracks, but it could not be seen from a distance whether the cracks formed a closed loop as in the previous decks. Crack widths could not be measured, but visually appeared similar to the wider cracks seen for Bridges 2 and 6.

Frequent transverse cracking was also observed along the underside of the deck, in a similar frequency as observed on the top surface. Several of the more closely-spaced transverse cracks had bridging longitudinal cracks connecting them, in a similar pattern as was observed for Bridges 2 and 6; a possible precursor to future deck damage. A road sign was affixed to the underside of the deck in the center of Span 2, which is believed to be the underside of an earlier full-depth repair of the deck (Figure 30).

There also appeared to be more efflorescence on the underside of the deck than had been observed on many of the previous bridge decks. The efflorescence not only filled the transverse cracks, but also coated the concrete surface surrounding the cracks. Corrosion stains were observed in a small percentage of the transverse cracks and in isolated areas on the girders, as well (Figure 31). Corrosion staining had not been observed associated with the cracks of any of the previous bridge decks.

Photos

Figure 29. General cracking on top surface of the deck. Transverse cracks are observed with high frequency.

Figure 30. General appearance of underside of deck. Frequent efflorescence-filled transverse cracks are visible. A road sign likely forms a full-depth repair.

Figure 31. Minor corrosion staining around a transverse crack (circled). Corrosion stains were observed for a small number of transverse cracks on the underside of the deck.

BRIDGE 9: HENDERSON-EAST, MP 23.325

Bridge ID # I00090023+03251
Investigation date: August 24, 2016
Investigation type: Cursory

Bridge Description*

The Henderson-East bridge over the St. Regis River (MP 23.325) is a 658 ft., 4-span bridge, with a welded plate girder superstructure. The original superstructure was constructed in 1979. The east-bound deck was replaced in 2009, and the west-bound deck received a 2 1/2" overlay, also in 2009.

The same Class SD mixture was used for the EB deck replacement as was used for Bridge 8 (Table 7). The mixture was designed with a w/c of 0.40. Air entrainment was used to provide a target air content of 5.5%. The 28-day compressive strength was designed to be a minimum of 4500 psi. No information was provided regarding the latex-modified concrete mix design used for the WB deck overlay.

The EB deck was designed with a 210 mm [8 1/4"] depth, a 60 mm [2 3/8"] cover to the top mat reinforcing bars, and a 25 mm [1"] cover to the bottom mat reinforcing bars. Transverse reinforcement is specified as #19 [#6] epoxy-coated steel with 125 mm [5"] spacing in both the top and bottom mats. Longitudinal reinforcement is specified as #13 [#4] epoxy-coated steel with 450 mm [1'-5 3/4"] spacing in the top mat and 90 mm [3 1/2"] spacing in the bottom mat.

The WB deck was originally designed with an 8 1/4" depth, a 2" cover to the top mat reinforcing bars, and a 1" cover to the bottom mat reinforcing bars. Transverse reinforcement is specified as #6 black-bar steel with 5" spacing in both the top and bottom mats. Longitudinal reinforcement is specified as #4 black-bar steel with 1'-6" spacing in the top mat and 4" spacing in the bottom mat. The 2009 construction removed the top 2 1/2" of the original deck and replaced it with a 2 1/2" latex-modified overlay.

Four welded plate girders support each deck, spaced at 12'-4" on center with a 2'-4 1/2" overhang on each side. The bridges are adjacent to one another, and connected at a median barrier.

** EB deck replacement design is in metric units. Customary unit equivalents are given in brackets. WB deck design is in customary units.*

Deck Construction

The EB deck was placed Sept. 3-6, 2008. Batch tickets indicate that the concrete was batched with a w/c of approximately 0.35. Notes on the batch tickets indicate that additional water (typically 5-10 gal but up to 35 gal for a 9 yd^3 batch) was added on site to increase workability. It is not known how long after batching the additional water was added. Batch ticket notes also indicate that fresh air contents between 5.2 and 7.0% were measured, with an average air content of 6.3%. It is not known whether these air contents were measured after batching or just prior to placement. Compressive strength tests on hardened concrete cylinders indicate an average 28-day compressive strength of 4700 psi (minimum reading = 4049 psi). Two of 16 cylinders tested had a compressive strength less than the 4500 psi design strength at 28 days. No information was provided regarding the WB latex-modified concrete overlay.

Field Investigation

A cursory field investigation was performed on August 24, 2016. The investigation consisted of visual observation and chain drag. No cores were taken.

Visual observations

Transverse and longitudinal cracks were observed in both the EB deck and the WB overlay (Figure 32). The cracks on the EB deck were similar in appearance and frequency to the cracks observed previously on the other bridge decks; the spacing of the transverse cracks was visually estimated to be between 2’ and 4’. Transverse cracks on the WB deck overlay were generally less frequent than on the EB deck, with an estimated spacing of 4’ to 8’. Very little map cracking was observed on the WB overlay.

Two transverse cracks in the WB overlay exhibited corrosion staining (Figure 33**Error! Reference source not found.**). Both stains affected only a small percentage of the total crack length.

The two bridge decks were separated from but immediately adjacent to one another, which enabled observation of live-load deflections of the EB deck. Under typical live loads, the EB deck was observed to deflect 1/4”, but under heavy truck loads, deflections of up to 1/2” were observed.

Chain drag

Delaminations were detected on the WB overlay around a small percentage of cracks (~10 delaminations detected in total). Most delaminations were 1’ × 1’ or less in area, with the largest delaminations measuring approximately 1’ × 3’ (Figure 34).

Photos

Figure 32. Transverse cracks on EB deck.

Figure 33. Corrosion staining on top of deck. Corrosion staining was observed in two isolated locations on the top of the deck.

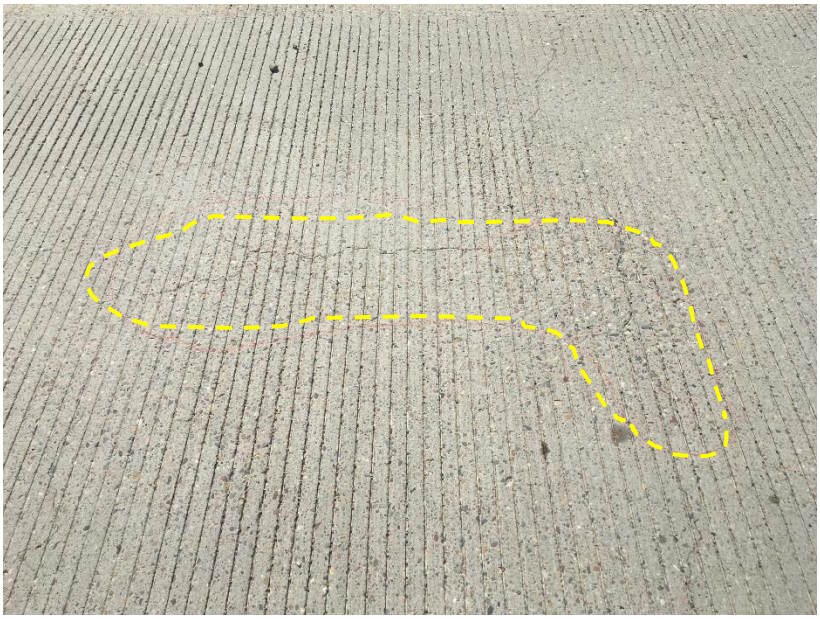

Figure 34. WB deck overlay. A delaminated region around the transverse crack and branching longitudinal crack is outlined. Delaminations were observed around a small percentage of cracks in the overlay.

BRIDGE 10: SUPERIOR AREA, MP 49.397 EB

Bridge ID # I00090049+03971
Investigation date: August 25, 2016
Investigation type: Cursory

Bridge Description

The east-bound Superior Area bridge over the Clark Fork (MP 49.397 EB) is an 800 ft., 6-span bridge with a welded plate girder superstructure. The original superstructure was constructed in 1966, and the deck was replaced in 2010.

The Class SD-L concrete mixture used for the deck (Table 8) was provided by Knife River and was designed with a w/cm of 0.40. The mixture contained partial substitution of cement with silica fume (4.8% by wt.). Air entrainment was used to provide a target air content of 6%. The 28-day compressive strength of the Class SD-L concrete was designed to be a minimum of 4000 psi.

Table 8. Superior Area Structures, Class SD-L concrete

Material	Batch weights, per yd^3 at SSD	Source
Water	205 lb (24.6 gal)	-
Cement	500 lb	Ash Grove Type I/II
Silica Fume	25 lb	WR Grace
Coarse Aggregate	1844 lb	TR
Fine Aggregate	1328 lb	TR
Air Entrainer	9 fl. oz.	MasterBuilders AE 90
Water reducer (mid-range)	30 fl. oz.	MasterBuilders Polyheed 1020
Retarder	30 fl. oz.	MasterBuilders Delvo Stabilizer

The superstructure design varies along the length of the bridge, but is symmetric about its midspan. In all spans, the transverse reinforcement is specified as #5 epoxy-coated steel, and the longitudinal reinforcement is specified as #4 epoxy-coated steel. A 2 3/8" cover to the top mat reinforcing bars and a 1" cover to the bottom mat reinforcing bars are specified for all spans.

- In spans 1 and 6 (0' to 75' and 725' to 800'), the deck was designed with an 8 1/4" depth. Transverse reinforcing bars are spaced at 6 1/4" on center in both the top and bottom mats, and longitudinal reinforcing bars are spaced at 1'-6" on center in the top mat and 6 7/16" on center in the bottom mat. Four welded plate girders support the deck, spaced at 9' on center, with a 2'-6 1/2" overhang at each side.

- In spans 2, 3, 4, and 5 (75' to 725') the deck was designed with a 7 1/2" depth. Transverse reinforcing bars are spaced at 7" on center in both the top and bottom mats, and longitudinal reinforcing bars are spaced at 1'-6" on center in the top mat and 7 11/16" on center in the bottom mat. Five welded plate girders support the deck, spaced at 6'-9" on center, with a 2'-6 1/2" overhang at each side.

Deck Construction

The deck was placed Sept. 21-28, 2010. No batch tickets were provided. Fresh concrete properties reported in the MDT-provided Concrete Diary indicate that air contents ranged from 5.3 to 7.0% with an average of

6.0%. Compressive strength measurements on hardened concrete cylinders indicate an average 28-day compressive strength of 5630 psi (minimum reading = 4480 psi). None of the 28 cylinders tested had a compressive strength less than 4000 psi at 28 days. ASTM C1202/AASHTO T277 Rapid Chloride Permeability (RCP) testing on the Class SD-L concrete indicated an average charge passed of 2560 C at 28 days for the 28 samples, with a standard deviation of 580 C (range between 1872 to 3918 Coulombs passed, 23% coefficient of variation).

Field Investigation

A cursory field investigation was performed on August 25, 2016, in the driving lane of Spans 1, 2, and 3. The investigation consisted of visual observation, chain dragging, coring, IR, and GPR. The deck temperature was periodically monitored.

Visual observations

Several regularly spaced transverse cracks were observed on the deck of Bridge 10, primarily in Spans 2-5. The transverse cracks appeared to be more closely spaced than on the previous bridges. Cracks in Span 2 were measured at approximately 2’ to 4’ spacing and had an average width between 0.010” and 0.015” (10 to 15 mil). Many of the closely-spaced transverse cracks appeared to also have longitudinal cracks that “jumped” between them; core 10B was taken over one such jumping crack. The jumping cracks measured less than 0.010” (10 mil) in width, and bridged cracks measuring 0.015” (15 mil), on average. The distance over which the cracks jumped was typically 6”, but jumps of up to 2’ were also observed (Figure 35).

Longitudinal cracks were observed above the girders, consistent with some previous bridge decks. Map cracks were also apparent, but were difficult to quantify due to the abrasion of the deck surface.

Two “chunks” of concrete measuring 6” × 6” were observed along the expansion joint between Spans 5 and 6 (Figure 37). One chunk had been fully separated from the deck, leaving the joint beneath exposed, while the other chunk remained intact. These “chunks” were similar in appearance to those previously photographed by MDT in July, and do not appear to have grown since that time; however, greater raveling was observed. A “chunk” of concrete delaminated from the top of the deck in July (previously observed by MDT personnel) had been repaired at the time of the field investigation.

The underside of the bridge deck showed some efflorescence-filled transverse cracks. Longitudinal cracks were also observed between several of the more closely-spaced transverse cracks, forming closed loops similar to what was observed for Bridges 2, 6, and 8.

Cores

Five cores in total were sampled from the deck (cores 10A-10E). Two cores were taken over cracks. No cores were intentionally taken over reinforcing bars:

- Core 10A: No cracks, no reinforcing bar
- Core 10B: Taken over “jumping” transverse crack (< 10 mil)
- Core 10C: No cracks, no reinforcing bar
- Core 10D: No cracks, no reinforcing bar
- Core 10E: Taken over longitudinal crack (10 mil)

GPR

The slab depth near the center of Span 2 was estimated from GPR scans to be approximately 7 5/8" on average, but varied locally between 7 1/4" and 8 1/8". The transverse and longitudinal bar covers were estimated to be 2 5/8" and 3 1/2", respectively.

Temperature

Deck temperatures were measured throughout the morning and early afternoon (Table 9) during the site visit on August 25, 2016.

Table 9. Deck temperatures, Bridge 10

Time	Deck Top Surface	Deck Underside	Ambient
7:30 AM	41 °F	40 °F	45 °F
10:30 AM	69 °F	49 °F	62 °F
12:00 PM	74 °F		
12:30 PM	83 °F	52 °F	68 °F

Sketches and Photos

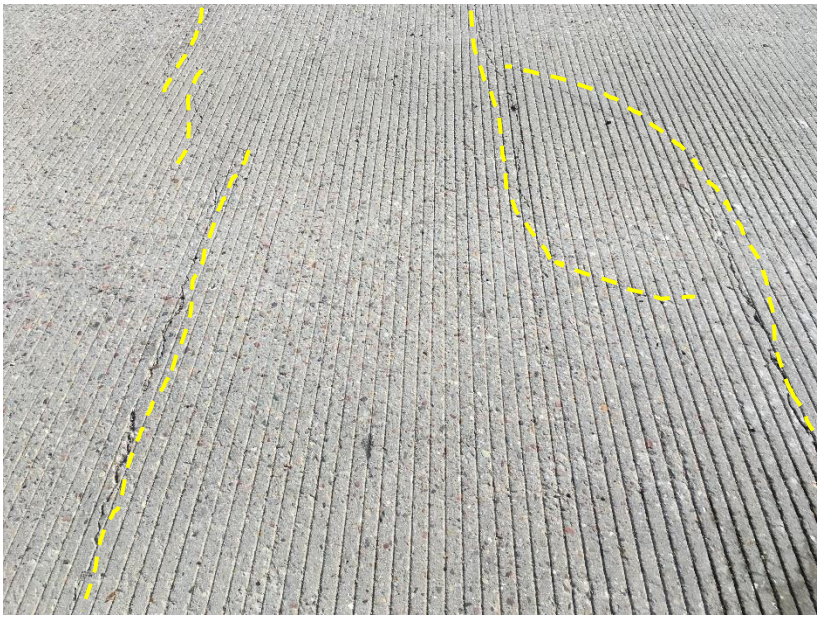

Figure 35. General crack appearance, Bridge 10. Transverse cracks are outlined. As closely-spaced transverse cracks progress, they appear to bend or branch toward adjacent transverse cracks.

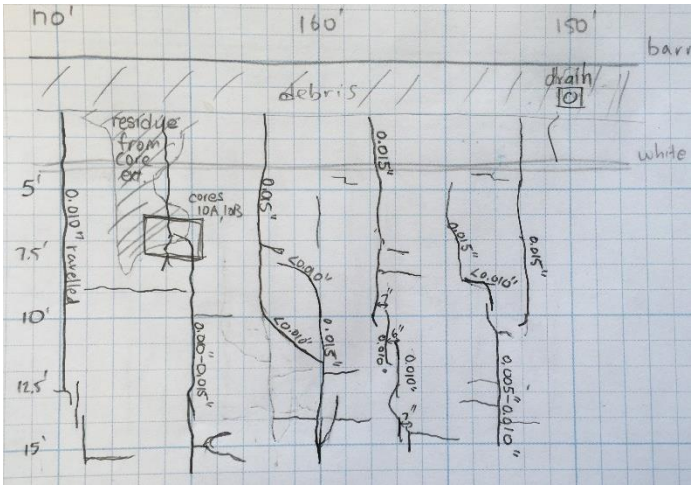

Figure 36. Sketch of cracks, 170' to 150'. Long bending cracks near 160' and long "jumping" crack near 162' are the same cracks shown in Figure 35. Sketch is drawn at 180 degrees rotation from Figure 35.

Figure 37. "Chunks" of concrete along expansion joint between Spans 5 and 6.

BRIDGE 11: SUPERIOR AREA, MP 49.397 WB

Bridge ID # I00090049+03972
Investigation date: August 25, 2016
Investigation type: Cursory

Bridge Description

The west-bound Superior Area bridge over the Clark Fork (MP 49.397 WB) is an 800 ft., 6-span bridge with a welded plate girder superstructure. The original superstructure was constructed in 1960, and the deck was replaced in 2011.

The Class SD concrete mixture used for the deck (Table 10) was provided by Knife River and was designed with a w/c of 0.36. Air entrainment was used to provide a target air content of 6%. The 28-day compressive strength of the Class SD concrete was designed to be a minimum of 4500 psi.

Table 10. Superior Area Structures, Class SD concrete

Material	Batch weights, per yd^3 at SSD	Source
Water	214 lb (25.6 gal)	-
Cement	600 lb	Ash Grove Type I/II
Coarse Aggregate	1779 lb	TR
Fine Aggregate	1334 lb	TR
Air Entrainer	8 fl. oz.	MasterBuilders AE 90
Water reducer (mid-range)	22 fl. oz.	MasterBuilders Polyheed 1020
Retarder	32 fl. oz.	MasterBuilders Delvo Stabilizer

Like its sister Bridge 10, the superstructure of Bridge 11 varies along its length, but is symmetric about its midspan. In all spans, the transverse and longitudinal reinforcement are specified as epoxy-coated steel bars, but bar diameters vary along the length. A 2 3/8" cover to the top mat reinforcing bars and a 1" cover to the bottom mat reinforcing bars are specified for all spans.

- In spans 1 and 6 (0' to 75' and 725' to 800'), the deck was designed with a 7" depth. #6 transverse reinforcing bars are spaced at 6" on center in both the top and bottom mats, and #4 longitudinal reinforcing bars are spaced at 1'-6" on center in the top mat and 4 1/4" on center in the bottom mat. Four welded plate girders support the deck, spaced at 8'-4" on center, with a 2'-6 1/2" overhang at each side.

- In spans 2, 3, 4, and 5 (75' to 875') the deck was designed with a 6 3/4" depth. #5 transverse reinforcing bars are spaced at 6 1/2" on center in both the top and bottom mats, and #4 longitudinal reinforcing bars are spaced at 1'-6" on center in the top mat and 7 1/8" on center in the bottom mat. Five riveted plate girders support the deck, spaced at 6'-3" on center, with a 2'-6 1/2" overhang at each side.

Deck Construction

The deck was placed June 21-24, 2011. No batch tickets were provided. Fresh concrete properties reported in the MDT-provided Concrete Diary indicate that air contents ranged from 5.2 to 5.8% with an average of 5.5%. Compressive strength measurements on hardened concrete cylinders indicate an average 28-day

compressive strength of 5430 psi (minimum reading = 4790 psi). None of the 12 cylinders tested had a compressive strength less than the 4500 psi design strength at 28 days.

Field Investigation

A cursory field investigation was performed on August 25, 2016, in the driving lane of Spans 4, 5, and 6. The investigation consisted of visual observation, chain dragging, coring, and GPR.

Visual observations

In general, Bridge 11 appeared to be in better condition than its sister Bridge 10. Cracks on the top side of the deck were primarily transverse, with very little map cracking observed. Transverse cracks were spaced at approximately 2' to 4', like on the EB bridge, but crack widths were tighter, typically 0.010" (10 mil) or less. Most of the cracks measuring more than 0.010" appeared filled with a polymer (HMWM) crack sealant (Figure 38); core 11A was taken over one such crack to examine the penetration of the sealant into the crack.

Longitudinal cracks were observed in Span 5, at approximately 7' and 10' from the north edge of the deck. These locations correspond to the edges of the top flange of Girder G2 and are consistent with the locations of the longitudinal cracks in the other bridges.

The underside of Bridge 11 generally looked better than the underside of Bridge 10. Transverse cracks were more sparsely spaced, but also contained efflorescence (Figure 41 and Figure 42).

Cores

Three cores in total were sampled from the deck (cores 11A-11C). One core was taken over a crack and reinforcing bar:

- Core 11A: Taken over transverse crack with sealant (< 10 mil)
- Core 11B: No cracks, no reinforcing bar
- Core 11C: No cracks, no reinforcing bar

GPR

The slab depth in Span 4, near core 11A, was estimated from GPR scans to be approximately 6 1/4", but varied locally between 6" and 6 3/4"; only three locations measured 6 1/2" or deeper. The transverse and longitudinal bar covers were estimated to be 2" and 3", respectively.

Sketches and Photos

Figure 38. General appearance of transverse cracks, Bridge 11. Cracks wider than ~10 mil were filled with a sealant (visible in photo).

Figure 39. Closely-spaced cracks on top surface of Bridge 11. Cracks are outlined.

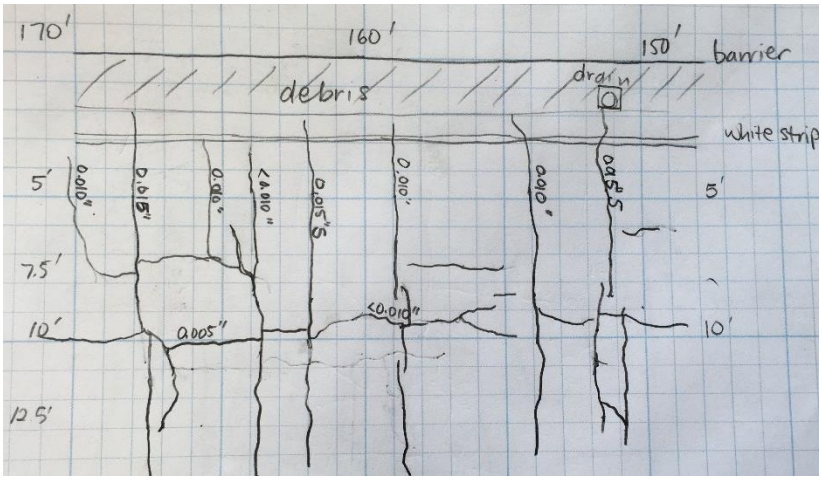

Figure 40. Sketch of cracks, 170' to 150'. Cracks are similar in location and frequency as on other bridge decks, but are tighter. Crack sealant ("S") was observed in cracks ~10 mil or wider.

Figure 41. General underside appearance, Bridge 11. Transverse cracks are more widely spaced, but showed efflorescence.

Figure 42. General underside appearance, Bridge 11.

BRIDGE 12: THOMPSON RIVER, MP 55-56

Bridge ID # STA 23+20.50
Investigation date: August 25, 2016
Investigation type: Cursory

Bridge Description

The bridge over the Thompson River is a 446 ft., 3-span bridge with a continuous welded plate girder superstructure. The bridge was constructed in 2015. Class SD concrete was used for the superstructure, but no information was provided regarding its composition.

The deck was designed with a 9" depth, 2 3/8" cover to the top mat reinforcing bars, and 1" cover to the bottom mat reinforcing bars. Transverse reinforcement is specified as #6 epoxy-coated steel with 6 1/4" spacing in the top mat and 9 3/4" spacing in the bottom mat. Longitudinal reinforcement is specified as #4 epoxy-coated steel with 1'-6" spacing in the top mat, and #5 epoxy-coated steel with 9" spacing in the bottom mat. Four welded plate girders support the deck. The girders are spaced at 11'-6" on center, with a 3'-9 1/2" overhang at each side of the deck. The girders are deep, with narrow flanges.

Deck Construction

The deck was placed in August 2015 on the new bridge and represents recent deck construction. No other details were provided regarding the deck construction or the quality of the concrete used.

Field Investigation

A cursory field investigation was performed on August 25, 2016 in the EB lane. The investigation consisted of visual observation, chain dragging, coring, and GPR.

Visual observations
Transverse cracks between 0.005" and 0.010" (5 to 10 mil) in width were observed over most of the deck in Spans 1 and 2; fewer cracks in general were observed in Span 3. The transverse cracks were spaced at 2' to 4' and appeared to be in the very initial stages of propagation/"jumping". Cracks were located in similar locations and frequencies as on the other bridge decks, but were much tighter due to the comparatively younger (1 year) age of the bridge deck (Figure 43). The transverse cracks often continued into the cast-in-place barrier. Some of the wider cracks (0.015" in width) were filled with a crack sealant (Figure 44**Error! Reference source not found.**).

Few efflorescence stains at transverse cracks were yet visible on the underside of the deck.

Cores
Three cores in total were identified for later sampling from the deck (cores 12A-12C). Two cores were located over cracks, and one core was intentionally located over a reinforcing bar:

- Core 12A: Taken over longitudinal hairline crack
- Core 12B: No cracks, no reinforcing bar
- Core 12C: Taken over transverse crack filled with sealant (10 mil), and over transverse reinforcing bar

GPR

The slab depth was estimated from one GPR scan to be approximately 8 1/4". The transverse bar cover was estimated to be 2 1/2".

Sketches and Photos

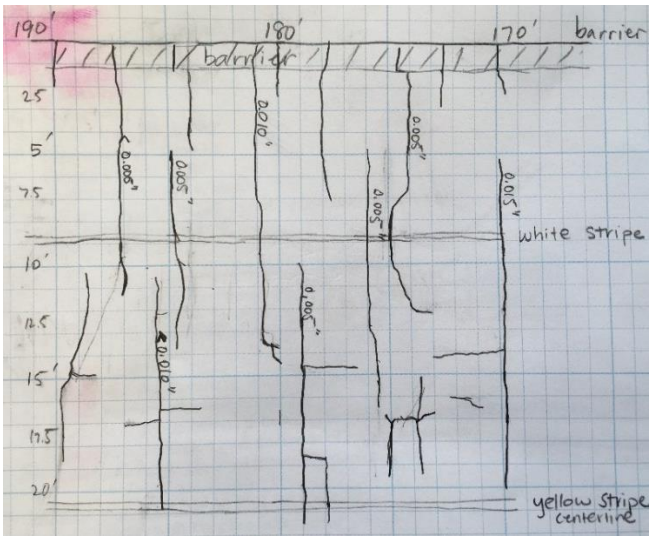

Figure 43. Sketch of cracks, 190' to 170'. Transverse cracks appear with similar frequency as for other bridges, but are typically less than 10 mil and width; longitudinal cracks are hairline.

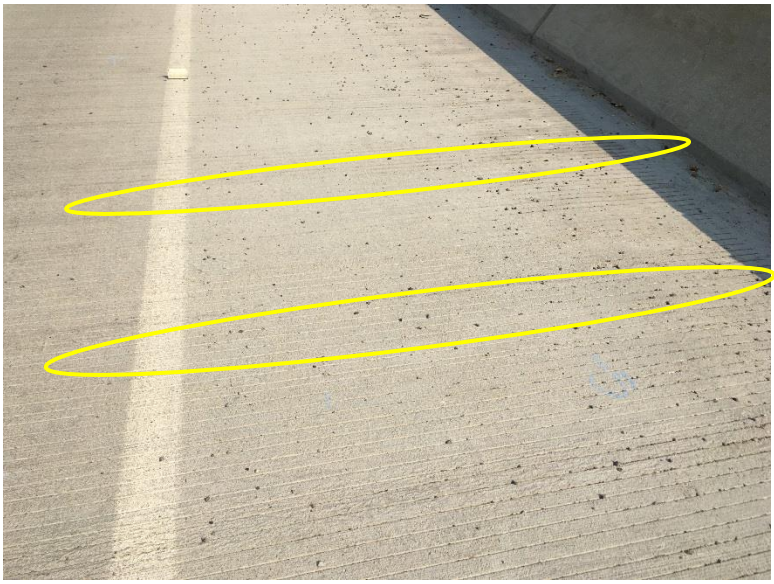

Figure 44. General crack appearance, Bridge 12. Cracks are generally too fine to see from photographs. The wider transverse cracks, circled, contain a crack sealant.

WJE ENGINEERS ARCHITECTS MATERIALS SCIENTISTS

APPENDIX B - INVESTIGATION REPORT

INVESTIGATION AND RESULTS

The investigation of the bridge deck distress consisted of a document review, field investigation, laboratory studies, and computer modeling and simulation.

Document Review

Prior to WJE's field investigations and laboratory studies, MDT personnel provided WJE with project documentation to better understand the design, construction, materials, and distress patterns exhibited by the Missoula-area bridge decks. Documentation was provided for the following projects:

- Florence - East, STPS-STPB 203-1(12)10
- Henderson - East, IM 90-1(175)23
- Henderson - West, IM 90-1(142)2
- Lozeau-Tarkio Structures, IM 90-1(168)29

Plan drawings were also provided for the bridge over the Thompson River in Thompson Falls, MT, although the bridge was not included in the original document review. In total, documentation was received for 22 bridges in the Missoula area and three additional bridges in the Billings area showing similar types of distress. Subsequent investigations by WJE focused primarily on the 22 Missoula-area bridge decks; the Billings-area bridges are not discussed in this report.

Bridge Design

The 22 Missoula-area bridge decks under investigation were all placed between 2007 and 2015, with many decks being replacement decks for bridges built between 1960 and 1980. At least three deck rehabilitations between 2007 and 2015 consisted only of overlays applied to the original decks from the 1960s to 1980s, while the remaining projects were full deck replacements. The two bridges at Florence-East and Thompson River were new construction.

The bridges varied in terms of the number of spans, total length, and structural type, but most of the superstructures consisted of either prestressed concrete beams or welded plate girders. Deck thicknesses varied between 6 1/2" and 9" but were most commonly specified between 7 1/4" and 8". Epoxy-coated steel reinforcing bar was specified for the transverse (No. 5 bar) and longitudinal (No. 4 bar) reinforcement in all new construction and replacement deck slabs. Transverse reinforcement was specified at the same spacing in the top and bottom mats for most of the bridges, and ranged between 5" and 10 1/2", with a typical spacing of 6" to 7". Longitudinal reinforcement for each deck was specified at 1'-6" on center in the top mat, and ranged between 3 1/2" and 9" in the bottom mat, with a typical spacing of 6" to 7 1/2". Top cover to the transverse bars was specified at 2 3/8" for all new bridge decks, and bottom cover to the lower bars was specified at 1".

Representative cross-sections cut parallel to the longitudinal and transverse reinforcement are shown in Figure 1 and Figure 2, respectively, for the Florence-East Bridge (MP 10.640) to illustrate typical bar locations within the deck. A summary of deck thicknesses and bar locations for 12 of the 22 bridges is presented in Table 1, and a detailed description of the superstructure and deck designs is included in Appendix A.

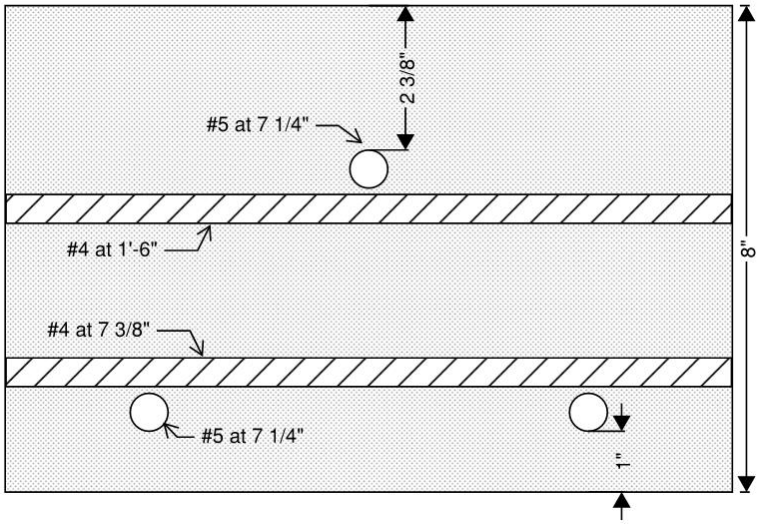

Figure 1. Representative cross-section for Florence-East, Bridge over the Bitterroot River, MP 10.640. Section shows cut parallel to longitudinal reinforcement.

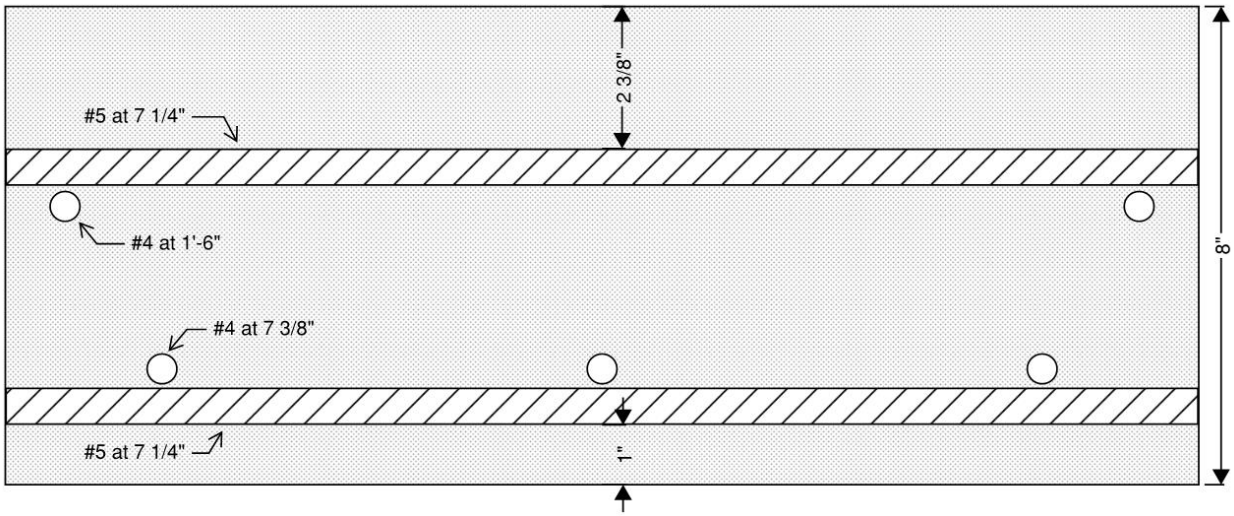

Figure 2. Representative cross-section for Florence-East, Bridge over the Bitterroot River, MP 10.640. Section shows cut parallel to transverse reinforcement.

Table 1. Specified Deck Thicknesses and Reinforcement Bar Spacing for Selected Bridge Decks

Bridge Location	Year of Construction (Reconstruction)	Specified Deck Thickness	Transverse Bar Spacing: Top and Bottom Mats	Longitudinal Bar Spacing: Top Mat	Longitudinal Bar Spacing: Bottom Mat
Florence-East, MP 10.640	2014	8”	7 1/4”	1’-6”	7 3/8”
Lozeau-Tarkio, MP 57.472 EB	1967 (2011 - redeck)	7 1/4” to 8”	7” or 7 1/2”	1’-6”	7 1/2”
Lozeau-Tarkio, MP 58.550 EB	1967 (2011 - overlay)	7 1/4” to 8” (+)	6” or 10 1/2”	1’-3” or 1’-8”	5” or 6”
Lozeau-Tarkio, MP 58.550 WB	1967 (2011 - redeck)	7 1/2” to 8 1/4”	7” or 7 3/4”	1’-6”	7” or 7 1/2”
Lozeau-Tarkio, MP 57.472 WB	1967 (2011 - redeck)	7 1/4” to 8”	7” or 7 1/2”	1’-6”	7 1/2”
Henderson-West, MP 22.013	1980 (2007 - redeck)	7 1/2”	5 3/4”	1’-5 3/4”	6 1/8”
Henderson-East, MP 25.393	1980 (2008 - overlay)	7” to 7 3/4”	5”, 5 3/4”, or 6 1/4”	1’-6”	5”, 6”, or 7”
Henderson-East, MP 24.603	1980 (2008 - redeck)	6 5/8”	6 1/8”	1’-5 3/4”	6”
Henderson-East, MP 23.325	1979 (2009 - redeck)	8 1/4”	5”	1’-5 3/4”	3 1/2”
Superior Area, MP 49.397 EB	1966 (2010 - redeck)	7 1/2” to 8 1/4”	6 1/4” or 7”	1’-6”	6 7/16” or 7 11/16”
Superior Area, MP 49.397 WB	1960 (2011 - redeck)	6 3/4” to 7”	6” or 6 1/2”	1’-6”	4 1/4” or 7 1/8”
Thompson River, MP 55-56	2015	9”	6 1/4” (top) 9 3/4” (bottom)	1’-6”	9”

(+) Includes 1/2” added from overlay.
Note: In-depth investigations were performed on highlighted bridges (see “Field Investigation” below).

Concrete Mixtures

The concrete used for each bridge deck was typically Class SD “special deck” concrete. Class SD concrete, as specified in Section 551 of the MDT *Standard Specifications for Road and Bridge Construction, 2006 Edition*, has a maximum water-cementitious materials ratio (w/cm) of 0.40, a target slump of 1 1/2 to 3 in. (40 - 80 mm), a required air content of 5-7%, and a minimum 28-day compressive strength of 4500 psi. Special provisions modifying the requirements for Class SD concrete were issued for the Florence-East project, but all other projects adhered to the then-current 2006 MDT requirements.[1] Class SD-L low-permeability deck concrete was also specified for one bridge deck in the Superior Area Structures project, and Class SF silica fume deck overlay concrete was specified for the Lozeau-Tarkio project.

[1] Class SD requirements were significantly revised in the 2014 edition of the *Standard Specifications*, but only the Thompson River bridge deck was placed after the changes were made. However, since project specifications and concrete mix designs were not included among the documentation received for the Thompson River Bridge, no conclusions can be made regarding the influence of the new Class SD requirements on the type and severity of the observed bridge deck distress.

The concrete mixtures and raw materials (cement, aggregates, admixtures, etc.) used for each project were provided by different suppliers, although similar mix designs were typically used for each bridge (see Table 2 and Table 3). Most concrete mixtures were designed with a nominal w/cm between 0.36 and 0.42, but the actual w/cm of the design mixture increases to 0.39 to 0.43 when the contributions of the liquid admixtures are also included. Air entraining admixtures were used in all mixtures to provide a target air content between 5.5 to 6.0%. Supplementary cementitious materials (SCMs) were used in the Florence - East (6% silica fume and 28% Class C fly ash) bridge, and on select bridge decks in the Lozeau-Tarkio (7% silica fume for Class SF deck overlays only) and Superior Area Structures (4.8% silica fume in Class SD-L concrete only) projects. A latex-modified concrete was used for the overlays in the Henderson-East and Henderson-West projects, but no information was provided regarding its mix design.

Quality control (QC) documentation provided by MDT consisted of batch tickets, concrete diaries (QC testing logs), and compressive strength data. Fresh concrete properties, including air content, slump, and occasionally temperature, were indicated on the batch tickets for every 3-5 trucks. The reported air contents were typically within 0.5% of the targeted air content, but air contents reported for the Florence - East bridge were significantly (up to 3.3%) higher than the targeted amount. It was not clear from the documents whether these air contents were measured before or after the concrete had been pumped or conveyed. Pumping and conveying methods could have a significant impact on the air content of the in-place concrete.

Some batch tickets also indicated that water or water-reducing admixtures were added to the concrete on site. The amounts of added water and water-reducing admixture were sometimes provided, but the same numbers were often reported for 12 yd^3 batches as for 3 yd^3 batches. It was not clear whether these quantities were measured or estimated, how long after batching they were added, or how much concrete was in the truck at the time of the addition. Addition of water at the job site could have a significant impact on the properties of the hardened concrete including its strength, permeability, and air void distribution.

Break data included 7 day compressive strength (typically 1 cylinder per pour) and 28 day compressive strength (typically 2 cylinders per pour). As shown in Table 4, the reported 28-day compressive strengths generally met or exceeded project specifications. However, two cylinders from the Lozeau-Tarkio Bridge at MP 57.472 EB and two cylinders from Henderson-East Bridge at MP 23.325 did not meet the required 4500 psi compressive strength at 28 days.

A detailed review of the concrete mix designs, QC data, and batch ticket reports is included in Appendix A for 12 of the 22 Missoula-area bridge decks included in this investigation.

Table 2. Mix Designs, Class SD Concrete

Material	Florence-East (Class SD)	Henderson-East (Class SD)	Henderson-West (Class SD)	Lozeau-Tarkio and Superior Area (Class SD)
Water, pcy	217	242	258	214
Cement, pcy	345	611	658	600
Fly ash, pcy	146	-	-	-
Silica fume, pcy	30	-	-	-
Stone, pcy	1821	1850	1875	1779
Sand, pcy	1299	1205	1100	1334
Air entrainer, fl. oz./cwt	2	4.6	6	8
Mid-range water reducer, fl. oz./cwt	12	31	33	22
High-range water reducer, fl. oz./cwt	4	-	-	-
Set retarder, fl. oz./cwt	4	-	-	32
w/cm (nominal)	0.42	0.40	0.39	0.36
w/cm (including admixtures)	0.43	0.42	0.41	0.39

Table 3. Mix Designs, Class SF and SD-L Concrete

Material	Lozeau-Tarkio (Class SF)	Superior Area (Class SD-L)
Water, pcy	243	205
Cement, pcy	570	500
Fly ash, pcy	-	-
Silica fume, pcy	43	25
Stone, pcy	1749	1844
Sand, pcy	1260	1328
Air entrainer, fl. oz./cwt	8	9
Mid-range water reducer, fl. oz./cwt	22	30
High-range water reducer, fl. oz./cwt	-	-
Set retarder, fl. oz./cwt	32	30
w/cm (nominal)	0.40	0.39
w/cm (including admixtures)	0.43	0.43

Table 4. Average Reported 28-day Compressive Strengths

Bridge Location	Average 28-day Compressive Strength (psi)
Florence-East, MP 10.640	6790 (Phase 1) 5840 (Phase 2)
Lozeau-Tarkio, MP 57.472 EB	4670
Lozeau-Tarkio, MP 58.550 EB	7320
Lozeau-Tarkio, MP 58.550 WB	5430
Lozeau-Tarkio, MP 57.472 WB	5590
Henderson-West, MP 22.013	4840 (EB) 5050 (WB)
Henderson-East, MP 25.393	No information provided
Henderson-East, MP 24.603	5230
Henderson-East, MP 23.325	4700
Superior Area, MP 49.397 EB	5630
Superior Area, MP 49.397 WB	5430
Thompson River, MP 55-56	No information provided

Note: In-depth investigations were performed on highlighted bridges (see "Field Investigation" below).

Deck Condition

Photographs were provided by MDT personnel for most of the bridges included in the investigation. The photographs showed varying levels of distress in each of the decks. Most of the decks showed transverse cracking on the underside, often highlighted by white or gray-white efflorescence that appeared in the older decks to leach out of the cracks and onto the underside of the deck. Some - but not all - of the bridge decks that received only an overlay (e.g., the east-bound Superior Area bridge at MP 45.180) also exhibited this type of distress, but there were generally fewer and less frequent cracks observed in the undersides of those decks. Transverse cracks were estimated to be spaced less than 1 ft. apart in the most severely distressed decks, and more widely spaced (~6 ft.) in the less severely distressed decks. The cracks generally appeared parallel to one another, but occasional longitudinal cracks (perpendicular to the predominant transverse cracks) were also observed in a few of the MDT photos. Some decks exhibited a darkening discoloration of the concrete surrounding the efflorescence-filled cracks that suggested the presence of moisture in or near the crack opening at the time of the photograph.

The top surfaces of the bridge decks showed wide-spread abrasion in decks both with SCMs (fly ash or silica fume) and without SCMs. Spalls in both the concrete and the asphalt could be seen at pavement and expansion joints in several of the photographs. Transverse and map cracks were also observed on the top surfaces of several of the decks, with the most severely distressed decks showing large transverse cracks throughout the top surfaces.

Two of the Missoula-area bridge decks exhibited severe cracking that broke the concrete free from the reinforcing steel. The Lozeau-Tarkio Bridge over the Montana Rail Link (MP 57.472) developed a full-depth crack that dropped a "chunk" (approximately 4 in. by 4 in.) of the deck concrete onto the ground below. A portion of this "chunk" was retrieved for laboratory study prior to WJE's field investigation. The Superior Area Bridge over the Clark Fork River (MP 49.397) also developed a deep crack that dislodged a "chunk" of concrete from the top of the deck, but not through the full depth of the deck. Photographs of the two holes were similar, with the cracks appearing directly above (or below) the reinforcing bars along their

lengths. The coatings of the bars in all photographs appeared to be in satisfactory condition, and no corrosion products were visible within the cracks.

Figure 3. Through-hole in east-bound Lozeau-Tarkio bridge at MP 57.472 (photo provided by MDT).

Figure 4. Through-hole in east-bound Lozeau-Tarkio bridge at MP 57.472, as seen from the underside of deck (photo provided by MDT).

Figure 5. Delaminated "chunk" in deck of east-bound Superior Area bridge at MP 49.397 (photo provided by MDT).

Figure 6. Delaminated "chunks" along expansion joint of east-bound Superior Area bridge at MP 49.397 (photo provided by MDT).

Field Investigation

Based on findings of the document review, four bridges were identified by WJE in consultation with MDT personnel for further in-depth field investigation. These bridges include:

- **Florence-East, Bridge over the Bitterroot River, MP 10.640**: A two-year old new construction bridge deck showing initial signs of distress. Extensive map cracking and deep transverse cracks were visible in MDT photographs of the top surface of the deck. Light efflorescence-filled cracks were also observed by MDT personnel on the underside of the deck. This bridge was selected for in-depth investigation due to its young age and the use of fly ash and silica fume in its mix design.

- **Lozeau-Tarkio, East-bound Bridge over the Montana Rail Link, MP 57.472**: A five-year old bridge deck replacement showing severe signs of distress, including deep cracks, spalls, and through-holes. The bridge was selected for in-depth investigation due primarily to the severity of its distress. MDT had completed repairs on the bridge by the time of the field investigation, but part of the "chunk" of concrete that had fallen through the deck was submitted to WJE for laboratory study.

- **Henderson-West, Henderson Interchange, MP 22.013**: A nine-year old bridge deck replacement showing distress representative of other area bridge decks. Frequent transverse cracks were visible in MDT-provided photographs of both the topside and underside of the bridge deck. This bridge was selected for in-depth investigation due to its older age, representative distress pattern, and straight cement mix design.

- **Superior Area Structures, East-bound Bridge over Clark Fork, MP 49.397**: A six-year old bridge deck replacement showing severe signs of distress, including deep cracks and large spalls. The severity of distress observed in the MDT photographs was comparable to that of the east-bound Lozeau-Tarkio Bridge at MP 57.472, but no through-holes had yet been formed. This bridge was selected for in-depth investigation due to the severity of its distress and its silica fume (Class SD-L) mix design. The adjacent west-bound bridge deck, which did not contain silica fume (Class SD mix) and did not show as severe distress in MDT photographs, was also investigated for comparison in a cursory investigation.

An additional eight bridges were also selected for cursory inspection, to provide supplemental information regarding the type and severity of distress exhibited by the area bridge decks. A total of twelve bridges were investigated, as described in Table 5. Bridges were numbered 1 through 12 for easier identification.

The field investigations were performed between August 22 and 25, 2016. Field investigations consisted of crack mapping, core extraction, delamination surveys, impulse response (IR) surveys, ground penetrating radar (GPR) scans, and infrared imaging. The field investigation also included visual observation of the undersides of each deck, periodic measurements of deck surface temperatures, and sampling of efflorescence from the underside of the bridge decks for further laboratory analysis. A table summarizing the methods used on each bridge deck is provided in Table 6. Plan drawings showing the locations of the cores, crack maps, and delaminations identified during the four in-depth investigations (Bridges 1, 2, 6, and 10) are provided in Figure 7 to Figure 10.

Table 5. Description of Bridges Investigated

Bridge #	Bridge Location	Date of Field Investigation	Year Constructed (Re-constructed)	Superstructure	Concrete Mixture	Notes
1	Florence-East, MP 10.640	Aug. 22, 2016	2014	Prestressed concrete beam, 378 ft.	Fly ash (28%) and silica fume (6%)	Two years old at time of investigation; early stages of distress documented by MDT personnel
2	Lozeau-Tarkio, MP 57.472 EB	Aug. 23, 2016	1967 (2011)	Prestressed concrete beam, 296 ft.	No SCMs	Deep cracks and through-holes documented by MDT personnel
3	Lozeau-Tarkio, MP 58.550 EB	Aug. 23, 2016	1967 (2011)	Welded plate girder, 826 ft.	Silica fume (7%)	2 1/2” overlay applied in 2011
4	Lozeau-Tarkio, MP 58.550 WB	Aug. 23, 2016	1967 (2011)	Welded plate girder, 826 ft.	No SCMs	Companion to Bridge 3, but full deck replacement used different concrete mixture than Bridge 3 overlay
5	Lozeau-Tarkio, MP 57.472 WB	Aug. 23, 2016	1967 (2011)	Prestressed concrete beam, 311 ft.	No SCMs	Companion to Bridge 2
6	Henderson-West, MP 22.013	Aug. 24, 2016	1980 (2007)	Prestressed concrete beam, 138 ft.	No SCMs	Oldest bridge deck
7	Henderson-East, MP 25.393	Aug. 24, 2016	1980 (2008)	Prestressed concrete beam, 122 ft.	No information provided	2 1/2” overlay applied in 2008
8	Henderson-East, MP 24.603	Aug. 24, 2016	1980 (2008)	Prestressed concrete beam, 402 ft.	No SCMs	Under two-way traffic at time of investigation; investigation only performed on underside
9	Henderson-East, MP 23.325	Aug. 24, 2016	1979 (2009)	Welded plate girder, 658 ft.	No SCMs	EB lanes under two-way traffic at time of investigation; investigation only performed on WB lanes
10	Superior Area, MP 49.397 EB	Aug. 25, 2016	1966 (2010)	Welded plate girder, 800 ft.	Silica fume (6%)	Deep cracks and spalls documented by MDT personnel
11	Superior Area, MP 49.397 WB	Aug. 25, 2016	1960 (2011)	Welded plate girder, 800 ft.	No SCMs	Companion to Bridge 10, but used different concrete mixture
12	Thompson River, MP 55-56	Aug. 25, 2016	2015	Prestressed concrete beam, 446 ft.	No information provided	Approximately one year old at time of investigation; early cracking observed by MDT personnel

Note: In-depth investigations were performed on highlighted bridges.

Table 6. Field Investigations Performed for Each Bridge

Bridge #	Crack Mapping	Core Extraction	Delamination Survey	Impulse Response Survey	GPR Survey	Infrared Imaging
1	X	X	X	X	X	X
2	X	X	X	X	X	X
3	X	X	X			
4	*Visual inspection only*					
5	X	X	X			
6	X	X	X	X	X	
7			X			
8	*Visual inspection of underside only*					
9		X				
10	X	X	X	X	X	
11	X	X	X		X	
12	X	X	X		X	X

Note: In-depth investigations were performed on highlighted bridges.

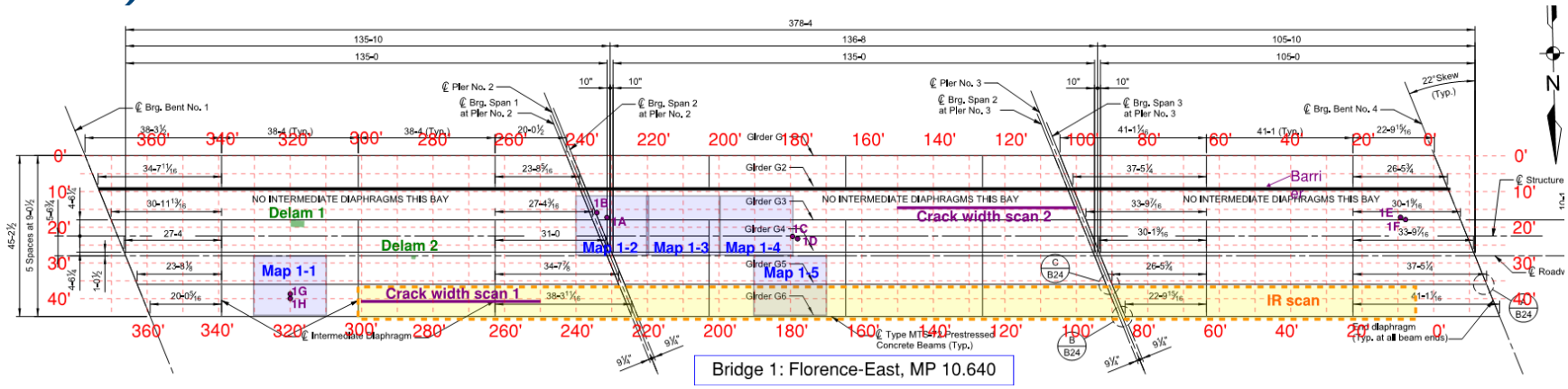

Figure 7. Annotated drawing of Bridge 1, Florence-East, MP 10.640. Station markings are shown in red. Cores are indicated by purple circles, delaminations by green polygons, crack maps by blue rectangles, and IR surveys by a yellow rectangle. Two small delaminations were identified in Span 1 of the deck.

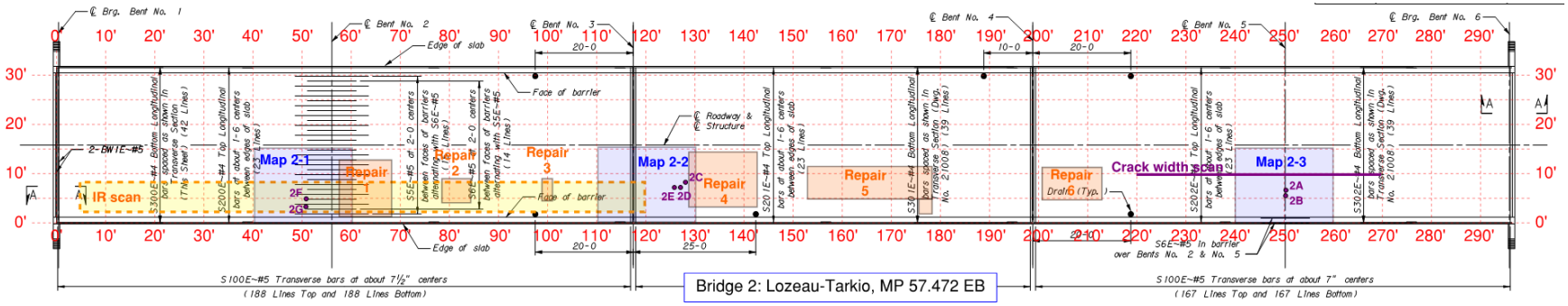

Figure 8. Annotated drawing of Bridge 2, Lozeau-Tarkio, MP 57.472 EB. Station markings are shown in red. Cores are indicated by purple circles and crack maps by blue rectangles. Previously repaired areas are shown in orange.

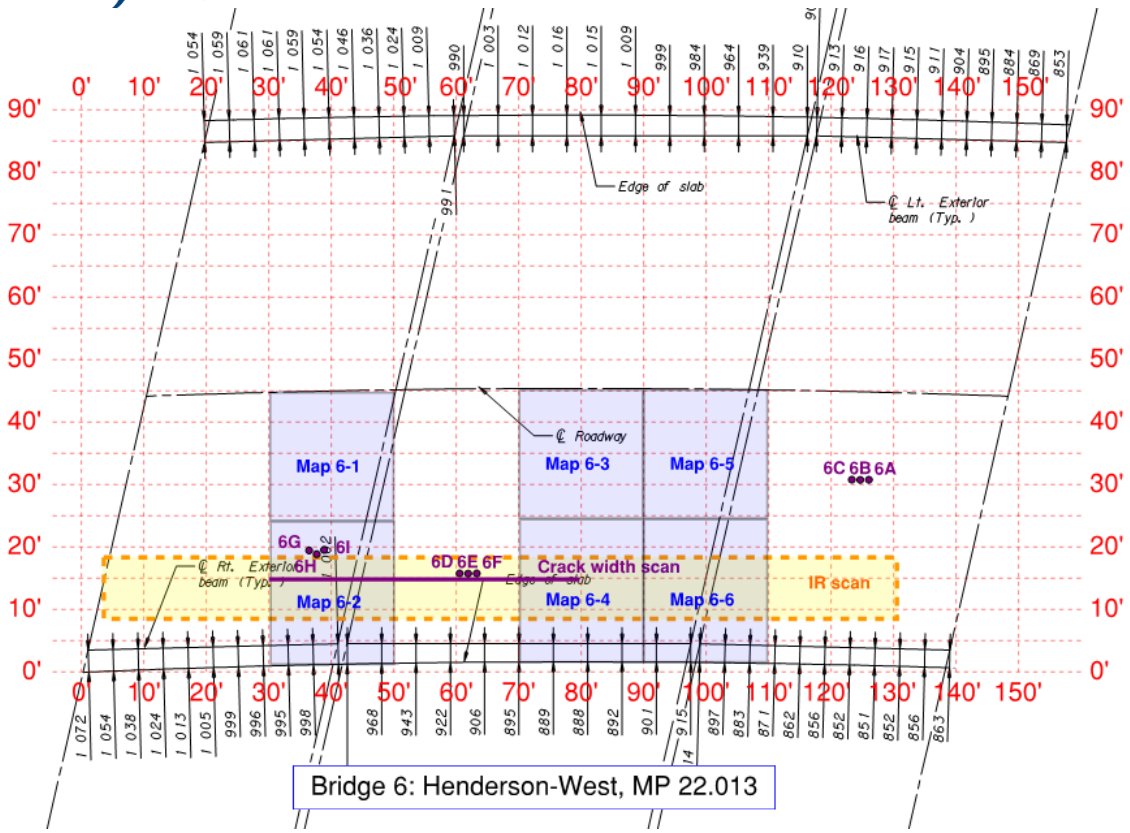

Figure 9. Annotated drawing of Bridge 6, Henderson-West, MP 22.013. Station markings are shown in red. Cores are indicated by purple circles and crack maps by blue rectangles. The slight curvature of the deck with respect to the longitudinal (East-West direction) was ignored in the subsequent sketches and analyses.

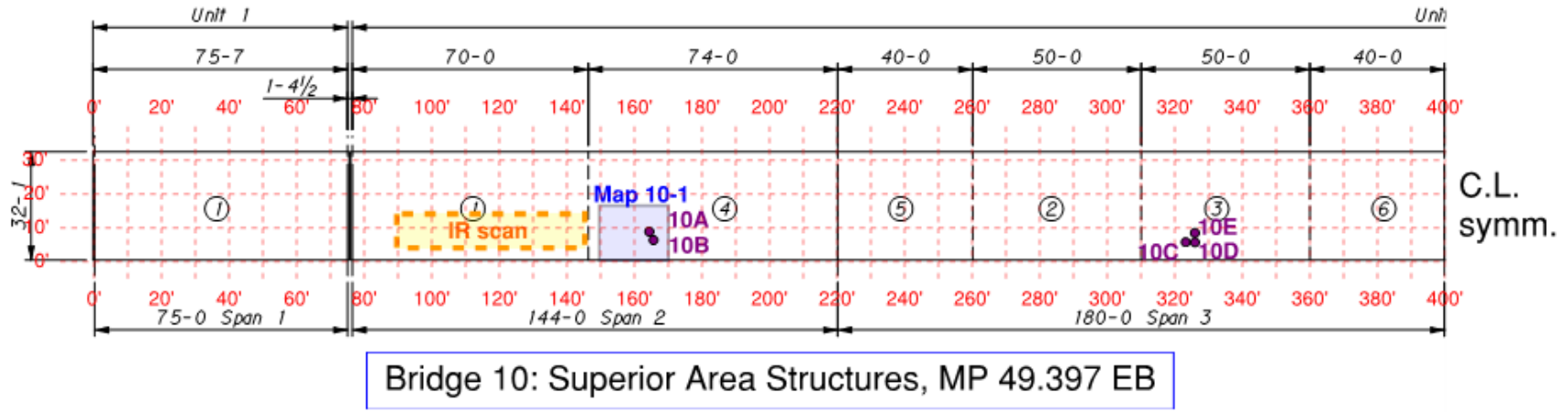

Figure 10. Annotated drawing of Bridge 10, Superior Area Structures, MP 49.397 EB. Station markings are shown in red and are reversed for the parallel span, Bridge 11. The structure is symmetric about its centerline (400' station marking). Cores are indicated by purple circles and crack maps by blue rectangles.

Crack Mapping

Transverse, longitudinal, and random cracks were sketched on plan drawings for 20-foot wide sections of each bridge deck. Multiple areas of Bridges 1, 2, 6, and 10 were mapped during the in-depth investigations, and individual areas of Bridges 3, 5, 11, and 12 were mapped during the cursory investigations. The crack maps are shown in Figure 11 to Figure 21. The total crack widths were also measured over 50-foot lengths of Bridges 1, 2, and 6 to estimate the total volume change of the decks. The results of these measurements are shown in Table 7.

All 12 bridge decks exhibited some degree of transverse and longitudinal cracking. The transverse cracks were more frequent and generally wider than the longitudinal cracks for all 12 of the bridges investigated. The transverse cracks typically extended from the girders or ran along the piers, while the longitudinal cracks typically formed over the girders and occasionally half-way between adjacent girders. The transverse cracks were spaced at 2 to 4 feet in most bridges, and ranged in top surface width from 5 to 35 mils (0.005 to 0.035 inches). Some decks also exhibited random map cracking, but these were not always visible on older decks. Map cracking was most pronounced for Bridge 1, which contained silica fume.

The frequency of wider cracks generally increased with the age of the bridge deck. The widest average crack widths were measured on the deck placed nine years ago (Bridge 6), while the finest cracks were measured on the deck placed one year ago (Bridge 12). Despite the finer cracks, however, the younger decks still showed similar crack patterns to the older decks, suggesting that the cracks initiate early in the life of the concrete and propagate and widen over time under environmental and live loads.

Based on the progression of the crack patterns from the youngest decks to the oldest decks, it is hypothesized that the transverse cracks initiate near the girders, where the restraint is the greatest, and propagate away from the girders with time. When the transverse cracks propagate past one another in close proximity (typically, within 6 to 18 inches), the crack tips bend toward one another, eventually "jumping" from one crack to another. Such "jump" crack patterns were observed in Bridges 2, 6, and 10, and were reflected on the top and bottom surfaces of the deck in Bridge 6 (see Figure 22 and Figure 23). It is hypothesized that the holes previously observed in Bridges 2 and 10 may have initiated at such "jump" crack locations.

Table 7. Crack width measurements, Bridges 1, 2, and 6

Bridge	Year	Measurement Location	Total Crack Width (inches)	Average Crack Width (inches)	Total Width (microstrain)
1	2014	East-bound driving lane, 100' to 150'	0.215	0.009	358
1	2014	West-bound driving lane, 250' to 300'	0.280	0.010	467
2	2011	East-bound driving lane, 220' to 270'	0.400	0.012	667
6	2007	East-bound driving lane, 30' to 80'	0.240	0.014	400

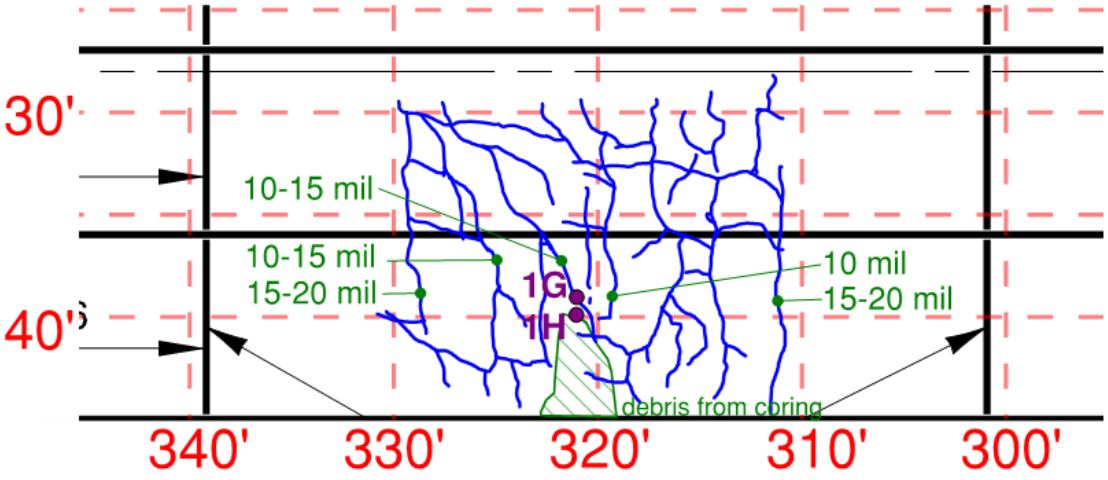

Figure 11. Crack map, Bridge 1, Map 1-1. Transverse cracks in this area measured 10-20 mil in width and were spaced at roughly 4-foot intervals.

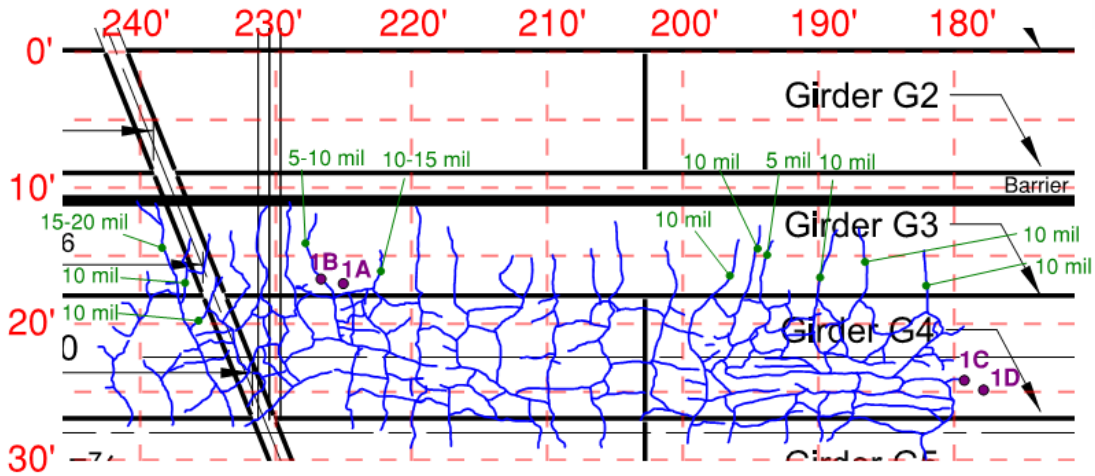

Figure 12. Crack maps, Bridge 1, Maps 1-2 (240' to 220'), 1-3 (220' to 200'), and 1-4 (200' to 180'). Transverse cracks in this area typically measured 10 mil in width and were spaced at 2- to 4-foot intervals. Dense map cracking was observed over large areas of the deck. The widest crack observed was over the pier; cracks in the vicinity of the pier were rotated relative to the transverse and longitudinal cracks observed elsewhere in the deck.

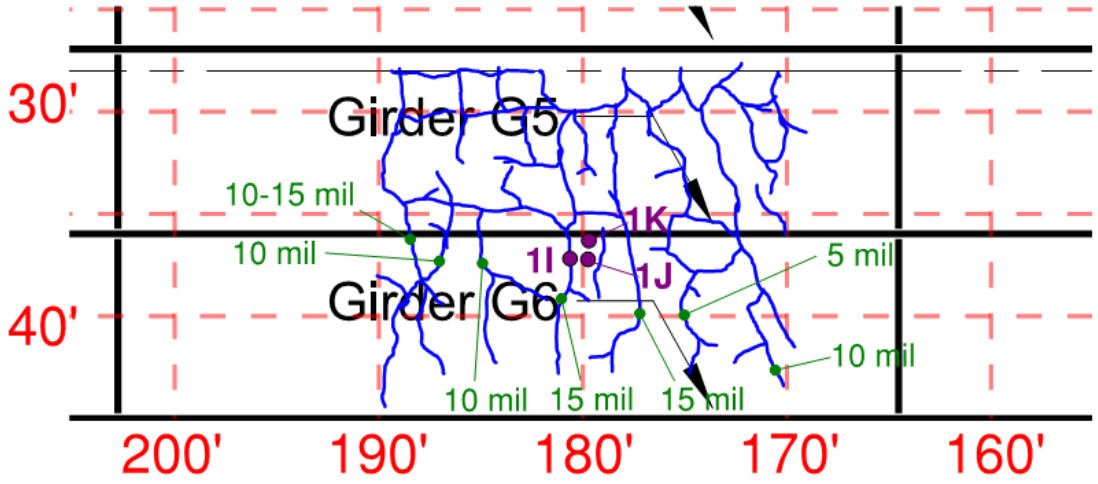

Figure 13. Crack map, Bridge 1, Map 1-5. Typical transverse cracks in this area measured 10-15 mil in width. Longitudinal cracks appeared primarily along girders G5 and G6.

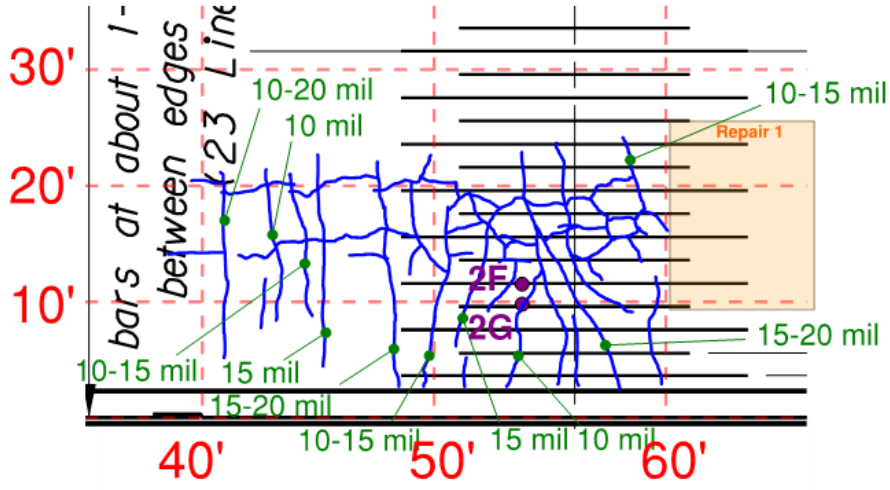

Figure 14. Crack map, Bridge 2, Map 2-1. Cracks in this area were primarily transverse (10-20 mil width), with longitudinal cracks along the girders at 16' and 22'. Some random cracking was also observed near the pier at 56'.

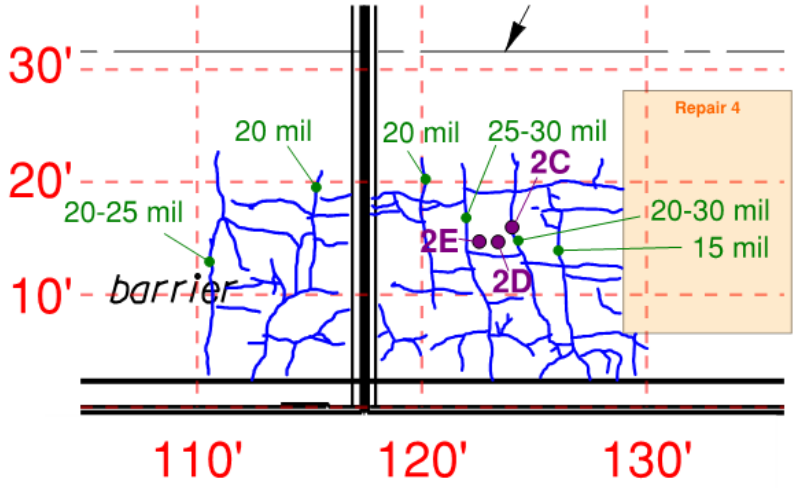

Figure 15. Crack map, Bridge 2, Map 2-2. Transverse cracks in this area measured 20-30 mil in width and were spaced at 2- to 4-foot intervals. Longitudinal cracks appeared primarily along the girders at 9' and 16' in Span 2 (left of expansion joint) and along the girders at 11' and 20' in Span 3 (right of expansion joint). Additional longitudinal cracks were also observed between the girders at 3' and 9' (or 10' in Span 3), with fine transverse cracks propagating outward from these longitudinal cracks.

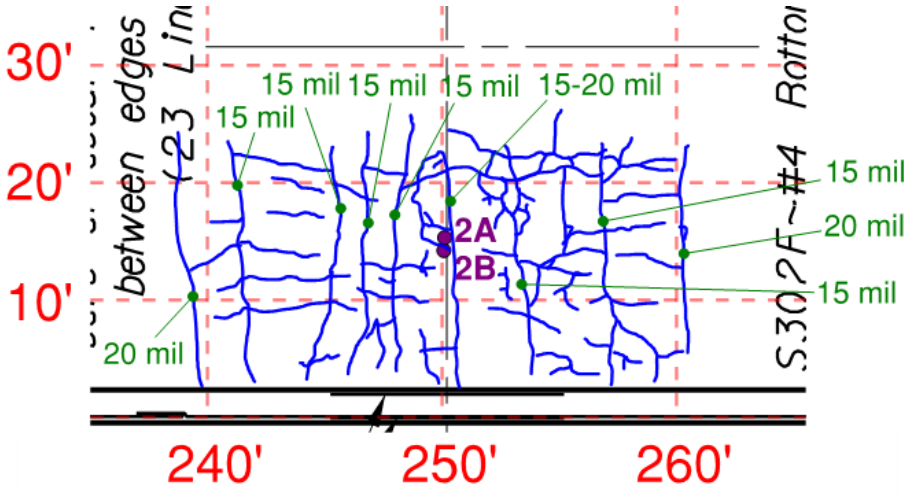

Figure 16. Crack map, Bridge 2, Map 2-3. Transverse cracks in this area measured 15-20 mil in width and were spaced at 2- to 4-foot intervals.

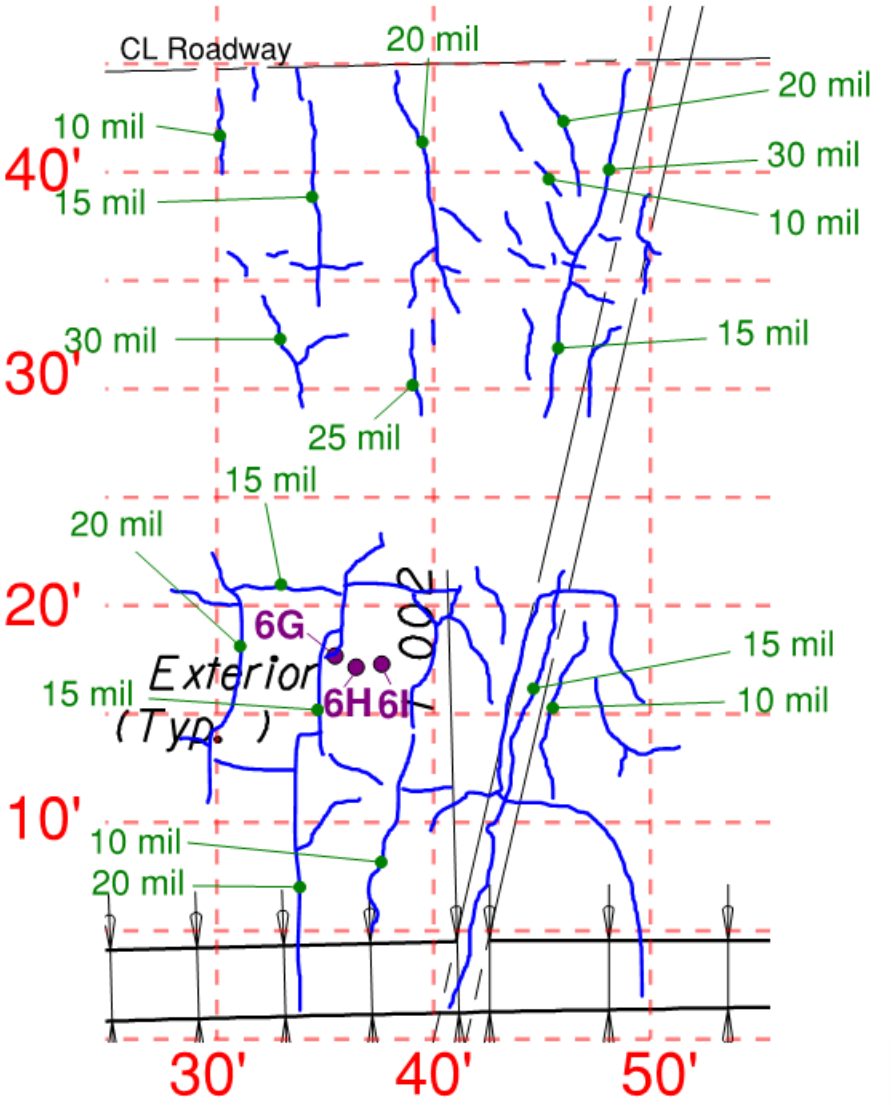

Figure 17. Crack map, Bridge 6, Maps 6-1 (passing lane) and 6-2 (driving lane). Transverse cracks in this area measured 10-30 mil in width and were more raveled than the cracks in the other bridges decks. Wide cracks propagated along the pier. A "jumping" crack is shown near core 6G.

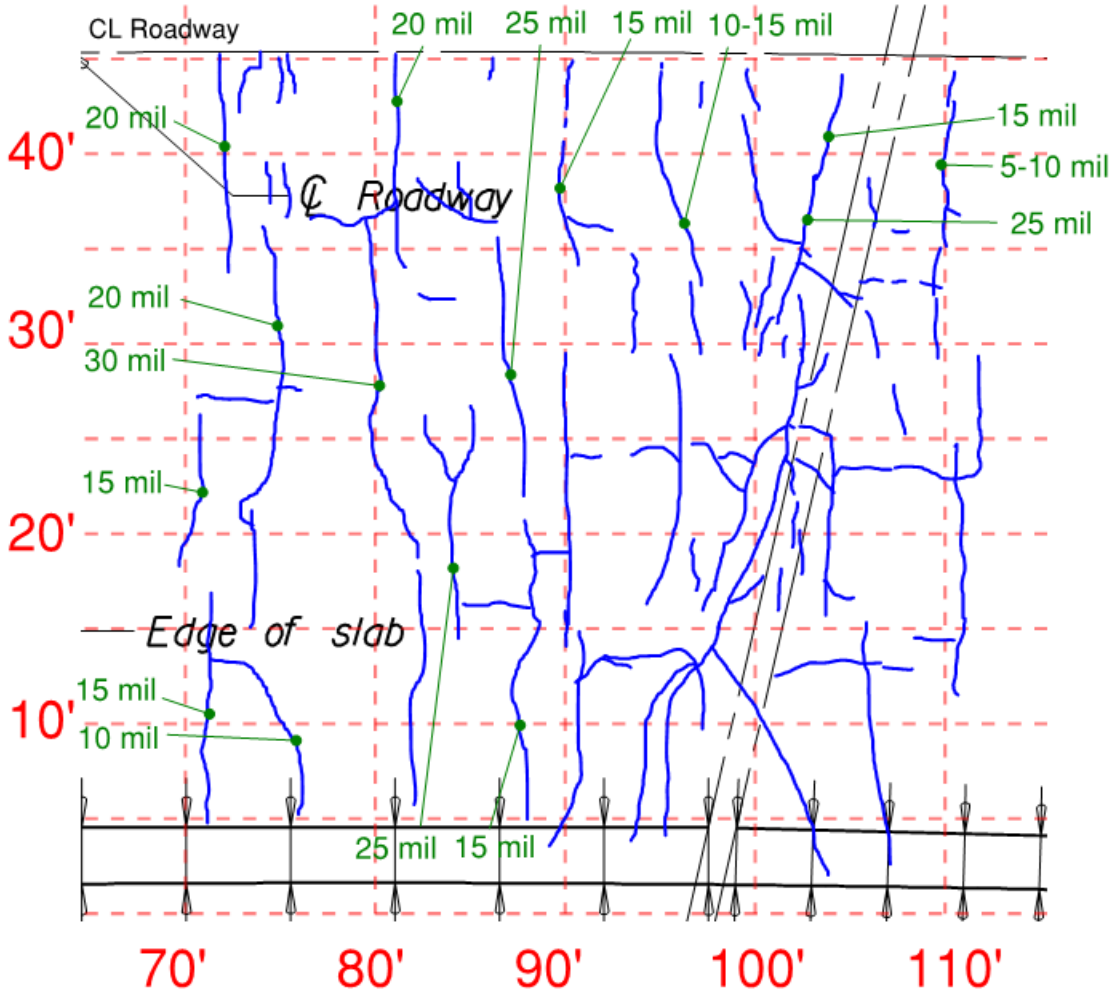

Figure 18. Crack map, Bridge 6, Maps 6-3 (passing lane, 70' to 90'), 6-4 (driving lane, 70' to 90'), 6-5 (passing lane, 90' to 110'), and 6-6 (driving lane, 90' to 110'). Transverse cracks in this area were raveled and measured 15-25 mil in width. Wide cracks propagated along the pier.

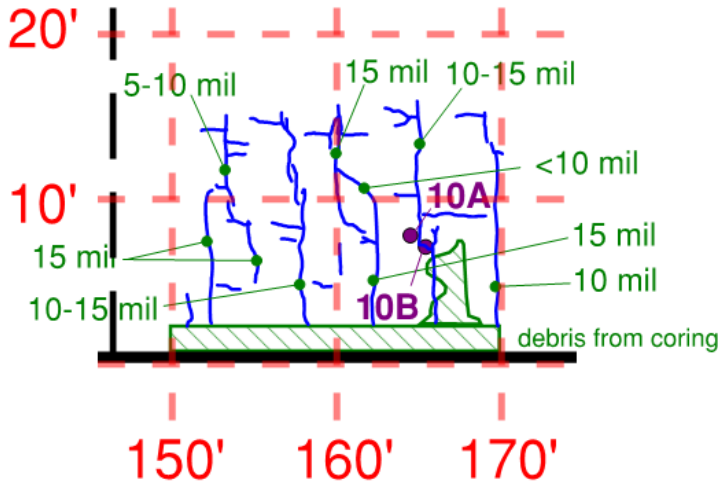

Figure 19. Crack map, Bridge 10, Map 10-1. Transverse cracks in this area measured 10-15 mil in width. A "jumping" crack is shown near core 10B, and a series of "jumping" crack is shown along the transverse crack at the 158' station marking.

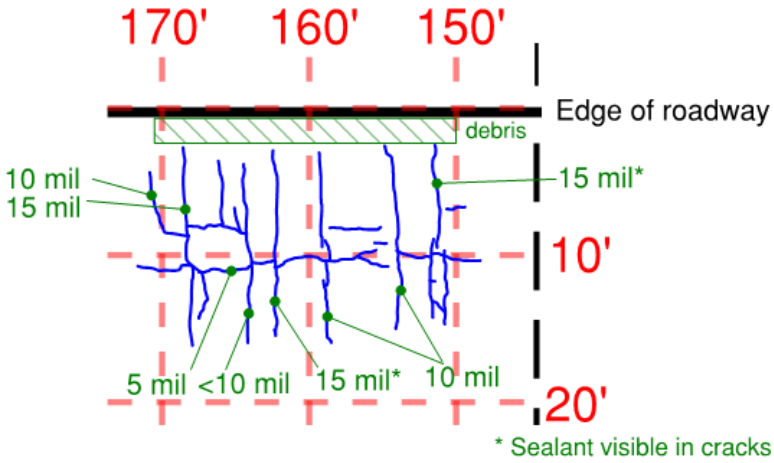

Figure 20. Crack map, Bridge 11, Map 11-1. Transverse cracks in this area measured 5-15 mil in width. A sealant was visible within the cracks measuring 15 mil in width. A longitudinal crack measuring 5 mil in width follows the girder at 10'.

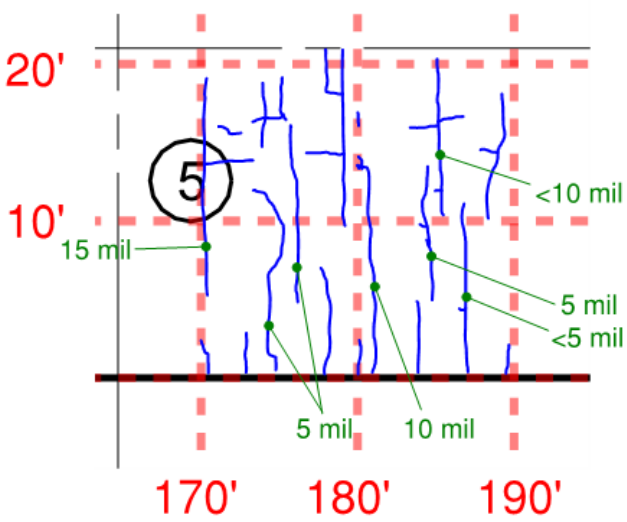

Figure 21. Crack map, Bridge 12, Map 12-1. Transverse cracks in this area typically measured less than 10 mil in width, but were consistent in pattern and spacing to the transverse cracks in the other bridges.

Figure 22. "Jump" cracks in top side of Bridge 6. Cracks are spaced approximately 6 inches apart.

Figure 23. "Jump" cracks from Figure 22, as reflected in the underside of the deck of Bridge 6.

Core Extraction

A total of 43 four-inch nominal diameter cores were extracted from the bridge decks for further laboratory study at WJE's Janney Technical Center (JTC) in Northbrook, IL. Cores were extracted in both cracked and uncracked areas of the deck and over reinforcing bars to for subsequent visual observation, physical testing, and chemical and petrographic analysis. The number and location of cores extracted from each bridge is summarized in Table 8, and the description of the cracks and reinforcing bar present in each core is summarized in Table 9. A complete description of the laboratory tests performed on each core is described in the "Laboratory Analysis" section of this report.

Table 8. Core Location Summary

Bridge #	# of Cores	Core Location(s)		Notes
1	11	Cores 1A, 1B: Cores 1C, 1D: Cores 1E, 1F: Cores 1G, 1H: Cores 1I, 1J, IK:	Span 2, EB lane, 220’ station marking, above Girder G3 Span 2, EB lane, 180’ station marking, C.L. of structure Span 3, EB lane, 10’ station marking, above Girder G3 Span 1, WB lane, 320’ station marking, 5’ from edge of deck Span 2, WB lane, 180’ station marking, 10’ from edge of deck	Core 1K fell through deck and was not retrieved
2	8	Cores 2A, 2B: Cores 2C, 2D-I/II, 2E: Cores 2F, 2G:	Pier 5, driving lane, 250’ station marking, 7’ from edge of deck Span 3, driving lane, 125’ station marking, 7’ from edge of deck Span 1, driving lane, 50’ station marking, 5’ from edge of deck	Core 2D-I fell through deck and was not retrieved; replaced by Core 2D-II from same location
3	3	Cores 3A, 3B: Core 3C:	Span 3, driving lane, 280’ station marking, 5’ from edge of deck Span 5, driving lane, 575’ station marking, 10’ from edge of deck	Cores taken through overlay
4	-	-		-
5	1	Core 5A:	Span 2, driving lane, 65’ station marking, 7’ from edge of deck	-
6	9	Cores 6A, 6B, 6C: Cores 6D, 6E, 6F: Cores 6G, 6H, 6I:	Span 3, passing lane, 125’ station marking, 15’ from C.L. barrier Span 1, driving lane, 35’ station marking, 15’ from edge of deck Span 2, driving lane, 65’ station marking, 10’ from edge of deck	Crack in core 6G was reflected through underside of deck
7	-	-		-
8	-	-		-
9	-	-		-
10	5	Cores 10A, 10B: Cores 10C, 10D, 10E:	Span 2, driving lane, 165’ station marking, 7’ from edge of deck Span 3, driving lane, 325’ station marking, 10’ from edge of deck	-
11	3	Cores 11A, 11B, 11C:	Span 4, driving lane, 330’ station marking, 10’ from edge of deck	Core 11A taken over crack with sealant
12	3	Cores 12A, 12B: Cores 12C:	Span 2, EB lane, 275’ station marking, 15’ from edge of deck Span 2, EB lane, 280’ station marking, 15’ from edge of deck	Core 12C taken over crack with sealant

Note: In-depth investigations are highlighted. C.L. = center line.

Table 9. Core Descriptions

Bridge #	Core ID	Crack	Rebar	Notes
1	1A			
	1B	X		Transverse crack, < 10 mil
	1C			
	1D	X		Longitudinal crack, < 10 mil
	1E			
	1F	X	X	Diagonal crack, < 10 mil Transverse reinforcing bar
	1G	X	X	Diagonal crack, 10 mil Longitudinal reinforcing bar
	1H	X		Transverse crack, 10 mil
	1I	X	X	Transverse crack, 15 mil Transverse reinforcing bar
	1J			
	1K			Fell through deck; not retrieved
2	2A			
	2B	X		Map crack, hairline
	2C	X	X	Transverse crack, 25 mil Transverse reinforcing bar
	2D-I	X		Longitudinal crack, hairline Fell through deck; retrieved
	2D-II	X		Longitudinal crack, hairline
	2E			
	2F			
	2G	X		Map crack, < 10 mil
3	3A	X		Map cracks, < 10 mil Crack in overlay does not appear to reflect from base concrete
	3B	X		Intersecting map cracks, < 10 mil Longitudinal crack in overlay appears to reflect from base concrete; transverse crack does not
	3C	X		Intersecting map cracks, < 10 mil Core taken close to midspan Crack in overlay reflected from base concrete
5	5A	X		Diagonal crack, 15 mil Appears to be in very early stages of progression
6	6A	X	X	Transverse crack, 15 mil Transverse reinforcing bar
	6B			
	6C			
	6D	X		Diagonal crack, 10 mil
	6E			
	6F			
	6G	X		Possible progression crack, 10 mil Crack reflected on underside of deck
	6H			
	6I			

Bridge #	Core ID	Crack	Rebar	Notes
10	10A			
	10B	X		Transverse progression crack, 10 mil
	10C			
	10D			
	10E	X		Longitudinal crack, 10 mil
11	11A	X	X	Transverse crack, < 10 mil with sealant Bottom reinforcing bar
	11B			
	11C			
12	12A	X		Longitudinal crack, < 5 mil Propagates between two transverse cracks
	12B			
	12C	X	X	Transverse crack, 10 mil with sealant Transverse reinforcing bar

Delamination Survey

Near-surface delaminations were identified by mechanical sounding of the bridge decks using chain dragging and hammering methods. The locations of the delaminations were identified, and their approximate areas were recorded. The total delaminated area was estimated for each deck. Delamination surveys were not performed on Bridges 4 and 8.

Delaminations were detected on Bridges 1, 3, 6, and 7. Most delaminations measured less than 1-foot by 1-foot, and in all cases, the total area delaminated was less than 0.5% of the deck area surveyed. Bridge decks 3 and 7, which had the largest delaminated fractions of the 12 bridge decks, both consisted of a 2 1/2-inch overlay applied to an existing concrete deck; the small fraction of delaminated areas in these decks suggests that the overlays are well-bonded to the concrete substrate.

Table 10. Delaminations Detected

Bridge	Estimated Total Area of Delaminations (ft^2)	Estimated Fraction of Surveyed Area (%)
1	3	0.03
2	None detected	0
3	10	0.08
4	*Not surveyed*	
5	None detected	0
6	1	0.02
7	13	0.26
8	*Not surveyed*	
9	None detected	0
10	None detected	0
11	None detected	0
12	None detected	0

Impulse Response (IR) Survey

Impulse response (IR) surveys were conducted using a Germann Instruments s'MASH unit on Bridges 1, 2, 6, and 10 to compare the relative modal response of the bridge decks and to identify areas potentially containing initiation of structural distress. Impulse response is a non-destructive test method in which a hammer is used to impact an element, and the nearby vibration response is collected and analyzed to obtain the mobility spectrum of the element. The mobility spectrum provides an indication of the relative flexibility (stiffness) of the element at the test location and can also be used to identify locations of poor consolidation (e.g., honeycombing), distress, or delamination within a concrete element.

The IR surveys were conducted over 5-foot intervals along the longitudinal direction of each bridge, as denoted by the yellow boxes outlined in Figure 7 through Figure 10. Three points were impacted at each longitudinal station, with points 1 and 3 typically over adjacent girders, and point 2 typically midway between the two girders. Contour plots of the average mobility and dynamic stiffness determined by IR for each bridge are shown in Figure 24 to Figure 27. The approximate locations of the girders and piers are overlaid for reference.

The mobility and stiffness plots both indicate that the deck is less flexible (i.e., has a lower average mobility or a higher dynamic stiffness) over the piers and girders than it is away from them. The higher mobility between the girders helps explain the occurrence of "jump" cracks and that through deck failures are most likely to occur mid-way between girders.

Overall, the baseline mobilities and stiffnesses are generally small (less than 20 units), compared to the mobilities and stiffnesses in areas that are affected by delaminations, voids, or other effects. The deck repairs to Bridge 2 appear to have only a small effect on the mobility and stiffness measured.

Two scanned areas of the Bridge 1 deck had significantly higher average mobilities than the surrounding bridge deck. Average mobilities in excess of 50 units were detected near the 285' and 195' station markings. Although delaminations or voids were not detected by chain drag at these locations, other delaminations of similar size were detected in the vicinity of these high-mobility regions, suggesting that intense cracking, delaminations, or voids may be present in the concrete at these locations. No other areas of high average mobility were identified for the other three bridge decks, which had infrequent incidence of delaminations and voids detected by chain drag. Due to the locality of the characteristic cracking that causes the deck penetrations, a general survey of the deck mobility may not pick up incipient areas of distress. Although IR testing was informative, identification of incipient deck distress is more easily done by visual inspection and recognition of tell-tale indicators rather than by measuring deck mobility.

Two scanned areas of the Bridge 6 deck had higher average stiffnesses than the surrounding deck. The stiff area at 5' is located near the intersection of the bridge deck and the approach slab, over Pier 1. No other field evaluation was performed in this area, however photographs of the area provided by MDT show a nearby patch in the pavement of the approach slab. The stiff area at 100' is located along Pier 2, in a region where several cracks were noted to initiate in the crack map shown in Figure 18. No other areas of high dynamic stiffness were identified for the other three bridge decks.

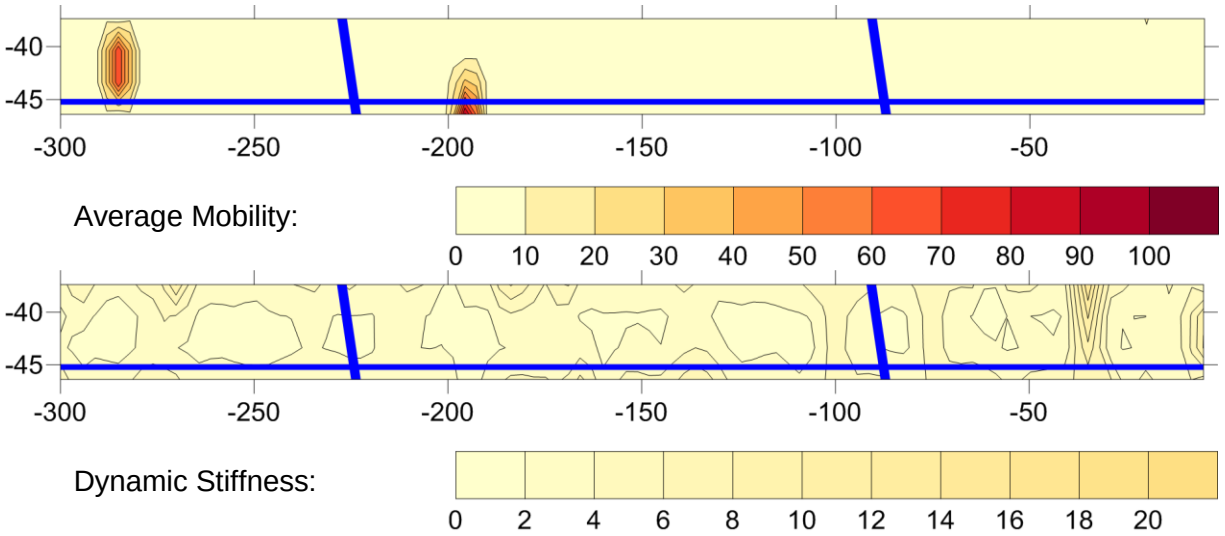

Figure 24. Mobility and stiffness contour plots, Bridge 1. Note: Station markings in this figure are shown with a negative sign to preserve orientation shown in Figure 7. Increased mobility may indicate incipient distress.

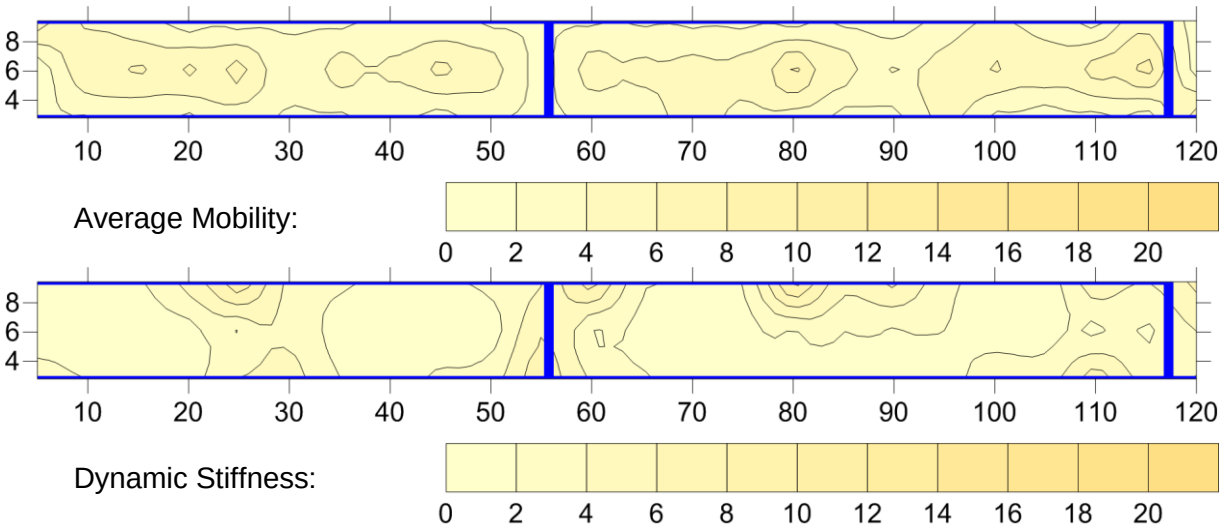

Figure 25. Mobility and stiffness contour plots, Bridge 2.

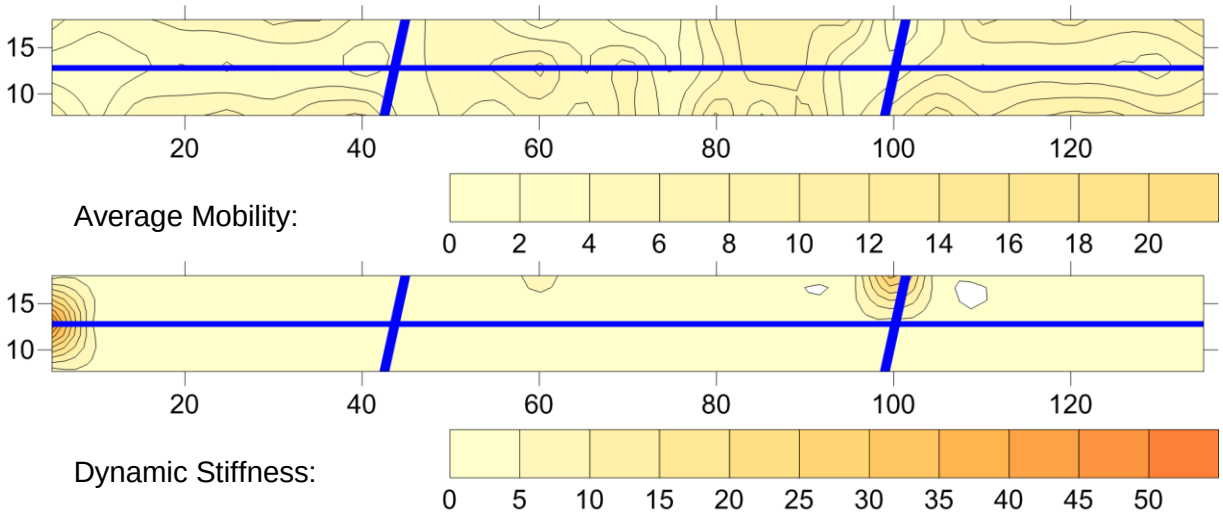

Figure 26. Mobility and stiffness contour plots, Bridge 6.

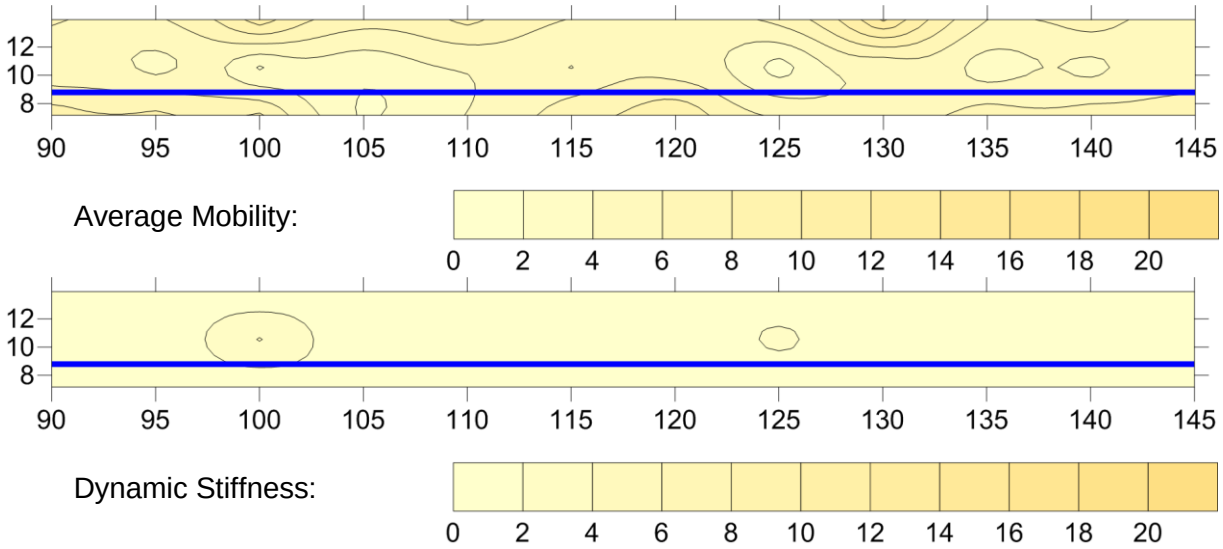

Figure 27. Mobility and stiffness contour plots, Bridge 10.

Ground Penetrating Radar (GPR) Scan

A Geophysical Survey Systems, Inc. (GSSI) StructureScan Mini ground penetrating radar (GPR) unit was used to estimate the thickness of the deck slab and to identify the location and depth of the reinforcing bars. GPR was also used during core extraction to determine the location of the reinforcing bar relative to the core extraction site.

Table 11 summarizes the average bar depths and deck thicknesses and estimated by the GPR scans. Bar depths are reported relative to the top surface of the deck, and measurements made on extracted cores are

also provided for comparison where available. Based on comparison of the GPR estimates and the measured bar locations, the GPR scans tend to underestimate the average slab depth and bar locations by approximately 1/2 inch. Therefore, although several of the decks had estimated depths less than that specified (as little as 6 inches locally), it cannot be stated on the basis of the GPR scans that the slab depths or bar depths differed significantly from those specified in the plans.

Table 11. Average Slab Depths and Bar Depths Estimated by GPR

Bridge	Range	Depth of Slab (inch)[1]			Top Transverse Bar Location (inch)			Bottom Transverse Bar Location (inch)		
		Spec.	Est.	Meas.	Spec.	Est.	Meas.	Spec.	Est.	Meas.
1	Entire length	8	7 3/4	8 1/4	2 3/8	2 1/2	2 1/2, 2 5/8	6 3/8	-	7 1/8, 6 5/8
2	0' to 117'-3"	7 1/4	-	-	2 3/8	-	-	5 5/8	-	-
	117'-3" to 198'-9"	7 3/4	-	7 5/8	2 3/8	-	2 1/2	6 1/8	-	6 1/4
	198'-9" to 296'	8	7 1/8		2 3/8	2 1/8	-	6 3/8	-	-
3	*Overlay*									
4	*Not measured*									
5	*Not measured*									
6	Entire length	7 1/2	7	-	2 3/8	2 1/4	2 5/8	5 7/8	-	-
7	*Overlay*									
8	*Not measured*									
9	*Not measured*									
10	0' to 75'	8 1/4	-	-	2 3/8		-	6 5/8	-	-
	75' to 725'	7 1/2	7 1/2	-	2 3/8	2 3/4	-	5 7/8	-	6 3/8
	725' to 800'	8 1/4	-	-	2 3/8	-	-	6 5/8	-	-
11	0' to 75'	7	-	-	2 3/8	-	-	5 3/8	-	-
	75' to 725'	6 3/4	6 1/4	-	2 3/8	2 1/8	2 5/8	5 1/8	4 7/8	-
	725' to 800'	7	-	-	2 3/8	-	-	5 3/8	-	-
12	Entire length	9	8 1/4	-	2 3/8	2 1/2	-	7 3/8	-	-

[1]Spec. = specified (plans), Est. = estimated (GPR), Meas. = measured (cores).

Infrared Imaging

Infrared videos of the deck surfaces were recorded for Bridges 1, 2, and 12 using a drone equipped with an infrared camera. Infrared images can be used to identify cracks, delaminations, areas of poor consolidation, and other features of the bridge decks where defects cause sharp, minute differences in surface temperature. Overhead videos without infrared imaging were also recorded for Bridges 1, 2, 10, and 12. All drone-recorded footage was provided to MDT personnel separate from this report.

Examples of infrared images recorded for Bridges 1, 2, and 12 are shown in Figure 28 through Figure 33, along with images of the corresponding features detected. Large cracks (Figure 28) and delaminations (Figure 30) were both clearly visible under infrared light, as were localized repairs (Figure 30) and surface crack sealants (Figure 32). In general, there were very few delaminated or poorly consolidated areas identified by the infrared camera, which was consistent with the low frequency of delaminated areas identified by chain drag, GPR, and impulse response surveys. The delaminated areas identified by the infrared camera tended to be on the order of 1 square foot in area, which is also similar in size to the areas identified by the other techniques.

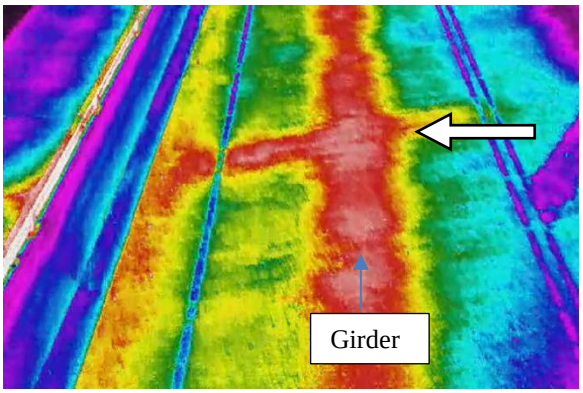

Figure 28. Overhead infrared photograph of Bridge 1 deck surface. A large transverse crack over Pier 3 of Bridge 1 is indicated by the arrow. Girder G3 and line stripping are also visible.

Figure 29. Overhead drone photograph of Bridge 1 deck surface. The large transverse crack over Pier 3 shown in Figure 28 is outlined by the dashed line.

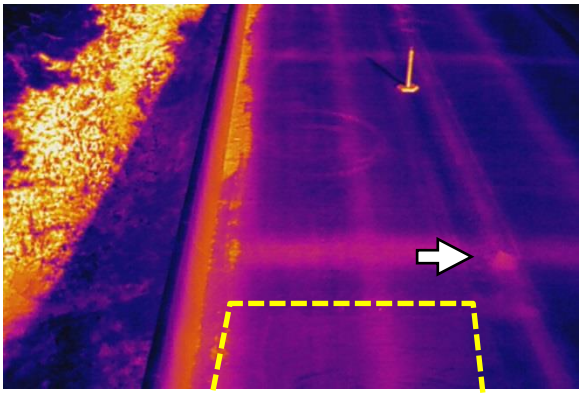

Figure 30. Overhead infrared photograph of Bridge 2 deck surface. The area shown approximately corresponds to the area mapped in Figure 14. Girders, piers, and diaphragms are clearly visible. A possible delamination or void is indicated by the arrow. Repair #1 (as shown in Figure 8) is outlined by the dashed line.

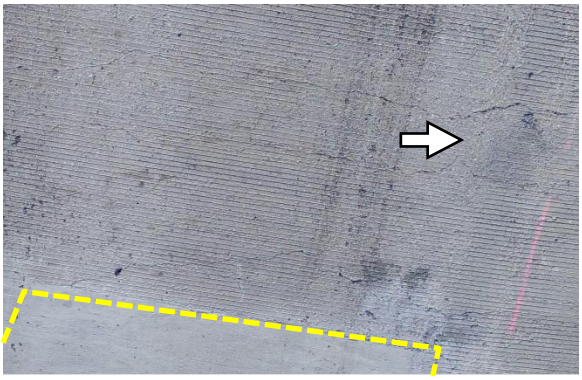

Figure 31. Overhead drone photograph of Bridge 2 deck surface. The area shown is a close-up of the area indicated in Figure 30. The possible delamination or void indicated by the arrow is surrounded on both sides by wide transverse cracks over Pier 2. Repair #1 is outlined by the dashed line.

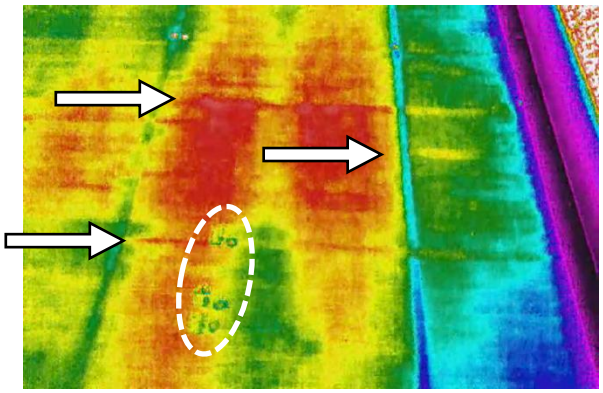

Figure 32. Overhead infrared photograph of Bridge 12 deck surface. Three transverse cracks (sealed) are indicated by white arrows. Cores 12A, 12B, and 12C were taken at the locations circled.

Figure 33. Photograph of Bridge 12 deck surface, near location shown in Figure 32. The sealed transverse crack through Core 12C was clearly visible by infrared imaging, while the narrower crack through Core 12A was not.

Other Field Observations

Temperature

Deck surface temperatures were measured during the in-depth investigations of Bridges 1, 2, 6, and 10, as summarized in Table 12. Overall, the top surfaces of the bridge decks experienced temperature swings of approximately 50 °F over 5 hours of measurements, from a low of about 40 °F to a high between 90 and 100+ °F. A peak deck surface temperature of 104 °F was recorded during the field investigation of Bridge 1.The undersides of the decks remained cooler throughout the day, with temperatures ranging between 40 and 60 °F. A maximum differential of 31 °F was observed between the top and bottom deck surfaces of Bridge 10. Such differences in temperature between the topside and the underside of the deck could lead to thermally-induced bending and thermal strains within the deck, and should be considered as a possible source for the initial cracking and/or subsequent crack propagation.

Table 12. Deck Temperatures

Bridge #	Time	Deck Surface	Underside	Ambient
1	Afternoon	104 °F	-	-
2	Morning	42-45 °F	-	50-52 °F
	Afternoon	86-91 °F	-	77-78 °F
6	8:00 AM	43 °F	-	48 °F
	9:00 AM	66 °F	58 °F	54 °F
	10:00 AM	74 °F	-	66 °F
	12:00 PM (cloudy)	72 °F	-	71 °F
	1:30 PM (sunny)	90 °F	-	71 °F
10	7:30 AM	41 °F	40 °F	45 °F
	10:30 AM	69 °F	49 °F	62 °F
	12:00 PM	74 °F	-	-
	12:30 PM	83 °F	52 °F	68 °F

Efflorescence

Efflorescence samples were collected from the undersides of Bridges 2 and 6 for further laboratory study. The sample from Bridge 2 was primarily white in color, while the sample from Bridge 6 contained both white and gray components.

Laboratory Studies

The cores and efflorescence samples taken during the field investigation were delivered to WJE's laboratories in Northbrook, IL for further study. A preliminary visual assessment was performed on each core to document the size of the core, the approximate depth of crack penetration, and the types and locations of the reinforcing bars. Based on the preliminary observations, specific cores were selected for physical testing, petrographic analysis, and chemical analysis. Each method is described briefly below. A list of samples used for each study is provided in Table 13.

Table 13. Summary of Laboratory Analyses Performed on Cores

Bridge #	Compressive Strength	Splitting Tensile Strength	Modulus of Elasticity	Coefficient of Thermal Expansion	Petrographic Analyses[1]	Air Void Analysis	Chloride Profiles
1	1E, 1J	1C	1A	1A	1D, 1I	1D	-
2	2D-II, 2E	2F	2A	2A	2C	2C	-
3	-	-	-	-	3A - overlay 3B - overlay	-	-
4	*No cores taken*						
5	-	-	-	-	-	-	-
6	6E, 6H	6I	6B	6B	6G	-	6A
7	*No cores taken*						
8	*No cores taken*						
9	*No cores taken*						
10	-	-	-	-	10B	-	10E
11	-	-	-	-	11A - sealant	-	-
12	-	-	-	-	12A	-	-

[1] Full petrographic analyses, including thin-section analyses, were performed on cores from Bridges 1, 2, 6, 10, and 12.

Physical Testing

The following physical properties of the concrete were determined from cores containing no cracks or reinforcing bar:

- **Compressive and Splitting Tensile Strength** were measured in accordance with ASTM C42, *Standard Test Method for Obtaining and Testing Drilled Cores and Sawed Beams of Concrete*. The ends of the compressive strength specimens were cut and capped prior to testing, and the edges of the tensile strength specimens were lapped free of any chatter as needed to provide a smooth testing surface.

- **Modulus of Elasticity** was measured in accordance with ASTM C469, *Standard Test Method for Static Modulus of Elasticity and Poisson's Ratio of Concrete in Compression*. The ends of the specimen were cut and capped prior to testing. Three wire strain gauges, located at approximately third points around the circumference, having an effective length of 2 inches were bonded to the surfaces of each specimen

to measure strains under the applied load. The modulus of elasticity was calculated from the stress-strain data averaged over two runs for each test specimen.

- **Coefficient of Thermal Expansion** was measured according to an in-house testing procedure. Three sides of each core, located at approximately third points around the circumference, were made plane by grinding. Two Whittemore strain buttons were installed on each planed surface at a 4 inch gauge length. The specimens were submerged in a water bath at room temperature (72 °F) for a minimum of 48 hours, and an initial reading was made with the Whittemore gauge. The temperature of the bath was cycled twice between 140 °F and 40 °F, holding each temperature for at least 48 hours prior to subsequent length change measurements. The coefficient of thermal expansion was determined after each temperature change as the average temperature-induced strain in the specimen divided by the change in temperature. The specimen's saturated coefficient of thermal expansion was taken as the average of the four individual measurements.

Table 14 gives a summary of the average physical properties measured on cores taken from Bridges 1, 2, and 6. Bridge 1 had the greatest compressive and tensile strengths and the stiffest modulus of elasticity of the three bridges examined, which is consistent with the use of fly ash and silica fume in its mixture. Bridges 2 and 6 had similar straight-cement concrete mixtures, and both consequently had similar compressive strengths and elastic moduli that were less than those measured for Bridge 1. All three bridges measured similar coefficients of thermal expansion between 3.6 and 5.0 × 10^{-6}/°F; typical thermal expansion coefficients for concrete reported in the literature range between 4 and 7 × 10^{-6}/°F (ACI Committee 207 2007).

Table 14. Summary of Measured Physical Properties

Bridge	Compressive Strength (psi)	Splitting Tensile Strength (psi)	Modulus of Elasticity (ksi)	Coefficient of Thermal Expansion (/ °F)
1	7370	770	4,450	4.8 × 10^{-6}
2	5090	600	3,300	3.6 × 10^{-6}
6	6090	605	3,950	5.0 × 10^{-6}

Petrographic Analyses

Petrographic analyses were conducted to examine the general quality of the concrete, the progression of the cracks within the concrete, the bond quality at the overlay/substrate interfaces, and the presence of internal distress mechanisms. Petrographic examinations were conducted in accordance with the applicable methods of ASTM C856, *Standard Practice for Petrographic Examination of Hardened Concrete*. Water-cement (w/c) ratio and total air contents were estimated by microscopic observation, and complete air void analyses were conducted according to ASTM C457, *Standard Test Method for Microscopical Determination of Parameters of the Air-Void System in Hardened Concrete*, on three cores (1D, 1I, and 2C). Detailed petrographic observations are reported in Appendix C.

The petrographic studies revealed no materials-related cause for the cracking. Proportions of constituents appeared normal, except for variations in air content. Evidence of internal distress mechanisms that could produce bulk volumetric instability was not observed. Pertinent observations include:

- The volume of fly ash in the concrete did not appear excessive.
- Water-cementitious materials ratios were variable and occasionally estimated higher than designed.

- Aggregates were sound and had performed adequately in service. The coarse aggregate included substantial amounts of high-absorption sedimentary rocks that could contribute to high shrinkage; however, evidence of adverse aggregate behavior was not observed.
- Measured air contents were high for cores 1D, and 2C, and estimated air contents were high for cores 1I, 3B, 6G, and 10B (at least locally – up to 12%). Despite the high air contents and local variations within the cores, the air void systems generally appeared adequate to protect the concrete against distress caused by cyclic freezing and thawing.
- Representative deck cracks commonly occurred inline or adjacent to steel reinforcement. Cracks predominantly passed around aggregate particles and appeared to be wider at the top of the concrete. Cracking through aggregate particles was less commonly observed and only seen in the bottom region of the concrete. Crack observations indicate that cracking was initiated early at the top of the concrete (before the concrete had gained strength and while paste-to-aggregate bond was weak). The cracks progressed deeper in the concrete after the concrete had gained appreciable strength.
- The frequency of paste microcracking was not excessive (generally infrequent except near the main cracks). Movement of the cracked sections of concrete probably caused these secondary cracks.
- White glaze that was observed on some crack surfaces was analyzed using SEM/EDX. The glaze mostly contained calcium, silicon, oxygen, and carbon. Smaller amounts of aluminum, potassium, sodium, magnesium, and iron were routinely detected. The composition of the glaze is consistent with precipitation from water saturated with elements leached from the cementitious paste.

Chemical Analyses

Chloride Contents

Acid-soluble chloride analyses were performed according to ASTM C1152, *Method for Acid Soluble Chloride in Mortar and Concrete* on a total of twelve slices sampled from cores 6A and 10E. Samples for analysis were taken at three different depths along the cracks in each core, and from three identical depths away from the cracks in each core. The chloride contents of the twelve slices are listed in Table 15. The chloride concentration profiles shown in Figure 34 were constructed from the results.

Table 15. Chloride Contents

Sample	Location	Acid-Soluble Chloride, percent by mass of sample
Core 6A Crack	Top Middle Bottom	0.359 0.196 0.171
Core 6A Non-Crack	Top Middle Bottom	0.332 0.210 0.205
Core 10E Crack	Top Middle Bottom	0.159 0.096 0.070
Core 10E Non-Crack	Top Middle Bottom	0.187 0.093 0.045
Bridge 6 Efflorescence White Portion	---	0.091

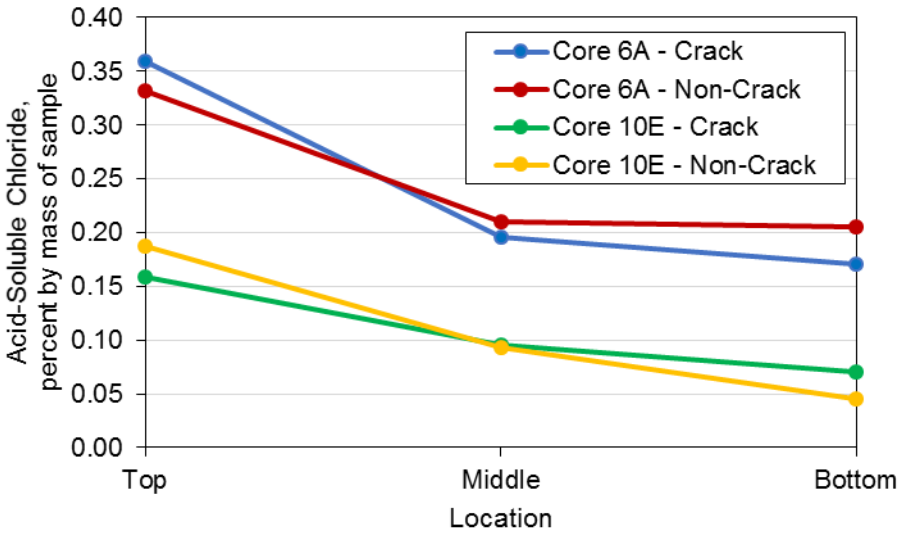

Figure 34. Acid-soluble chloride contents measured along the cracks ("crack") and away from cracks ("non-crack") in cores 6A and 10E.

The chloride concentrations were similar in both the cracked and non-cracked areas of both cores. Studies have shown that chloride contents above 0.02 to 0.03 percent by mass of concrete, depending on the cement content, can promote corrosion of embedded uncoated carbon steel in non-carbonated normal weight concrete. The chloride contents of all the samples analyzed were above to well above this threshold level, and therefore, may promote the corrosion of uncoated or damaged spots on coated steel in the presence of sufficient moisture and oxygen.

Efflorescence

Two efflorescence samples from Bridges 2 and 6 were analyzed for crystalline components by x-ray diffraction (XRD). The efflorescence sample from Bridge 2 was separated into grey and white portions prior to analysis. The efflorescence sample from Bridge 6 was mostly white and was analyzed as received.

During x-ray diffraction analysis, radiation produced from an x-ray source is diffracted off the sample at various angles. A detector measures the intensity of the diffracted energy, and the location (angle) and intensity are recorded as a graph. This graph, which displays a pattern of peaks, can be interpreted to identify the crystalline components of the sample. The peaks are compared to a library of diffraction patterns of known components to identify the crystalline materials present. The results are listed in Table 16.

Calcite was the only crystalline component detected in the white portions of the efflorescence samples. The crystalline components detected in the grey portion of the Bridge 2 efflorescence sample were typical of crystalline components normally found in concrete or dirt.

Acid-soluble chloride analysis was also performed essentially according to ASTM C1152 on the efflorescence sample from Bridge 6. The sample contained 0.091 percent chloride by mass of sample.

Table 16. X-ray Diffraction Analysis

Sample	Crystalline Components Detected
Bridge 6	Major--Calcite ($CaCO_3$)
Bridge 2 White Portion	Major--Calcite
Bridge 2 Grey Portion	Major--Quartz (SiO_2), calcite, Minor--Feldspar Possibly--Clay
Bridge 2 Spall Residue From Water Extraction	Major--Calcite Minor--Halite (NaCl), sylvite (KCl)

Modeling

Petrographic observations of the cracked cores indicate that the transverse cracks initiated early at the top of the concrete deck and progressed deeper after the concrete had gained appreciable strength. Early transverse cracking may develop primarily due to autogenous shrinkage of the deck concrete or to thermal changes or gradients in the deck and supporting beams. Because there is no information available regarding the early-age temperature and crack development in the bridge decks under investigation, two models were used to simulate the conditions under which early cracks may have developed in the bridge decks.

ConcreteWorks Thermal Model

Temperature histories were simulated for the decks of Bridges 1, 2, and 6 using ConcreteWorks[11]. To simulate the temperature history of a bridge deck element, the ConcreteWorks software uses user-defined mixture proportions and cement compositions to approximate the heat of hydration of the concrete (an internal source of heat), and historical or user-defined environmental conditions to generate air temperature, wind velocity, and solar radiation histories (external sources of heat). The thermal properties of the concrete - thermal conductivity and specific heat capacity - are assumed by the software based on the materials and mix proportions. The deck thickness and the thermal properties of the formwork and insulation (if used) are entered as additional inputs. The model combines these parameters with fundamental models for heat transfer to generate an approximate temperature profile history for the bridge deck element.

Temperature histories were simulated for the decks of Bridges 1, 2, and 6, assuming placement times as indicated on the batch tickets. Three additional simulations were performed for placement times of 6:00 a.m., 12:00 p.m. (noon), and 6:00 p.m. to demonstrate how temperatures develop in the bridge decks at different deck placement times. Table 17 summarizes the ConcreteWorks input parameters and the values assumed for each model. Figure 35 to Figure 37 show the maximum simulated deck temperatures for each bridge deck at each assumed placement time. A constant plastic concrete temperature of 65 °F was assumed for all models.

The simulation results demonstrate that temperatures develop in the concrete deck at different rates depending on the placement time. In every case, the deck experiences the greatest temperature increase due to its internal heat of hydration. When the concrete is placed in the morning (e.g., 12:00 am. - 12:00 p.m.), the peak hydration temperatures occur at approximately the same time as the peak ambient temperatures and solar radiation. This rapidly warms the deck, so that the concrete reaches its peak temperature approximately 18 hours after placement, or at about the time that the air is coolest; creating the largest temperature differential. When the concrete is placed in the late afternoon or early evening, the hydration temperatures build while the air temperatures and solar radiation are lower. This restricts the rate at which the deck heats up, so that the peak concrete temperature is reduced and the peak does not occur until approximately 24 hours after placement, when the daytime air and solar radiation are near or just past their peak. These different rates of heat development likely can have potentially significant effects on the stresses that are generated in the decks.

Table 17. Inputs for ConcreteWorks Thermal History Model

Input Category	Parameter	Assumed Values
General Inputs	Placement Time	Earliest time indicated on batch tickets +6:00 a.m., 12:00 p.m. (noon), and 6:00 p.m.
	Location	Missoula, MT
	Duration of Simulation	7 days
Shape Inputs	Type of Structure	Bridge deck w/ removable wood forms
Member Dimensions	Deck Thickness	Thickness as specified in plans
	Cover to Top Reinforcing Bar	2 3/8 inches, as specified
Mixture Proportions	Mixture Proportions and Chemical Admixture Types	Proportions and admixtures indicated in approved mix design
Material Properties	Cement Composition	Bogue compositions indicated on cement mill certificates
	Aggregate Types	Siliceous river gravel and siliceous river sand
	Thermal Properties	Coefficient of thermal expansion (CTE): 5.0×10^{-6}/ °F Thermal conductivity (k): 1.73 BTU/hr/ft/°F (default) Aggregate specific heat capacity (C_p): 0.18 BTU/lb/°F (default)
	Hydration Parameters	Default software values based on mix proportions and cement composition
Construction Inputs	Concrete Placement Temperature	65 °F (based on average value measured for Bridge 1)
	Formwork Type	Plywood
	Curing Blanket Insulation R-Value	1.0 (manual-recommended value for burlap)
	Plastic Layer on Top of Blanket	White or clear plastic (polyethylene sheeting, as specified)
	Age of Blanket and Form Removal	≥ 7 days
Environment Inputs	Air Temperature	Daily high and low temperatures recorded at Missoula International Airport for first week after deck placement (NCDC database[12])
	Wind Speed	Daily peak wind speed recorded at Missoula International Airport for first week after deck placement (NCDC database[12])
	Solar Radiation	Default software values based on historic averages for Missoula
	Relative Humidity	Default software values based on historic averages for Missoula

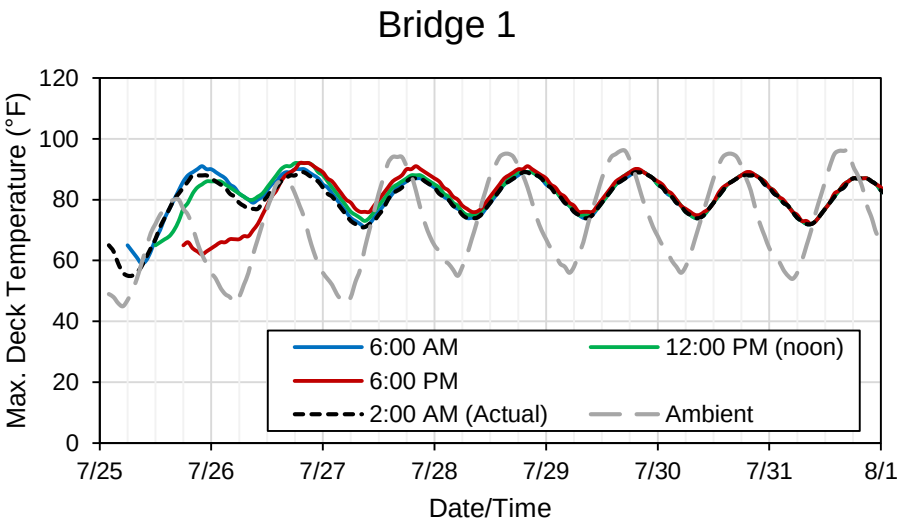

Figure 35. Maximum deck temperature simulated for Bridge 1 in ConcreteWorks for various placement times.

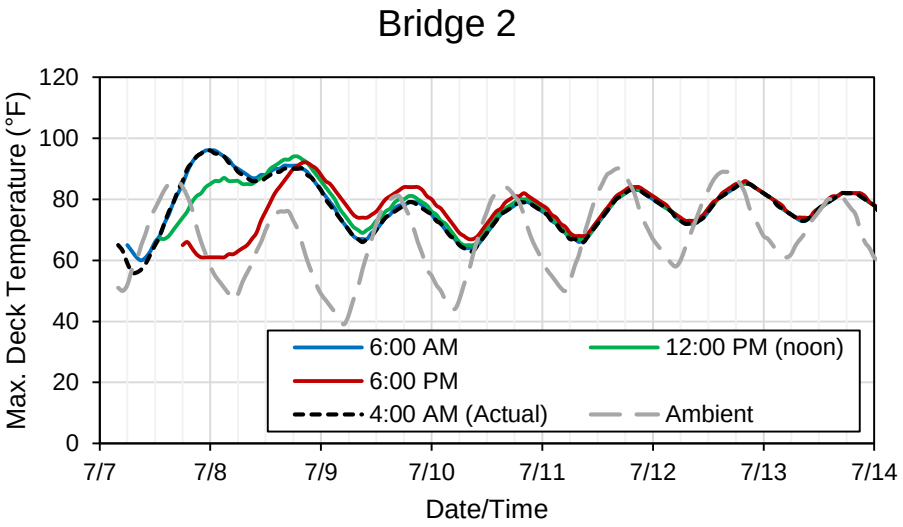

Figure 36. Maximum deck temperature simulated for Bridge 2 in ConcreteWorks for various placement times.

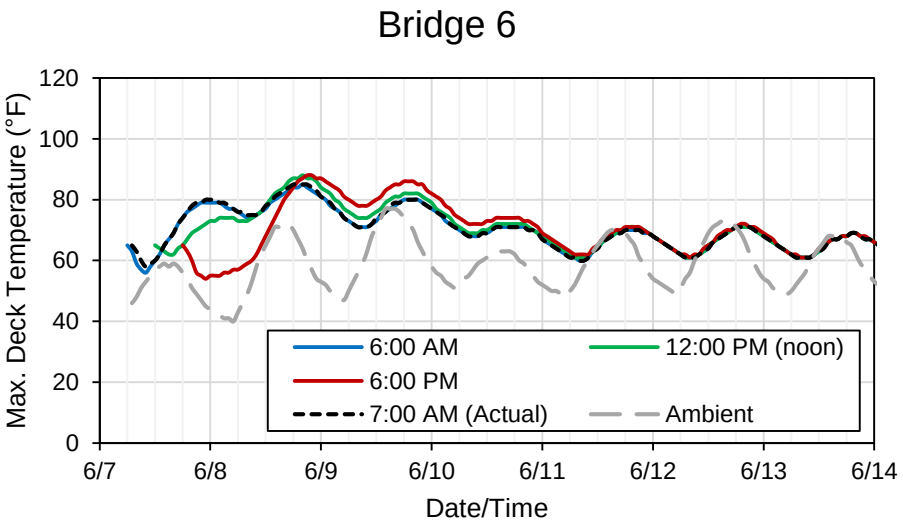

Figure 37. Maximum deck temperature simulated for Bridge 6 in ConcreteWorks for various placement times.

Stress Model

To simulate the stresses generated in the bridge decks under various thermal and shrinkage strains, a basic stress analysis model was developed in Mathcad, based on the analysis of W. Zuk[13]. The model first separates the deck into three horizontal sections (Figure 38) and calculates the free (unrestrained) strain in the girder and in each section of the deck due to a specified linear temperature or shrinkage profile over the section. For thermal strains, the free strains are calculated from the temperature profiles as:

$$\begin{pmatrix}\epsilon_{top}\\ \epsilon_{bot}\end{pmatrix}=\alpha\begin{pmatrix}\Delta T_{top}\\ \Delta T_{bot}\end{pmatrix}$$

where $\varepsilon_{top,\ bot}$ are the free strains at the top and bottom of the section, respectively, α is the coefficient of thermal expansion for the material, and $\Delta T_{top,\ bot}$ are the temperature change in the top and bottom of the section, respectively, relative to an initial, strain-free temperature T_0.[2]

After calculating free strains in each section, the model then applies compatibility requirements to force equal strains and curvatures at all deck/deck and deck/girder interfaces. The shear forces and moments required to maintain this compatibility are calculated and then used to determine the overall stresses developed at the top and bottom surfaces of the deck under the applied thermal and shrinkage profiles.

[2] The initial, strain-free temperature is the temperature of the concrete at the time when the concrete first gains measurable strength, typically 9 to 12 hours after placement.

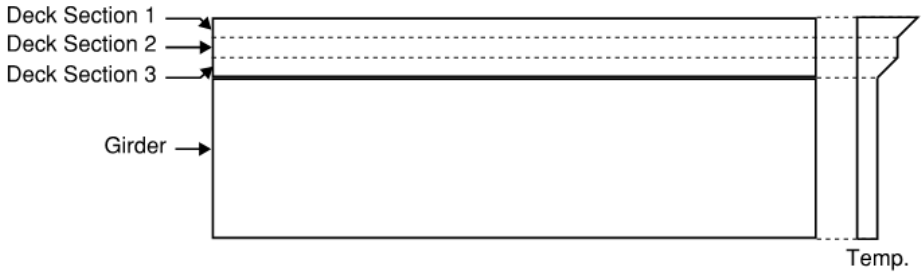

Figure 38. Sketch of sections used in stress model. A possible temperature profile is shown to the right.

Three models were developed to simulate the thermal and shrinkage stresses generated in Bridges 1, 2, and 6. A parameter sensitivity study was conducted using the Bridge 1 model to determine which factors most influence the development of tensile stresses in the decks. Additional simulations were performed on all three bridge decks to investigate early-age and long-term stress development under various temperature and shrinkage profiles.

Table 18 lists the parameters included in each model and defines the values assumed for each simulation. The thermal and mechanical properties used in the simulations were either obtained by physical testing on cores or assumed based on prior experience. Creep of the deck concrete is implicitly included in the model by reducing the elastic modulus of the young concrete by one-half and the mature concrete by one-third. The creep adjustment factor reduces the stresses estimated for the bridge deck to account for stress recovery under sustained loads.

For early-age concrete, the tensile strength was assumed to be approximately 10% of the assumed compressive strength; for mature concrete, the tensile strength was assumed to be approximately the value measured for the cores. In both cases, the concrete was considered “at risk” for cracking if the tensile stresses in the deck exceeded 80% of the tensile strength, due to the effect of fatigue.

Table 18. Inputs for Mathcad Stress Model

Input	Parameter	Bridge 1	Bridge 2	Bridge 6
Thermal and Mechanical Properties: Deck	Coefficient of Thermal Expansion	5.0×10^{-6}/°F (measured on cores)		
	Poisson's Ratio	0.20 (assumed)		
	Compressive Strength	Early-age: 1500 psi, or as indicated Mature: 7370 psi (measured on cores)	Early-age: 1500 psi, or as indicated Mature: 5090 psi (measured on cores)	Early-age: 1500 psi, or as indicated Mature: 6090 psi (measured on cores)
	Modulus of Elasticity	Early-age: $57{,}000\sqrt{f_c(psi)}$, where f_c is the compressive strength of the concrete Mature: 4450 ksi (measured on cores)	Early-age: $57{,}000\sqrt{f_c(psi)}$, where f_c is the compressive strength of the concrete Mature: 3300 ksi (measured on cores)	Early-age: $57{,}000\sqrt{f_c(psi)}$, where f_c is the compressive strength of the concrete Mature: 3950 ksi (measured on cores)
Thermal and Mechanical Properties: Beam	Coefficient of Thermal Expansion	5.0×10^{-6}/°F for concrete		
	Modulus of Elasticity	$57{,}000\sqrt{8000(psi)}$ = 5,098 ksi for concrete		
Deck Geometry	Thickness	8 in.	Spans 1-2: 7 1/4 in. Span 3: 7 3/4 in. Spans 4-5: 8 in.	7.5 in.
Beam Geometry	Depth	6 ft. 0 in.	Spans 1-2: 3 ft. 4 in. Span 3: 4 ft. 6 in. Spans 4-5: 3 ft. 4 in.	3 ft. 4 in.
	Area	886 in^2	Spans 1-2: 438 in^2 Span 3: 789 in^2 Spans 4-5: 438 in^2	438 in^2
	Moment of Inertia	636,612 in^4	Spans 1-2: 79,494 in^4 Span 3: 260,730 in^4 Spans 4-5: 79,494 in^4	79,494 in^2
	Centroid Location	32.29 in.	Spans 1-2: 17.93 in. Span 3: 24.73 in. Spans 4-5: 17.93 in.	17.93 in.
	Section Modulus	Calculated from moment of inertia and centroid location		
	Typical Spacing	9 ft. 0.5 in.	Spans 1-2: 6 ft. 7.5 in. Span 3: 8 ft. 10 in. Spans 4-5: 8 ft. 10 in.	9 ft. 5 in.
Temperature	Deck Temperature	Variable		
	Beam Temperature	Variable, constant		
Shrinkage	Deck Shrinkage	Variable		

Sensitivity Analysis

A parameter sensitivity study was initially performed using the model for Bridge 1. Factors investigated include the compressive strength of the deck concrete, the thickness of the deck, the spacing of the girders, the magnitude of autogenous and drying shrinkage, a uniform temperature change in the deck and beam, and a linear temperature change through the deck. Each factor was varied independently and the resulting stresses in the top and bottom of the deck were evaluated. A complete summary of the sensitivity analysis is provided in Appendix D. The key findings are summarized below:

- The compressive strength (elastic modulus) of the deck concrete has a small effect on the stresses that are developed. While doubling the compressive strength of the deck concrete approximately doubles its tensile strength, it only increases the thermal stresses in the deck by an estimated 20-25%. This implies that the risk of thermal cracking is the greatest at early ages, when the magnitude of the thermal stress is large relative to the tensile strength of the concrete.

- Thermal and shrinkage stresses are larger in thin decks than in thicker decks. A 2-inch increase in the thickness of the deck (e.g., from 6 inches to 8 inches) can reduce the magnitude of thermal and shrinkage stresses generated in the deck by 10-25%.

- Thermal and shrinkage stresses are larger in bridge decks with more closely spaced girders, influencing deck stresses by about 10 to 20%.

- The initial temperature rise caused by the heat of hydration generates compressive stresses in the deck. Tensile stresses are generated only after the deck has cooled below its strain-free temperature, T_0. Larger stresses are generated by temperature gradients in the deck than by uniform temperature changes, increasing stresses by about 30 percent.

- Autogenous shrinkage is a potentially significant contributor of tensile stresses in young concrete. An autogenous shrinkage of 40 microstrain generates tensile stresses of approximately 30 psi in the deck of Bridge 1, or about 20% of the assumed early-age tensile strength of the deck concrete.

- Drying shrinkage is the largest contributor of tensile stresses in mature concrete but would not be expected until after wet curing is complete. A uniform autogenous shrinkage of 500 microstrain generates tensile stresses of 413 and 477 psi in the top and bottom of the Bridge 1 deck, respectively, or approximately 60% of the measured splitting tensile strength of the deck concrete.

Stresses Generated by Realistic Temperature and Shrinkage Profiles

Simulation 1: Young Concrete, Uniform Temperature

The early-age stress development in Bridges 1, 2, and 6 was simulated using "realistic" temperature and shrinkage profiles. For the first set of simulations, uniform deck temperatures were assumed for each bridge, as shown in Table 19. This assumption is reasonable but not conservative for thin elements like bridge decks that are insulated at their top and bottom surfaces (by formwork, curing or insulating blankets, etc.). The temperatures used for each simulation were obtained from the ConcreteWorks temperature models. A strain-free temperature, T_0, was selected as the temperature of a deck concrete 12 hours after placement.

Stresses were evaluated at the peak temperature on Day 1 (500 psi compressive strength assumed) and at the low temperature on Day 3 (2000 psi compressive strength assumed). No autogenous shrinkage was

assumed for Day 1, and a moderate 20 microstrain of autogenous shrinkage was assumed for Day 3. Because the peak temperature on Day 1 occurs near the lowest ambient temperature, a uniform temperature decrease of 10 °F was assumed for the girder on Day 1; no temperature change was assumed for Day 3.

The simulated stresses for each bridge deck are shown in Table 20 (Day 1) and Table 21 (Day 3). At the peak hydration temperature for Day 1, all three bridge decks are under compression, with the assumed 10 °F temperature decrease in the girder contributing approximately 30% of the total modeled compressive stresses. Bridge 2 has the largest simulated compressive stresses, consistent with its comparatively larger temperature increase and close spacing of the girders.

At the lower temperature simulated for Day 3, all three bridge decks are under tension. Bridge 2 again had the largest simulated thermal stresses, consistent with the large temperature decrease relative to the other two bridge decks. For Bridge 2, the 20 microstrain of autogenous shrinkage contributed 20% of the total simulated tensile stress. Bridges 1 and 6 experienced much lower temperature decreases, and autogenous shrinkage contributed a much larger 40-60% of the total tensile stresses modeled for those bridges.

The largest tensile stress simulated for Day 3 was 71 psi, located at the bottom of Bridge 2, Span 3. During the field investigation, Span 3 was observed to have a somewhat higher frequency of transverse cracking compared to the adjacent spans of Bridge 2, and the cracks were generally wider. In general, Bridge 2 had a higher frequency of transverse cracking than either Bridge 1 or Bridge 6. Therefore, although the peak tensile stresses simulated by the first series of models are less than 35% of the assumed tensile strength (200 psi), the relative magnitudes of the stresses are consistent with the relative severity of transverse cracking observed in the bridge decks.

Simulation 2: Young Concrete, Temperature Gradient
The second set of simulations considered non-uniform deck temperatures during early hydration. This is more closely related to actual deck temperatures. The deck temperatures given in Table 19 were assumed to apply uniformly over the lower two-thirds of the deck, but the top surface was assumed to be 10 °F cooler than the rest of the concrete due to cooler air temperatures or contact with cooler curing water. The stresses developed under these conditions are given in Table 22 (Day 1) and Table 23 (Day 3).

In both scenarios, the 10 °F cooling of the top surface of the deck significantly increased the tensile stresses (or decreased the compressive stresses) at the top surface of the deck with little impact on the stresses at the bottom surface of the deck. Stresses at the top surface of the deck still remained mostly compressive on Day 1, but tensile stresses of up to 130 psi were found for the Day 3 model (65% of the assumed tensile strength). Even greater tensile stresses would be anticipated if the top deck surface cooled more than 10 °F relative to the rest of the bridge deck or if greater autogenous strains were generated.

Simulation 3: Mature Concrete, Temperature and Shrinkage Gradient
The third set of simulations considered "realistic" temperature and shrinkage gradients for mature concrete. In these simulations, temperature profiles were assumed based on the temperatures measured during the field investigation. For the high-temperature simulation, it was assumed that the lower two-thirds of the deck was at a constant 52 °F (measured at 12:30 p.m. on the bottom surface of the Bridge 10 deck) and the top surface of the deck was at 104 °F (measured in the afternoon on the top surface of the Bridge 1 deck). For the low-temperature simulation, it was assumed that the deck was at a uniform 40 °F (measured at 7:30 a.m. on the Bridge 10 deck).

A non-uniform shrinkage profile was assumed for both simulations. It was assumed that the top surface of the deck (exposed to the most drying) experienced 500 microstrain of drying shrinkage, but that the lower two-thirds of the deck (exposed to less drying) experienced 300 microstrain of drying shrinkage. Girder temperature changes were ignored for both simulations.

The assumed temperature profiles are shown in Table 24. The results of the simulations are given in Table 25 (high temperature) and Table 26 (low temperature). In both cases, the largest contributor to the tensile stresses developed is drying shrinkage. At high temperatures, compression in the top surface of the deck reduces tensile stresses generated by drying, but large tensile stresses are still developed in the bottom of the deck (approximately 50% of the measured tensile strength). At low temperatures, tension in the top surface of the deck adds to the tensile stresses generated by drying, producing very large shrinkage stresses at the top surface that exceed 90% of the splitting tensile strength measured on cores for Bridges 1 and 2. These drying shrinkage assumptions for these simulations may be un-conservative; however, the results demonstrate that there is a continued risk for drying shrinkage cracks to develop both in the top and bottom surfaces of the bridge decks.

Table 19. Early-Age Temperature and Shrinkage Profiles Simulated

Bridge #	T_0 degrees F	Day 1 (f_c = 500 psi)			Day 3 (f_c = 2000 psi)		
		Peak Temp. degrees F	Girder Temp. degrees F	Autogenous Shrinkage microstrain	Low Temp. degrees F	Girder Temp. degrees F	Autogenous Shrinkage microstrain
1	74	88 (ΔT = +14)	ΔT = -10	0	71 (ΔT = -3)	ΔT = 0	20
2	79	96 (ΔT = +17)	ΔT = -10	0	66 (ΔT = -13)	ΔT = 0	20
6	76	80 (ΔT = +4)	ΔT = -10	0	71 (ΔT = -5)	ΔT = 0	20

Table 20. Stresses Generated in Young Bridge Decks due to Day 1 Temperature and Shrinkage, psi

Driving Force	Stress Location in Deck	Bridge 1, All Spans	Bridge 2, Spans 1-2	Bridge 2, Span 3	Bridge 2, Spans 4-5	Bridge 6, All Spans
Deck temperature change	Top	-37	-36	-42	-28	-7
	Bottom	-40	-42	-46	-36	-9
Girder temperature change	Top	-22	-18	-20	-14	-14
	Bottom	-24	-21	-22	-18	-18
Autogenous shrinkage in deck	Top	-	-	-	-	-
	Bottom	-	-	-	-	-
Total	Top	-59	-54	-62	-42	-21
	Bottom	-64	-63	-68	-54	-27

Table 21. Stresses Generated in Young Bridge Decks due to Day 3 Temperature and Shrinkage, psi

Driving Force	Stress Location in Deck	Bridge 1, All Spans	Bridge 2, Spans 1-2	Bridge 2, Span 3	Bridge 2, Spans 4-5	Bridge 6, All Spans
Deck temperature change	Top	12	35	44	24	10
	Bottom	13	49	54	41	16
Girder temperature change	Top	-	-	-	-	-
	Bottom	-	-	-	-	-
Autogenous shrinkage in deck	Top	16	11	14	7	8
	Bottom	18	15	17	13	12
Total	Top	28	46	58	31	18
	Bottom	31	64	71	54	28

Table 22. Stresses Generated in Young Bridge Decks due to Day 1 Temperature Gradient, psi

Driving Force	Stress Location in Deck	Bridge 1, All Spans	Bridge 2, Spans 1-2	Bridge 2, Span 3	Bridge 2, Spans 4-5	Bridge 6, All Spans
Deck temperature change	Top	0	1	-4	8	29
	Bottom	-42	-45	-48	-40	-12
Girder temperature change	Top	-22	-18	-20	-14	-14
	Bottom	-24	-21	-22	-18	-18
Autogenous shrinkage in deck	Top	-	-	-	-	-
	Bottom	-	-	-	-	-
Total	Top	-22	-17	-24	-6	15
	Bottom	-66	-66	-70	-58	-30

Table 23. Stresses Generated in Bridge Decks due to Day 3 Temperature Gradient, psi

Driving Force	Stress Location in Deck	Bridge 1, All Spans	Bridge 2, Spans 1-2	Bridge 2, Span 3	Bridge 2, Spans 4-5	Bridge 6, All Spans
Deck temperature change	Top	85	106	116	93	79
	Bottom	7	41	48	33	7
Girder temperature change	Top	-	-	-	-	-
	Bottom	-	-	-	-	-
Autogenous shrinkage in deck	Top	16	11	14	7	8
	Bottom	18	15	17	13	12
Total	Top	101	117	130	100	87
	Bottom	25	56	65	46	19

Table 24. Long-Term Temperature and Shrinkage Profiles Simulated

Deck Section	Location in Section	High-Temperature		Low-Temperature	
		Temp. degrees F	Drying Shrinkage microstrain	Temp. degrees F	Drying Shrinkage microstrain
1 (top third)	Top	104	500	40	500
	Bottom	52	300	40	300
2 (middle third)	Entire section	52	300	40	300
3 (bottom third)	Entire section	52	300	40	300

Table 25. Stresses Generated in Mature Bridge Decks due to High-Temperature and Shrinkage, psi

Driving Force	Stress Location in Deck	Bridge 1, All Spans	Bridge 2, Spans 1-2	Bridge 2, Span 3	Bridge 2, Spans 4-5	Bridge 6, All Spans
Deck temperature change	Top	-345	-249	-238	-263	-327
	Bottom	145	123	130	113	121
Drying shrinkage in deck	Top	591	403	444	351	401
	Bottom	262	184	209	148	156
Total	Top	246	154	206	88	74
	Bottom	407	307	339	261	277

Table 26. Stresses Generated in Mature Bridge Decks due to Low-Temperature and Shrinkage, psi

Driving Force	Stress Location in Deck	Bridge 1, All Spans	Bridge 2, Spans 1-2	Bridge 2, Span 3	Bridge 2, Spans 4-5	Bridge 6, All Spans
Deck temperature change	Top	144	102	126	72	69
	Bottom	165	134	149	113	114
Drying shrinkage in deck	Top	591	403	444	351	401
	Bottom	262	184	209	148	156
Total	Top	**735**	505	**570**	423	470
	Bottom	427	318	358	261	270

Red: exceeds 80% of the measured splitting tensile strength of the concrete.

APPENDIX C - PETROGRAPHY

ASTM C457 Standard Test Method for Microscopical Determination of Air-Void System in Hardened Concrete: Modified Point-Count Method

Operator:	Hugh Hou	**Dates of Testing:**	September 27, 2016
Approved By:	Laura Powers	**WJE Project No.:**	2016.3598
Client:	Montana State DOT	**Magnification Used:**	90X

Core ID	1D
Air Content %	11.5
Paste Content %	23.6
Sand Content %	28.1
Coarse Aggregate %	36.8
Void Frequency	19.2
Paste-Air Ratio	2.0
Average Chord Length (inch)	0.006
Specific Surface inch^2/inch^3	666
Spacing Factor (inch)	0.003
Total Transverse (inch)	90.8
Total Points Counted	1363
Tested Area (inch^2)	21.0
Aggregate Top Size (inch)	3/4

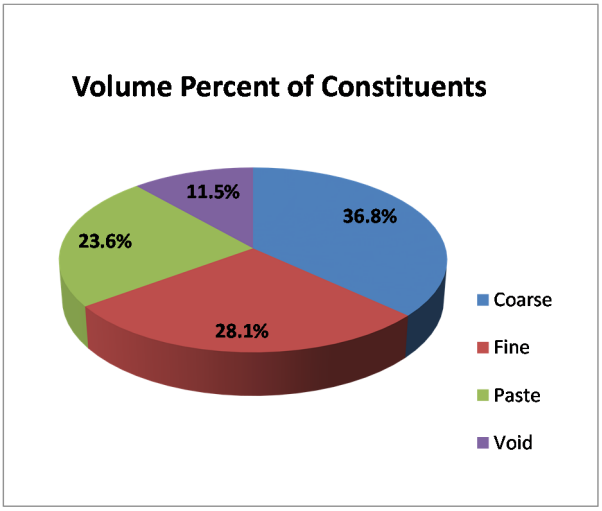

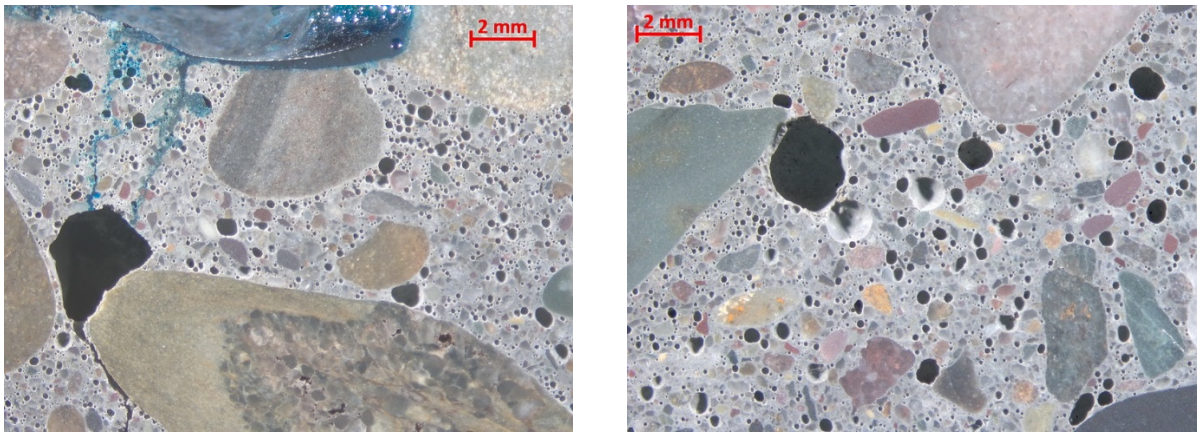

Appearance of air-void system.

CORE LOG - VISUAL OBSERVATIONS

Sample ID: 1D	**WJE Project No.: 2016.3598**
Sample Location: Florence - East, MP 10.640 EB	**Petrographer: Hugh Hou/L. Powers November 1, 2016**
Project Name: Forensic Deck Analysis -2016	**Date: September 16 to 26, 2016**

Figure 1. Core 1D. Side view. Top surface is on left.

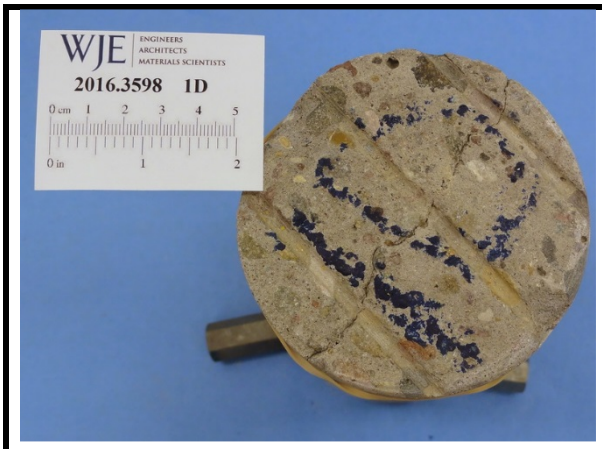

Figure 2. Core 1D. Top surface.

Figure 3. Core 1D. Bottom surface

Dimensions	Diameter: 3.7 inches Length: 7.0 inches
End Surfaces	Saw-grooved top surface. Fractured bottom surface extended both around and through aggregate particles.
Reinforcement	None observed.
Consolidation	A few scattered entrapped voids; well consolidated overall.
Distribution of Constituents	Aggregate and paste are uniformly distributed.
Cracks, Joints	0.002-0.004 inch wide vertical, longitudinal (relative to deck lanes in field) crack extended to a depth approximately 3 inches, and mainly around aggregate particles.
General Observations	Concrete is mainly composed of natural siliceous sand and gravel aggregates uniformly dispersed in air-entrained cementitious paste.

STEREOMICROSCOPE AND PETROGRAPHIC MICROSCOPE EXAMINATION

Aggregate Characteristics	CA: Gravel composed of sandstone, graywacke sandstone, meta-sandstone, quartzite, siltstone, and meta-siltstone. Small amounts of mudstone, limestone, schist, and igneous rock were also observed. Top size: 3/4 inch. FA: Natural siliceous sand mainly composed of quartz/quartzite, sandstone, and siltstone; small amounts of schist, chert, mudstone, mica, limestone, and other rocks and minerals were also observed. Measured volume percentages: CA 36.8%, FA 28.1% (see separate report).
Potentially Reactive Components	Chert, siltstone, mudstone, greywacke sandstone, and quartzite, or certain components of these rocks are potentially alkali-silica reactive (ASR). No evidence of ASR was observed in the core.
Paste-Aggregate Bond	Fracture surfaces created in the laboratory examination extended through substantially more aggregate particles than the crack.
Paste Characteristics	Medium to dark gray, subvitreous to vitreous, and hard. Measured paste volume is 23.6%. Residual portland cement and fly ash particles, and trace amount of agglomerated silica fume.

	Residual portland cement estimated at 3 to 5% by volume of paste. Hydration of cement is advanced. Residual fly ash estimated at 6 to 9% by volume of paste. Calcium hydroxide generally small in size, estimated at 1 to 2 %. Replacement rate of fly ash estimated at approximately 20%.
Water-Cementitious Materials Ratio (w/cm)	Estimated at 0.38 to 0.43 on average, with micro-scale regions of higher w/cm around some aggregate particles.
Carbonation	Approximately 0.1 inch.
Air-Void System (AVS) Characteristics	Air-entrained. Measured air content is 11.5%, spacing factor 0.003 inch, and specific surface 666 in^2/in^3. Abundant small spherical air voids. Distribution of entrained air voids is non-uniform (see micrographs in AVS report). Air-void system appears adequate to protect against cyclic freeze-thaw distress. Entrapped voids frequently observed.
Secondary Deposits	Traces of ettringite in several air voids, but overall uncommon.
Microcracking	Minor microcracks near the major crack. Infrequent microcracks in remainder of concrete.
Comments and Distinctive Features	Interfacial transition zone appears narrow. No gaps or regions of high w/cm were observed adjacent to the sedimentary aggregate particles. Substantial amount of clastic sedimentary rocks in coarse and fine aggregate but no specific distress associated with higher absorption and weaker rock types.

Figure 4. Lapped cross section showing the appearance and condition of the concrete. Top surface is on left.

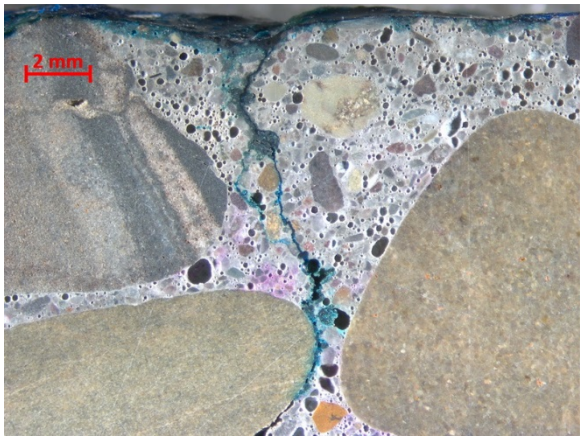

Figure 5. Close-up view of concrete in the top region.

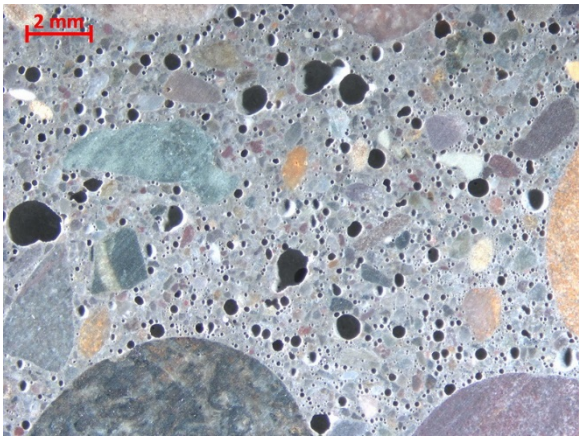

Figure 6. Close-up region in the body of the concrete.

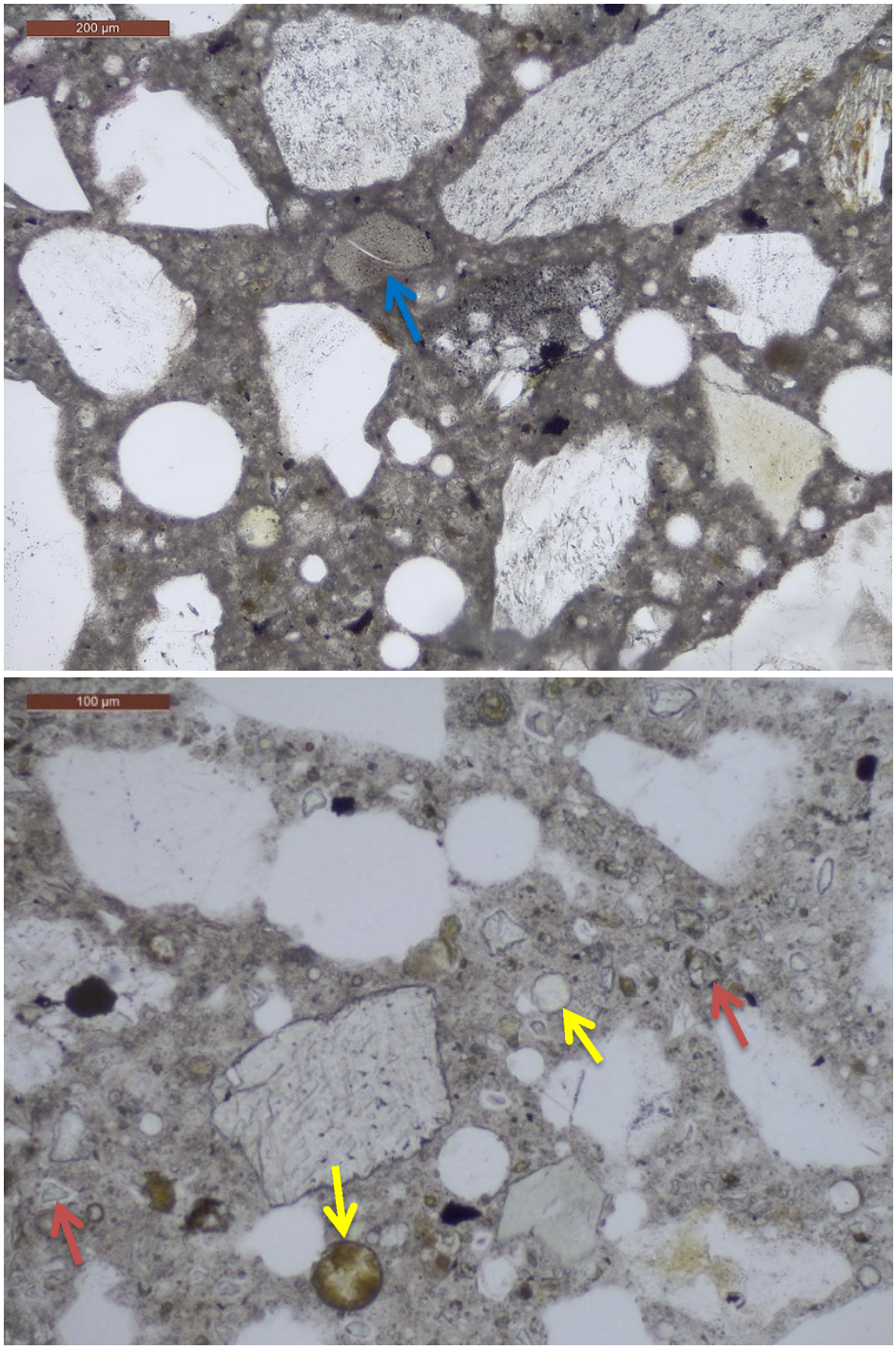

Figure 7. Plane-polarized thin section photomicrographs showing paste composition and texture. Portland cement (red arrows), fly ash (yellow arrows) and a few silica fume aggregations (blue arrow) were observed.

CORE LOG - VISUAL OBSERVATIONS

Sample ID: 1I	**WJE Project No.: 2016.3598**
Sample Location: Florence - East, MP 10.640 WB	**Petrographer: Hugh Hou/ L. Powers October 31, 2016**
Project Name: Forensic Deck Analysis -2016	**Date: September 16 to 27, 2016**

Figure 1. Core 1I. Side view. Top surface is on left.

Figure 2. Core 1I. Top surface.

Figure 3. Core 1I. Bottom surface

Dimensions	Diameter: 3.7 inches Length: 6.1 to 6.7 inches
End Surfaces	Saw-grooved top surface; bottom end broke exposing embedded epoxy-coated rebar.
Reinforcement	No. 5 epoxy coated deformed rebar (transverse relative to lane orientation); concrete cover is 2.7 inches. No. 4 epoxy coated deformed longitudinal rebar at bottom. Both rebars are in good condition. Short rebar imprint perpendicular to the bottom rebar. No gaps or secondary deposits were observed at the interface with the paste. No evidence of relative displacement at plastic stage of concrete was observed.
Consolidation	Generally well consolidated.
Distribution of Constituents	Aggregate and paste are uniformly distributed.
Cracks, Joints	Full-depth crack (transverse to the lanes in the field), approximately 0.015 inch wide, extended around aggregate particles. A crack traverse to the core axis was observed at the location of the top rebar, likely generated from sample handling and preparation.
General Observations	Concrete is mainly composed of natural siliceous sand and gravel aggregates uniformly dispersed in air-entrained cementitious paste.

STEREOMICROSCOPE AND PETROGRAPHIC MICROSCOPE EXAMINATION

Aggregate Characteristics	CA: Gravel composed of sandstone, graywacke sandstone, meta-sandstone, quartzite, siltstone, and meta-siltstone. Small amounts of mudstone, limestone, schist, and igneous rock were also observed. Top size: 3/4 inch. FA: Natural siliceous sand mainly composed of quartz/quartzite, sandstone, and siltstone; small amounts of schist, chert/chalcedony, volcanic rocks, mudstone, mica, limestone, and other rocks and minerals were also observed.
Potentially Reactive Components	Chert/chalcedony, siltstone, mudstone, and quartzite, or certain components of these rocks are potentially alkali-silica reactive (ASR). No evidence of ASR was observed in the core.
Paste-Aggregate Bond	Moderately tight to tight. Laboratory created fresh fracture surfaces generally extended through more aggregate particles compared to the full-depth major crack.

Paste Characteristics	Medium to dark gray, subvitreous to vitreous, and hard. Paste contains residual portland cement and fly ash particles, and small amounts of silica fume. Residual portland cement estimated at 4 to 6% by volume of paste. Hydration of the cement is advanced. Residual fly ash estimated at 7 to 10% by volume of paste. Calcium hydroxide generally small in size, estimated at 1 to 2% by volume of paste. Replacement rate of fly ash estimated at approximately 20%.
Water-Cementitious Materials Ratio	Estimated at 0.38 to 0.43.
Carbonation	Approximately 0.04 inch.
Air-Void System Characteristics	Air-entrained. Estimated air content 9 to 12%. Abundant small spherical voids. Air-void system appear adequate to protect the concrete from cyclic freeze-thaw distress. Entrapped voids were frequently observed.
Secondary Deposits	Ettringite lines or fills a few voids, more frequently near the crack.
Microcracking	Microcracks were infrequent. Where observed, microcracks pass between aggregate particles.
Distinctive Features	The interfacial transition zone between the paste and the sedimentary aggregate particles appears to be narrow. No gaps or regions of high w/cm were observed. Concrete characteristics were similar to Core 1D overall. The core appeared to contain slightly higher residual cementitious materials than Core 1D.

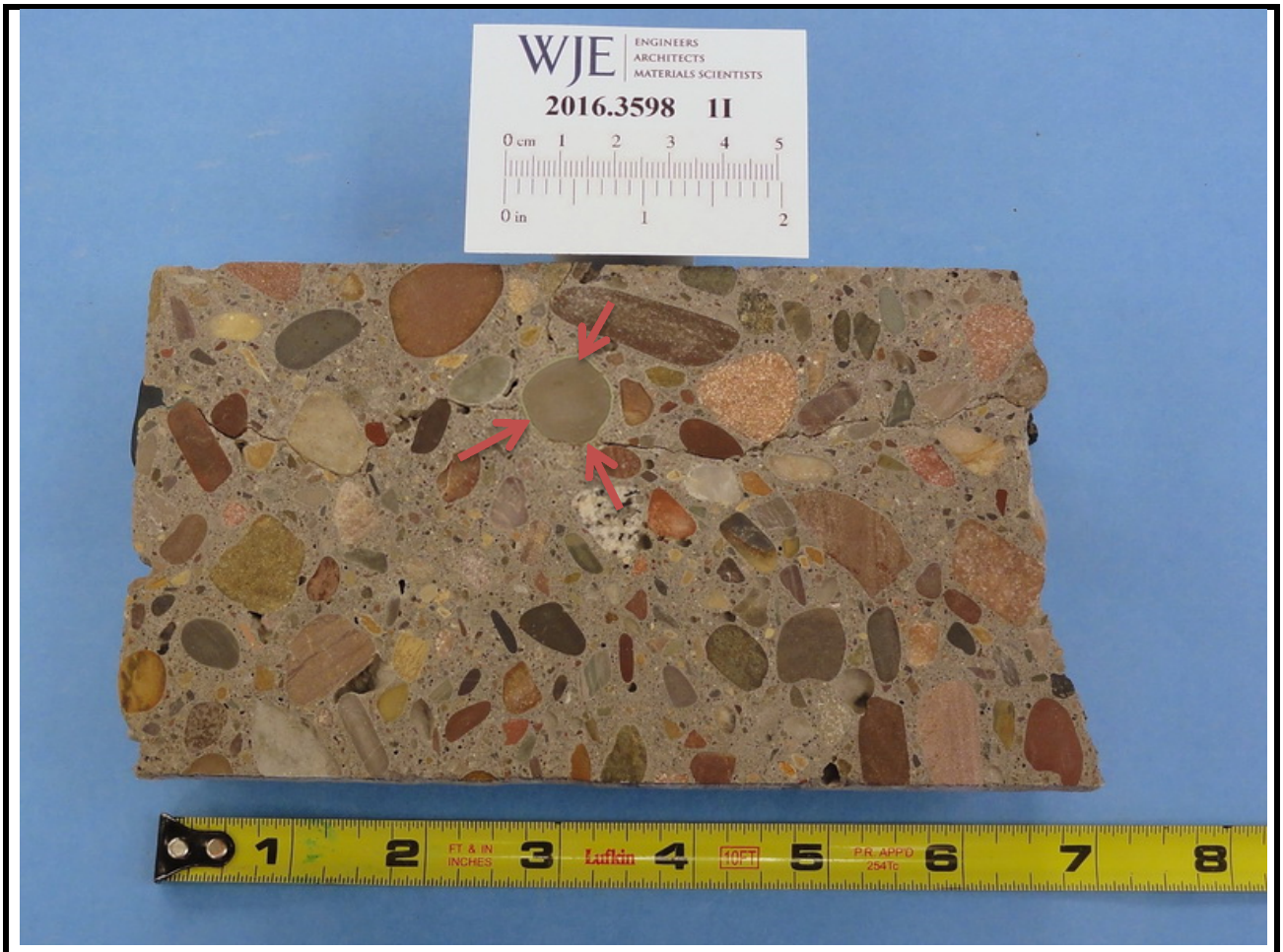

Figure 4. Lapped cross section showing the appearance and condition of the concrete. Arrows indicate embedded rebar. Top surface is on the left.

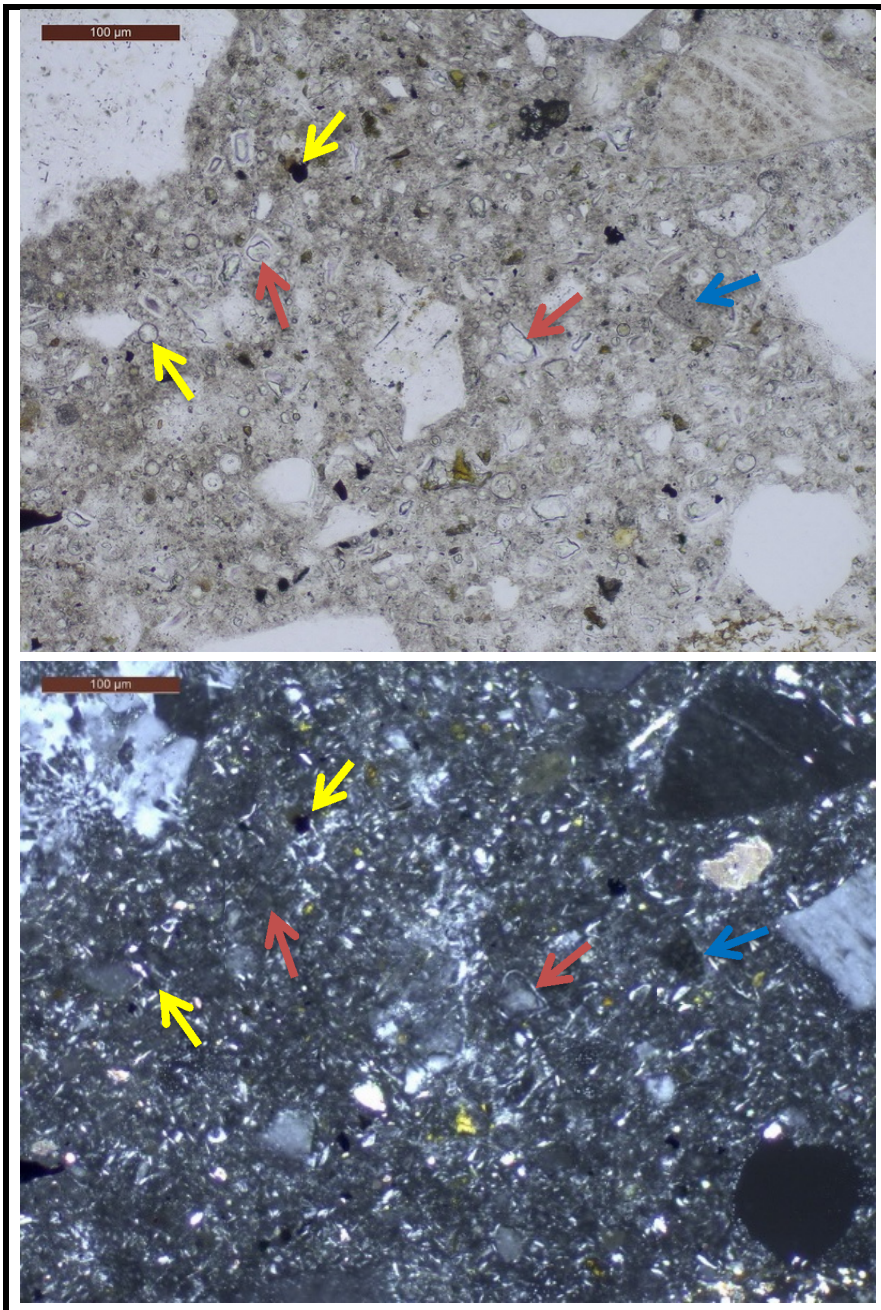

Figure 5. Thin section photomicrographs showing paste composition and texture. Portland cement (red arrows), fly ash (yellow arrows) and silica fume agglomerates (blue arrow) were observed. Top photo: plane-polarized light. Bottom photo: cross-polarized light.

ASTM C457 Standard Test Method for Microscopical Determination of Air-Void System in Hardened Concrete: Modified Point-Count Method

Operator:	Hugh Hou	**Dates of Testing:**	September 27, 2016
Approved By:	Laura Powers	**WJE Project No.:**	2016.3598
Client:	Montana State DOT	**Magnification Used:**	90X

Core ID	2C
Air Content %	11.5
Paste Content %	27.5
Sand Content %	30.9
Coarse Aggregate %	30.1
Void Frequency	15.4
Paste-Air Ratio	2.4
Average Chord Length (inch)	0.007
Specific Surface inch^2/inch^3	536
Spacing Factor (inch)	0.004
Total Transverse (inch)	91.7
Total Points Counted	1377
Tested Area (inch^2)	21.0
Aggregate Top Size (inch)	1/2

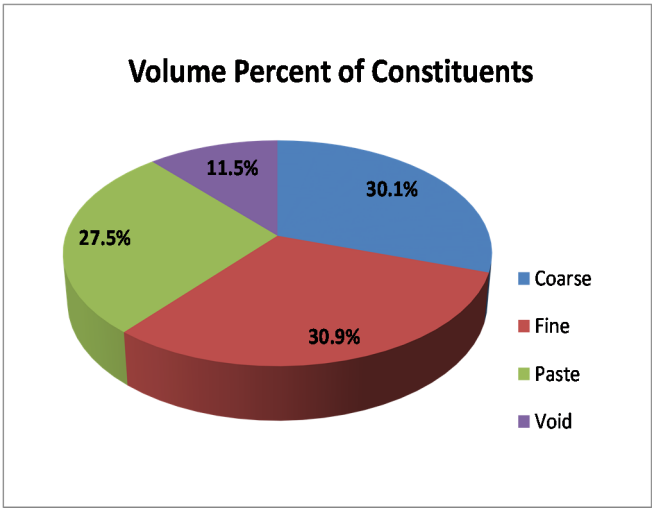

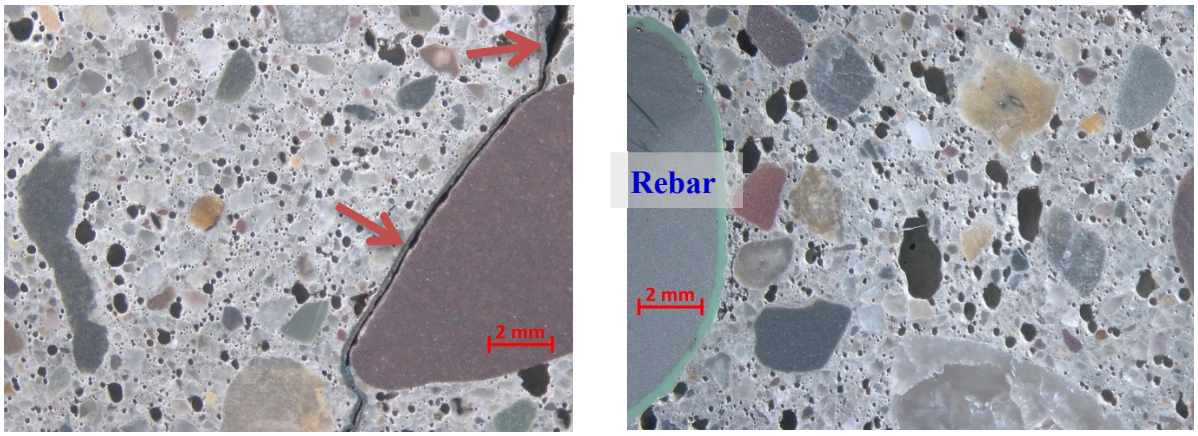

Appearance of air-void system. Arrows indicate crack and crack filler/sealer.

CORE LOG - VISUAL OBSERVATIONS

Sample ID: 2C	**WJE Project No.: 2016.3598**
Sample Location: Lozeau - Tarkio, MP 57.4721 EB	**Petrographer: Hugh Hou / L. Powers October 28, 2016**
Project Name: Forensic Deck Analysis -2016	**Date: September 20 to 27, 2016**

Figure 1. Core 2C. Side view. Top surface is on the left.

Figure 2. Core 2C. Top surface.

Figure 3. Core 2C. Bottom surface

Dimensions	Diameter: 3.7 inches Length: 6.7 to 7.6 inches
End Surfaces	Substantially worn, saw-grooved or tined top surface; fractured bottom surface broke mainly around aggregate.
Reinforcement	Two transverse No. 5 rebars with concrete cover 2.5 and 6.2 inches. No.4 rebar with 5.6-inch concrete cover, longitudinal and above the bottom No. 5 bar. Rebars are in good condition. No gaps, separations, or secondary deposits were observed between the rebar and the paste. No evidence of relative displacement at concrete plastic stage was observed.
Consolidation	Well consolidated. No large entrapped voids were observed.
Distribution of Constituents	Aggregate and paste are uniformly distributed.
Cracks, Joints	Full-depth crack transverse to the deck lanes in the field. The crack intercepts the upper and lower rebar and is up to 0.025 inch wide in the top region. Crack extends around coarse aggregate particles.
General Observations	Concrete is mainly composed of natural siliceous sand and gravel aggregates uniformly dispersed in air-entrained cementitious paste.

STEREOMICROSCOPE AND PETROGRAPHIC MICROSCOPE EXAMINATION

Aggregate Characteristics	CA: Gravel composed of sandstone, graywacke sandstone, meta-sandstone, quartzite, siltstone, and meta-siltstone. Small amounts of mudstone, limestone, schist, and igneous rock were also observed. Top size: 1/2 inch. FA: Natural siliceous sand mainly composed of quartz/quartzite, sandstone, and siltstone; small amounts of schist, chert, mudstone, mica, limestone, volcanic rocks, and other rocks and minerals were also observed.
Potentially Reactive Components	Chert, siltstone, mudstone, graywacke sandstone, and quartzite, or certain components of these rocks are potentially alkali-silica reactive (ASR). No evidence of ASR was observed in the core.
Paste-Aggregate Bond	Moderately weak. Laboratory created fractures extended through more aggregate particles than were transected by the major crack.

Paste Characteristics	Light beige gray, subvitreous, moderately hard. Measured paste volume was 27.5%. UPCs estimated at 7 to 10% by volume of paste. Calcium hydroxide crystals are moderately large, estimated at 8 to 12% by volume of paste. Cement and calcium hydroxide are non-uniformly distributed. No supplementary cementitious materials such as fly ash were observed.
Water-Cementitious Materials Ratio	Estimated at 0.46 to 0.51 on average and variable on a micro-scale.
Carbonation	Approximately 0.06 inch.
Air-Void System Characteristics	Air-entrained. Measured air content is 11.5%, spacing factor 0.004 inch, and specific surface 536 in^2/in^3. Air-void system appeared adequate to protect the concrete against cyclic freeze-thaw distress despite average low specific surface. Both spherical and non-spherical air voids were common.
Secondary Deposits	Ettringite frequently fills or lines small air voids. Carbonate secondary deposits were observed in leached paste near the crack. Leached paste is characterized by removal of calcium hydroxide.
Cracks	Microcrack branches extend from the major crack (described above) locally over most of the length of the core. Microcracks were generally infrequent in the concrete distant from the crack. Where present, the microcracks extend between aggregate particles.
Distinctive Features / Comments	Measured volume of coarse aggregate was 30.1% and is considered low (smaller observed maximum top size). Interfacial transition zone is variable and generally wider than observed in the concrete mixtures that contain fly ash. The major crack and some of the wider branches are lined with fine-grained material that was deposited in thin layers. Material in the crack includes quartz particles less than 0.002 inch in diameter, opaque particles of similar and smaller size, wood, and amorphous or nearly amorphous material. These materials appear to have been washed into the crack and were observed lining the crack to a depth of 3.8 inches.

Figure 4. Lapped cross section showing the appearance and condition of the concrete. Top surface is on the left.

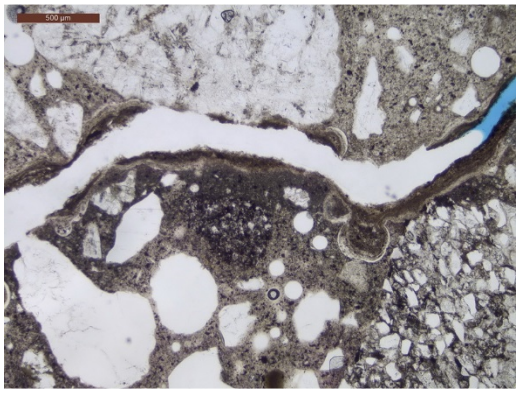

Figure 5. Thin-section photomicrograph showing a brown material lining the vertical crack (rotated in micrograph). Plane-polarized light.

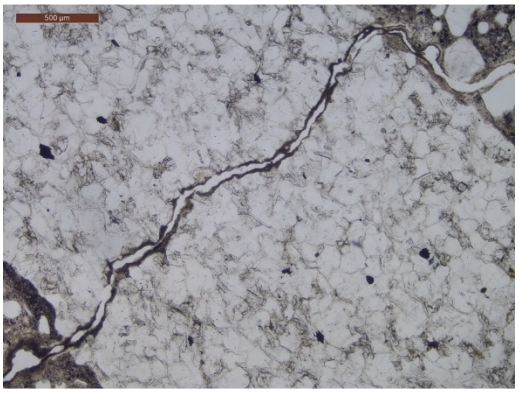

Figure 6. Thin-section photomicrograph showing a branch crack extending through a sandstone particle. Note brown material lining the crack. Plane-polarized light.

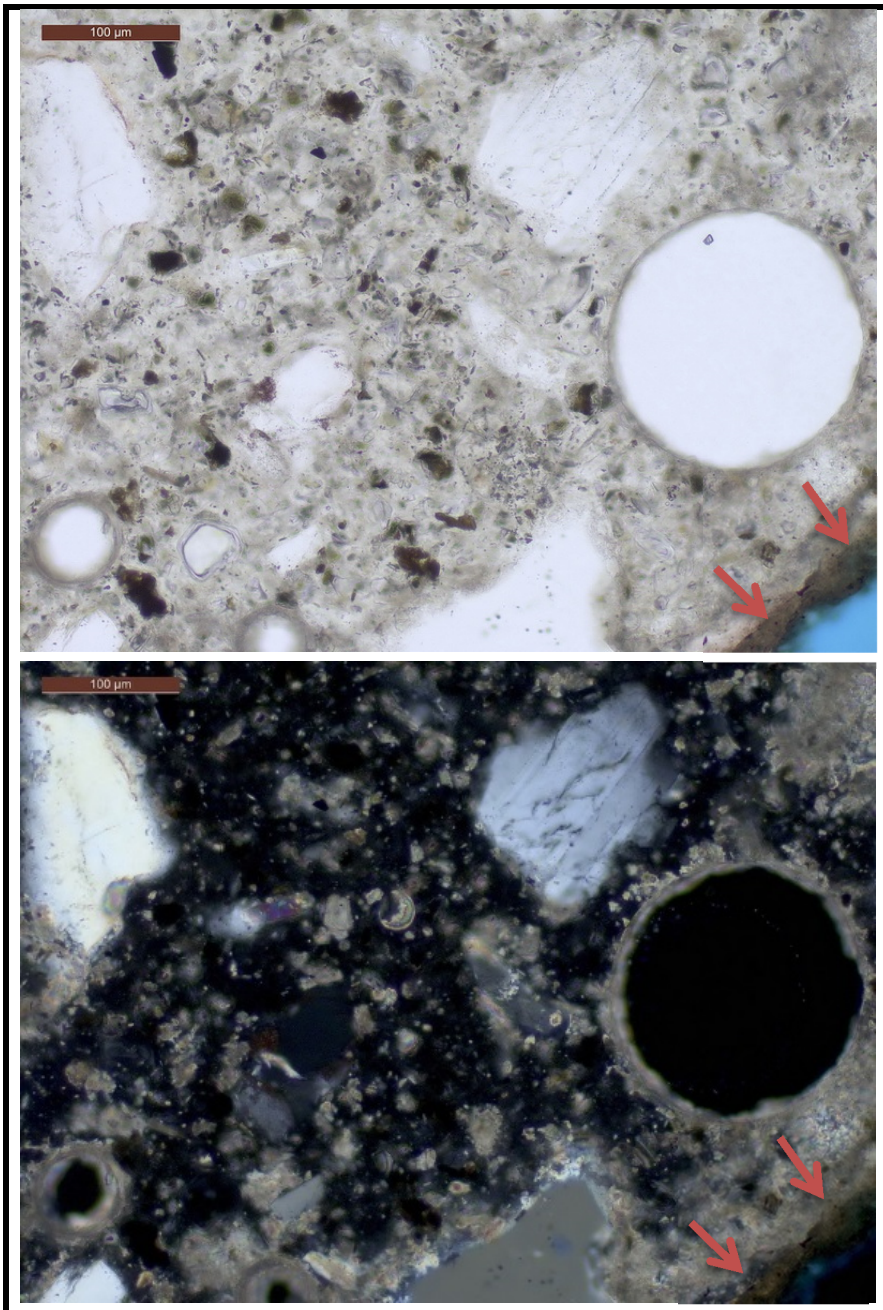

Figure 7. Thin-section photomicrographs show a leached region near the major crack (arrows). Secondary carbonate lines voids and has re-crystallized in the body of the paste.

CORE LOG - VISUAL OBSERVATIONS

Sample ID: 3A	**WJE Project No.: 2016.3598**
Sample Location: Lozeau-Tarkio - West, MP 58.5501 EB	**Petrographer: Hugh Hou / L. Powers October 28, 2016**
Project Name: Forensic Deck Analysis -2016	**Date: September 20 to 27, 2016**

Figure 1. Core 3A. Side view. Top surface is on the left.

Figure 2. Core 3A. Top surface.

Figure 3. Core 3A. Bottom surface

Dimensions	Diameter: 3.7 inches Length: 3.5 to 5.0 inches. Overlay 2.5-inch thick. Remainder is substrate concrete
End Surfaces	Saw-grooved top surface. Uneven fractured bottom surface with portion missing likely at the intersection of a horizontal crack and a vertical crack in the substrate.
Reinforcement	None observed.
Consolidation	Generally well consolidated.
Distribution of Constituents	Aggregate and paste are uniformly distributed in both overlay and substrate concrete.
Cracks, Joints	A hairline crack, less than 0.005 inch wide, extends from top surface to contact with substrate. The crack passes through a few aggregate particles, but around most. Short horizontal cracks and microcracks observed in the interfacial region.
General Observations: Overlay Concrete	Concrete is mainly composed of natural siliceous sand and gravel or partially crushed gravel aggregates uniformly dispersed in light to medium gray, air-entrained cementitious paste. Air content estimated at 6 to 9%. Top size: 3/8 inch.
Overlay-Substrate Interface	Substantially roughened substrate top surface. The two concretes are tightly adhered.
General Observations: Substrate Concrete	Concrete is mainly composed of natural siliceous sand and gravel aggregates uniformly dispersed in medium-dark gray, air-entrained cementitious paste. Air content estimated at 5 to 6%. Top size: 3/4 inch.

Figure 4. Lapped cross section showing the appearance and condition of the concrete. Top surface is on the left.

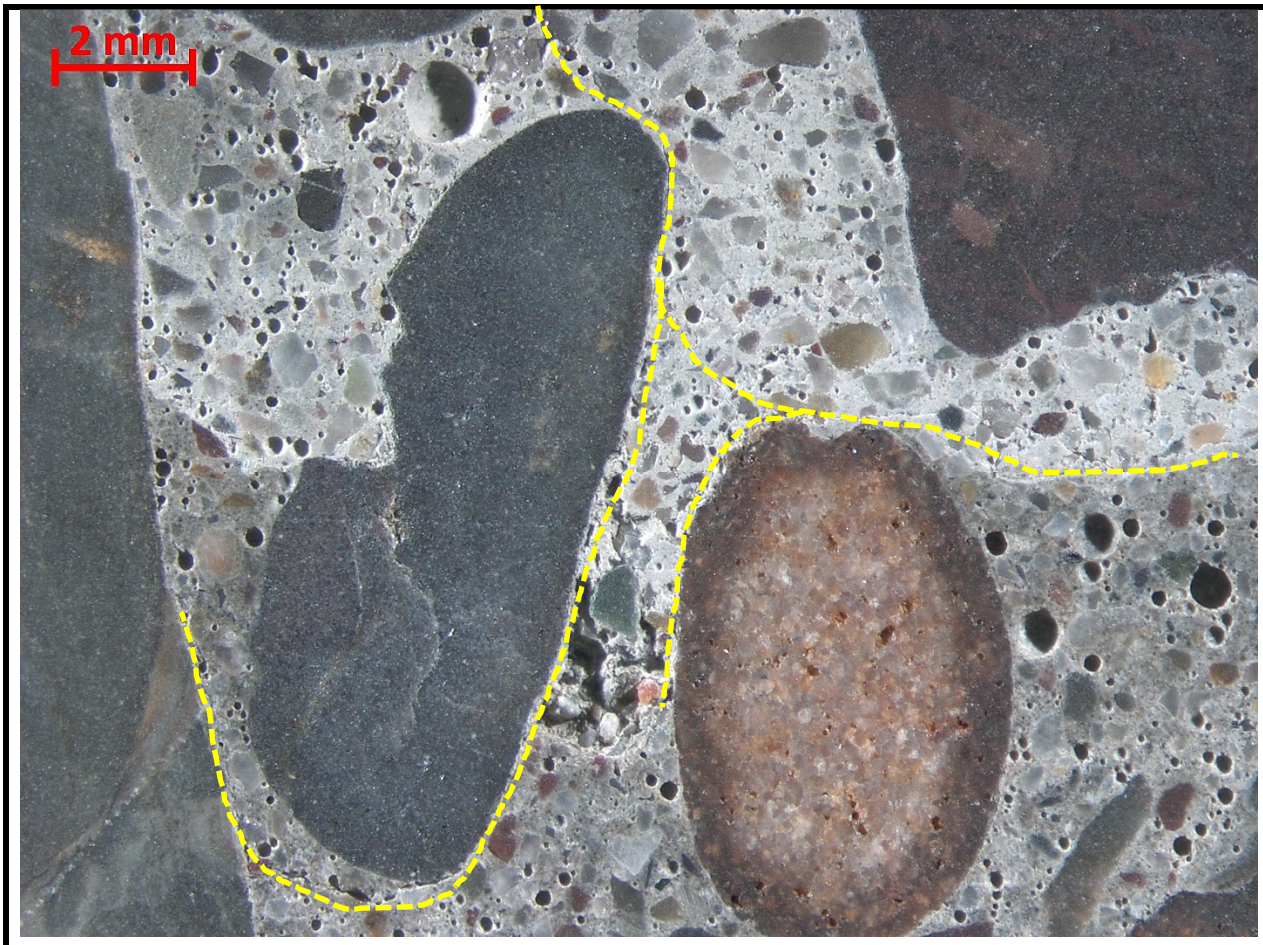

Figure 5. Close-up view of the overlay-substrate contact region. Dotted lines trace the vertical crack from the overlay that extended to region.

CORE LOG - VISUAL OBSERVATIONS

Sample ID: 3B	**WJE Project No.: 2016.3598**
Sample Location: Lozeau-Tarkio - West, MP 58.5501 EB	**Petrographer: Hugh Hou / L. Powers November 1, 2016**
Project Name: Forensic Deck Analysis -2016	**Date: September 20 to 27, 2016**

Figure 1. Core 3B. Side views. Top surface is on left. Top surface is on the left.

Figure 2. Core 3B. Top surface.

Figure 3. Core 3B. Bottom surface

Dimensions	Diameter: 3.7 inches Length: 5.5 to 6.4 inches. 2.5-inch thick overlay adhered to 3.0 to 3.9 inches substrate concrete.

End Surfaces	Saw-grooved top surface. Mainly uneven fractured bottom surface with a small area of flat formed surface.
Reinforcement	None in core.
Consolidation	Generally well consolidated.
Distribution of Constituents	Aggregates and paste are uniformly distributed in both overlay and substrate concrete.
Cracks, Joints	A full-depth vertical hairline crack, approximately 0.004 inch wide, mainly passes around aggregates; a few aggregate particles in the substrate are transected by the crack.
General Observations: Overlay Concrete	The concrete is mainly composed of natural siliceous sand and gravel or partially crushed gravel aggregates with a top size of 3/8 inch uniformly dispersed in light to medium gray, air-entrained cementitious paste. Air content estimated at 6 to 8%.
Overlay-Substrate Interface	Substantially roughened substrate top surface; tightly bonded each other.
General Observations: Substrate Concrete	The concrete mainly contains siliceous natural sand and gravel aggregates with a top size of 3/4 inch. Aggregates are uniformly dispersed in medium-dark gray, air-entrained cementitious paste. Air content was estimated at 4 to 6%.

Figure 4. Lapped cross section showing the appearance and condition of the concrete. Wearing surface is on the left. Arrows show the interface between overlay and substrate.

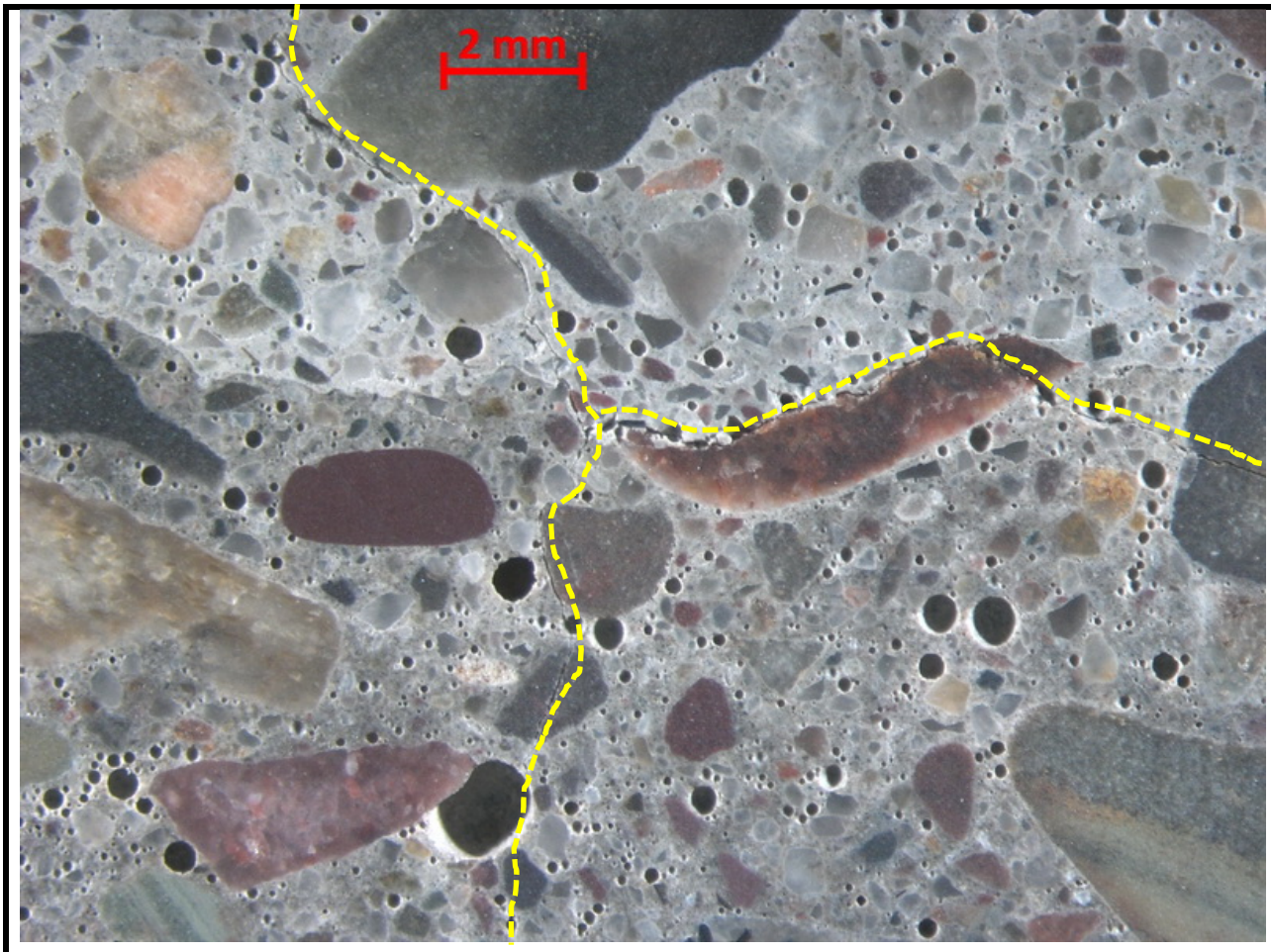

Figure 5. Close-up view of the overlay-substrate contact region. Dotted lines trace the crack from the top of the overlay into the substrate.

CORE LOG - VISUAL OBSERVATIONS

Sample ID: 6G	**WJE Project No.: 2016.3598**
Sample Location: Henderson - West, MP 22.013 EB	**Petrographer: Hugh Hou / L. Powers November 2, 2016**
Project Name: Forensic Deck Analysis -2016	**Date: September 20 to 27, 2016**

Figure 1. Core 6G. Side view. Red arrows indicate aggregate particles that exhibited minor evidence of ASR. Wearing surface is on the left.

Figure 2. Core 6G. Top surface.

Figure 3. Core 6G. Bottom surface

Dimensions	Diameter: 3.7 inches Length: 5.4 inches
End Surfaces	Abraded, tined or saw-grooved top surface with worn coarse aggregate particles exposed; fractured bottom surface exhibits rebar impression.
Reinforcement	Imprint of No.4 rebar on bottom surface. No evidence of corrosion was observed.
Consolidation	Generally well consolidated. A few scattered entrapped voids.
Distribution of Constituents	Aggregate and paste are uniformly distributed.
Cracks, Joints	Full-depth crack approximately 0.010 inch wide in the top 1 inch of the core mainly passes around CA particles.
General Observations	The concrete is mainly composed of siliceous natural sand and gravel aggregates uniformly dispersed in air-entrained cementitious paste.

STEREOMICROSCOPE AND PETROGRAPHIC MICROSCOPE EXAMINATION

Aggregate Characteristics	CA: Gravel mainly composed of mudstone, siltstone, limestone, dolomite, sandstone, and transitional rocks of these rock types. Small amounts of quartzite, calc-silicate and other metamorphosed equivalents of the sedimentary rocks. Top size: 1/2 inch. FA: Siliceous and calcareous natural sand mainly composed of quartz/quartzite, chert, limestone, and rock and mineral fragments found in the coarse aggregate
Potentially Reactive Components	The fine-grained clastic rocks and quartzite, or certain components of these rocks are potentially alkali-silica reactive. Dark reaction rims around a few aggregate particles and trace amounts of ASR gel were observed. No ASR-related cracks or microcracks were observed.
Paste-Aggregate Bond	Moderately tight.
Paste Characteristics	Medium gray, subvitreous, moderately hard. UPC estimated at 7 to 11% by volume of paste. Residual cement particles appeared to contain greater amounts of ferrite than the remaining three cores, 1D, 1I, and 2C studied, possibly indicating different cement source. Calcium hydroxide generally

	occurred as small crystals and abundance was estimated at 4 to 6% by volume of paste. No supplementary cementitious materials were observed.
Water-Cementitious Materials Ratio	Estimated at 0.42 to 0.47.
Carbonation	Approximately 0.04 inch.
Air-Void System Characteristics	Air-entrained with an estimated air content of 6 to 9%. Distribution of entrained air voids is fairly uniform. Air-void system is considered adequate to protect the concrete against cyclic freeze-thaw distress.
Secondary Deposits	Ettringite frequently fills small air voids, and lines many larger air voids. Alkali-silica gel was observed in two air voids. A few fine-grained clastic aggregate particles exhibited wet appearance due to ASR. ASR however did not appear to have contributed to cracking.
Cracks	Apart from the full-depth vertical crack, a hairline crack was observed in the bottom 2 inches of the concrete. The crack mainly passed around aggregate particles. The top 1.5 inches of the crack was filled with fine-grained, dark-colored debris that had been deposited in thin layers. Paste microcracking was infrequent.
Distinctive Features	The aggregates in 6G contained more carbonate and argillaceous, fine-grained clastic components compared to 1D, 1I, and 2C. The long axis of elongate aggregate particles was frequently parallel to the top surface.

Figure 4. Lapped cross section showing the appearance and condition of the concrete. The long axis of aggregate particles was frequently parallel to the top surface (on left).

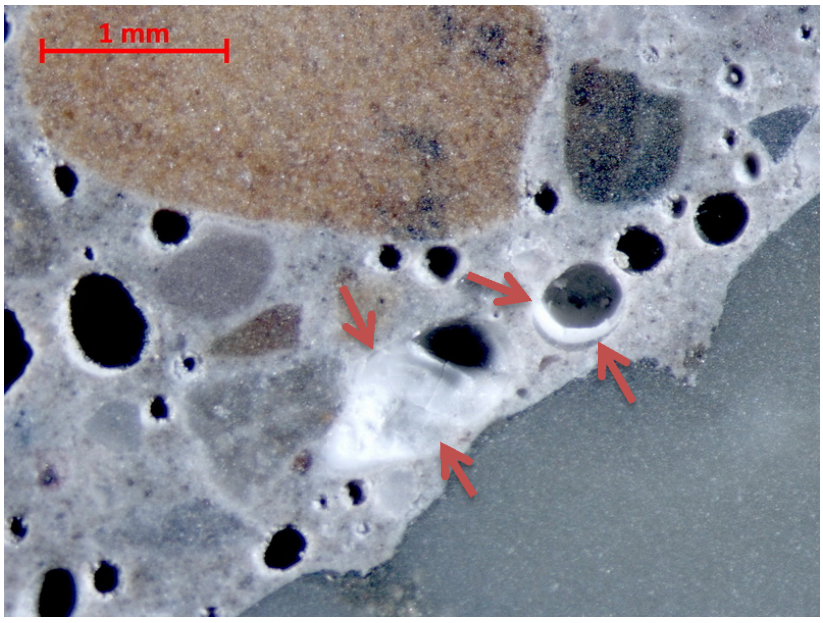

Figure 5. Close-up view of the concrete showing alkali-silica gel lining two air voids (arrows).

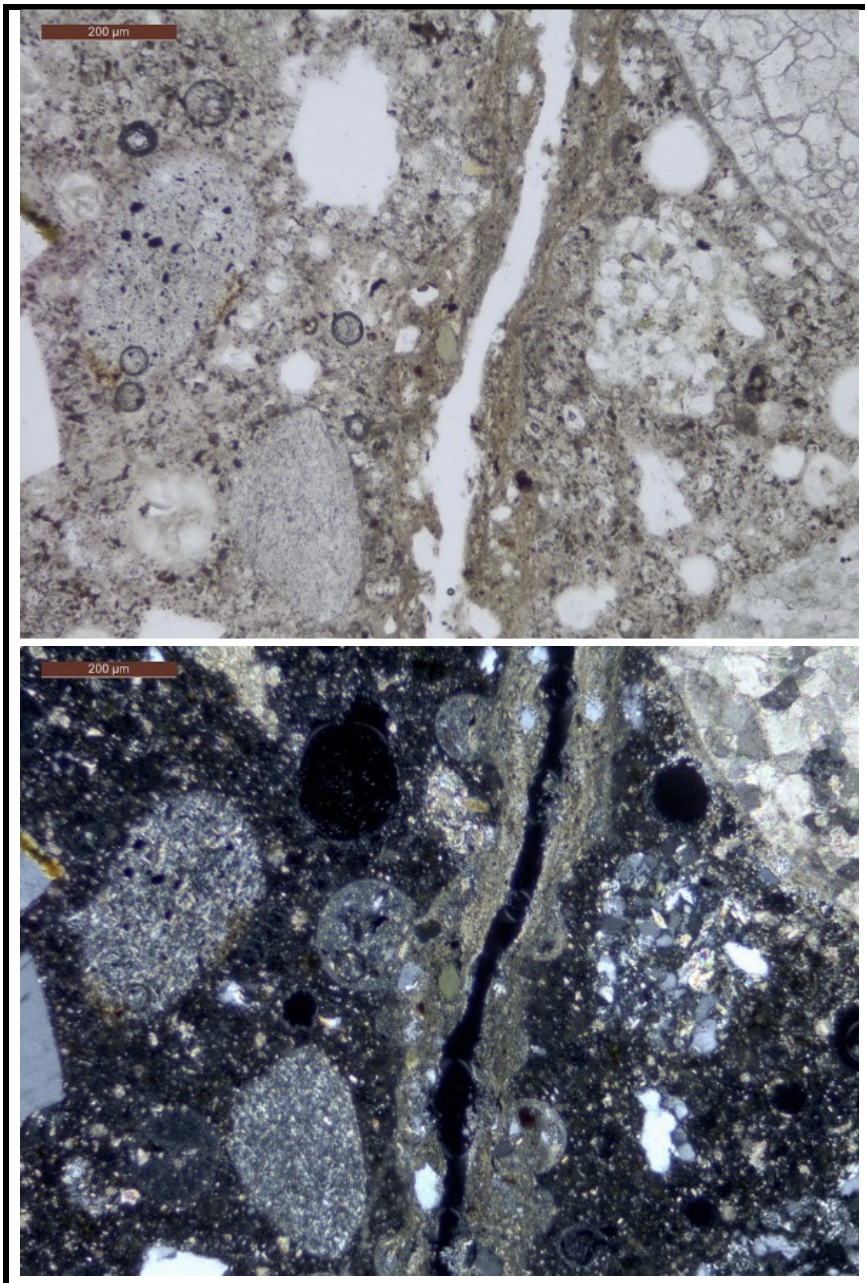

Figure 6. Thin-section photomicrographs show the vertical crack lined with fine-grained brown deposits. Top photo: plane-polarized light. Bottom photo: cross-polarized light.

CORE LOG - VISUAL OBSERVATIONS

Sample ID: 10B	**WJE Project No.: 2016.3598**
Sample Location: Superior Area - MP 49.3971 EB	**Petrographer: Hugh Hou / L. Powers November 2, 2016**
Project Name: Forensic Deck Analysis -2016	**Date: September 29, 2016**

Figure 1. Core 10B. Side views. Wearing surface is on left.

Figure 2. Core 10B. Top surface.

Figure 3. Core 10B. Bottom surface

Dimensions	Diameter: 3.7 inches Length: 6.6 inches

End Surfaces	Slightly abraded saw-grooved top surface. Uneven fractured bottom surface mainly broke off around coarse aggregate particles.
Reinforcement	None in core.
Consolidation	Well consolidated. Entrapped air void 0.7 inch across was observed at a depth of approximately 2 inches.
Distribution of Constituents	Aggregates and paste are uniformly distributed.
Cracks, Joints	Diagonal crack approximately 0.01 inch wide extended from the wearing surface and terminated at a depth of 3.5 inches. The crack transected one coarse aggregate particle at a depth of approximately 2 inches. A hairline crack extends from the top surface to a depth of 0.7 inch and a horizontal hairline crack connects the vertical crack with the major crack. A hairline crack at the bottom surface extended 1.5 inches from the bottom surface.
General Observations	The concrete is mainly composed of siliceous natural sand and gravel aggregates uniformly dispersed in air-entrained cementitious paste.

STEREOMICROSCOPE EXAMINATION

Aggregate Characteristics	CA: Siliceous gravel mainly composed of clastic sedimentary rocks including red sandstone and siltstone, granite, yellow and brown sandstone and siltstone, meta-sandstone, quartzite, schist, and minor purple-red ironstone. Top size: 3/4 inch. FA: Siliceous natural sand mainly composed of quartz/quartzite, sandstone, siltstone; schist, chert, mica, limestone, and smaller amounts of other rocks and minerals.
Potentially Reactive Components	Chert, siltstone, mudstone, graywacke sandstone, and quartzite, or certain components of these rocks are potentially alkali-silica reactive (ASR). No evidence of ASR was observed in the core.
Paste-Aggregate Bond	Moderately tight. Fresh fractures mainly pass through coarse aggregate particles.
Paste Characteristics	Medium gray, subvitreous, moderately hard. No fly ash was observed based on examination of lapped section. No thin section was prepared.
Water-Cementitious Materials Ratio	Estimated at 0.45 to 0.50 based on physical characteristics. No thin section was prepared.
Carbonation	Approximately 0.04 inch.
Air-Void System Characteristics	Air-entrained. The distribution of air voids is non-uniform, varying from estimated 10 to 12% to locally 4 to 6%. Air content is higher and the air voids are generally smaller in the top half of the core compared to the bottom half. The air-void system appears to be adequate to protect the concrete against cyclic freeze-thaw distress, despite of the nonuniform distribution of voids.
Secondary Deposits	None observed in stereomicroscope examination.

Microcracks	The body of the concrete contains infrequent microcracks that extend between aggregate particles. Microcracking is not excessive.
Distinctive Features	The major crack is lined with dark brown-gray fine-grained deposits to a depth of 2 inches.

Figure 4. Lapped cross section showing the appearance and condition of the concrete. Wearing surface is on the left.

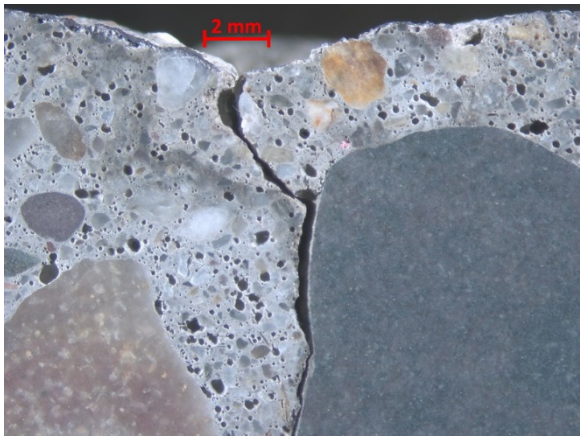

Figure 5. Close-up view of top region.

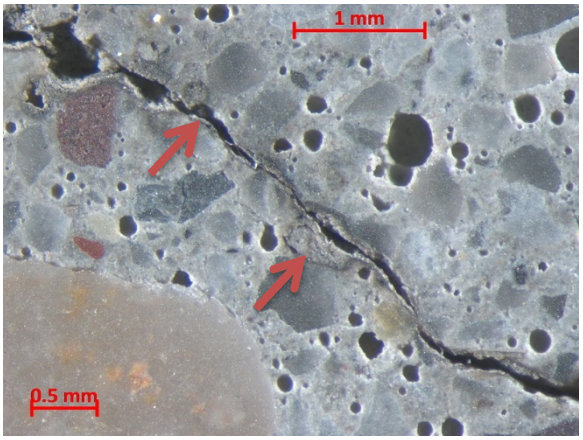

Figure 6. Close-up view at approximately 1 inch depth. Arrows show dark-colored fine-grained deposits lining the crack.

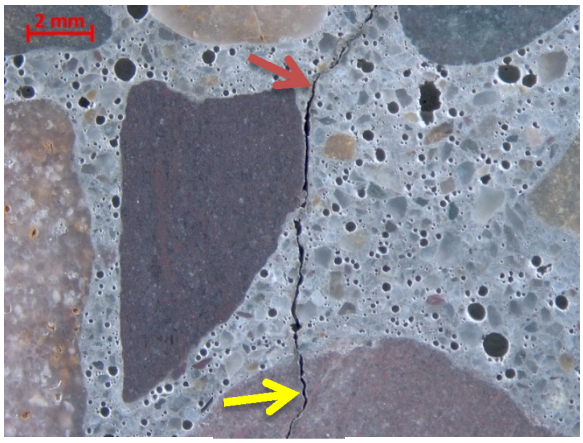

Figure 7. Close-up view at approximately 1.3 inches depth. Major crack transects a coarse aggregate particle at the bottom of the view (yellow arrow). Red arrow shows dark deposits lining the crack.

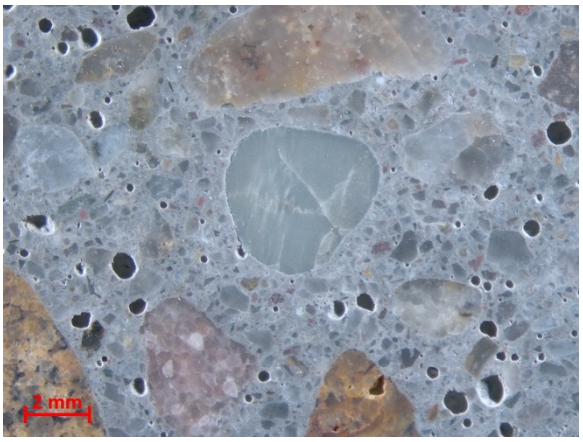

Figure 8. Close-up view at approximately 4.6 inches depth shows an region of low air content.

CORE LOG - VISUAL OBSERVATIONS

Sample ID: 11A	**WJE Project No.: 2016.3598**
Sample Location: Superior Area, MP 49.3972 WB	**Petrographer: Hugh Hou / L. Powers November 1, 2016**
Project Name: Forensic Deck Analysis -2016	**Date: September 20 to 27, 2016**

Figure 1. Core 11A. Side view. Top surface is on the left.

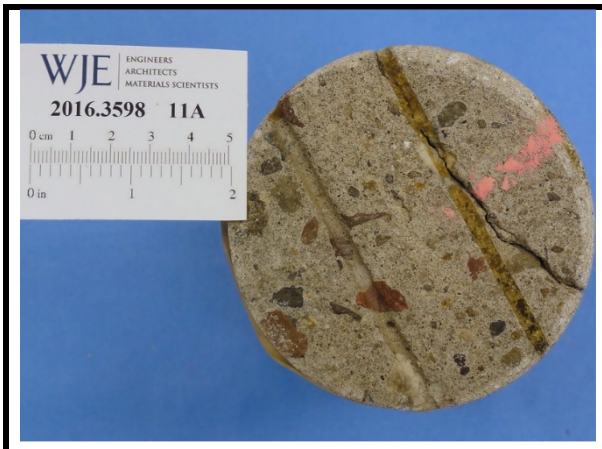

Figure 2. Core 11A. Top surface.

Figure 3. Core 11A. Bottom surface

Dimensions	Diameter: 3.7 inches Length: 5.5 to 6.5 inches
End Surfaces	Saw-grooved and abraded top surface; fractured bottom surface.
Reinforcement	No. 5 rebars with 2.6 and 5.3-inch cover; No. 4 rebar with 4.7-inch cover (above the bottom No. 5 bar and oriented perpendicular each other in the horizontal plane).
Consolidation	Generally well consolidated.
Distribution of Constituents	Aggregate and paste are uniformly distributed.
Cracks and Depth of Penetration of Crack Repair Material	Full-depth crack. Resinous (possibly epoxy) repair material penetrated to a maximum depth of 0.8 inch from top surface. Below this depth, and to the bottom of the crack, brown fine-grained material was observed lining the crack. This material appears to be debris that has washed into the crack and is similar to the fine-grained material lining the crack in Core 2C. The dark deposits also line the upper portion of the crack that was filled with the resinous repair material. No lapped cross section or thin section were prepared.

CORE LOG - VISUAL OBSERVATIONS

Sample ID: 12A	**WJE Project No.: 2016.3598**
Sample Location: Thompson River, MP 55 -56	**Petrographer: Hugh Hou / L. Powers November 3, 2016**
Project Name: Forensic Deck Analysis -2016	**Date: September 20 to 27, 2016**

Figure 1. Core 12A. Side view. Red arrows indicate aggregate particles that exhibited evidence of minor ASR.

Figure 2. Core 12A. Top surface.

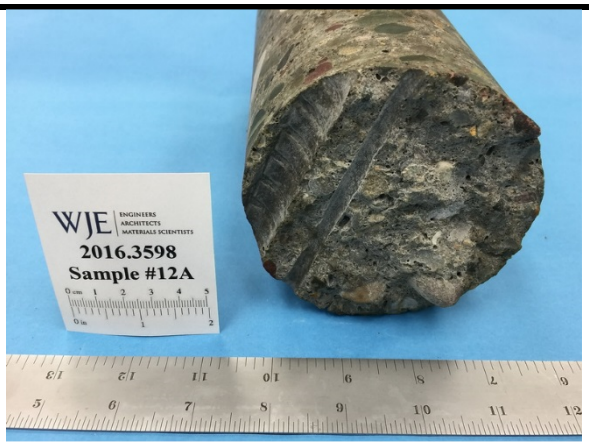

Figure 3. Core 12A. Bottom surface

Dimensions	Diameter: 3.7 inches Length: 6.8 to 7.8 inches
End Surfaces	Saw-grooved wearing surface. Uneven bottom surface broke around coarse aggregate particles and had an impression of a deformed rebar (No. 4 or No. 5) and a smooth wire (diameter approximately 0.25 inch).
Reinforcement	No reinforcement was embedded in the core. Impressions of steel reinforcement as described above. Impressions were clean; no evidence of corrosion.
Consolidation	Well consolidated. No large air voids observed.
Distribution of Constituents	Aggregate and paste are uniformly distributed.
Cracks, Joints	A vertical hairline crack approximately 0.003 inch wide extends to a depth of 4.5 inches. The hairline crack becomes a microcrack at a depth of approximately 1.5 inch. The crack/microcrack passes through a few aggregate particles.
General Observations	The concrete is mainly composed of siliceous natural sand and gravel aggregates uniformly dispersed in air-entrained cementitious paste.

STEREOMICROSCOPE EXAMINATION

Aggregate Characteristics	CA: Gravel is mainly composed of thinly bedded siltstone and fine-grained sandstone, medium-grained sandstone, and transitional rocks of these rock types. A few rock particles that were softer than the siltstone are classified as mudstone. Smaller amounts of quartzite, calc-silicate schist, and volcanic rocks were observed. Elongated aggregate particles are randomly oriented (not aligned). Top size is 1/2 inch. FA: Siliceous natural sand generally similar to the coarse aggregate, but with greater amounts of quartz/quartzite and other fragmental minerals.
Potentially Reactive Components	The fine-grained clastic rocks and quartzite, or certain components of these rocks are potentially alkali-silica reactive (ASR). No evidence of ASR was observed.
Paste-Aggregate Bond	Moderately tight. Fresh fractures induce din the laboratory mainly pass through coarse aggregate particles.

Paste Characteristics	Medium to dark gray, subvitreous, hard to moderately hard. No fly ash particles were observed in the stereomicroscope examination; the paste does not appear to contain supplementary cementitious materials.
Water-Cementitious Materials Ratio	Estimated at 0.40 to 0.45, based on paste characteristics. No thin-section analysis was performed.
Carbonation	Approximately 0.02 inch.
Air-Void System Characteristics	Air-entrained. Estimated air content is 5 to 8% and the small spherical entrained air voids are fairly uniformly distributed. The air-void system appears to be adequate to protect the concrete against cyclic freeze-thaw distress.
Secondary Deposits	No deposits were observed in air voids or cracks.
Cracks	Short microcracks that extend between aggregate particles were common. These cracks are only observed as the wet, lapped surface dried.
Distinctive Features	The proportion of fine-grained clastic sedimentary rocks is high.

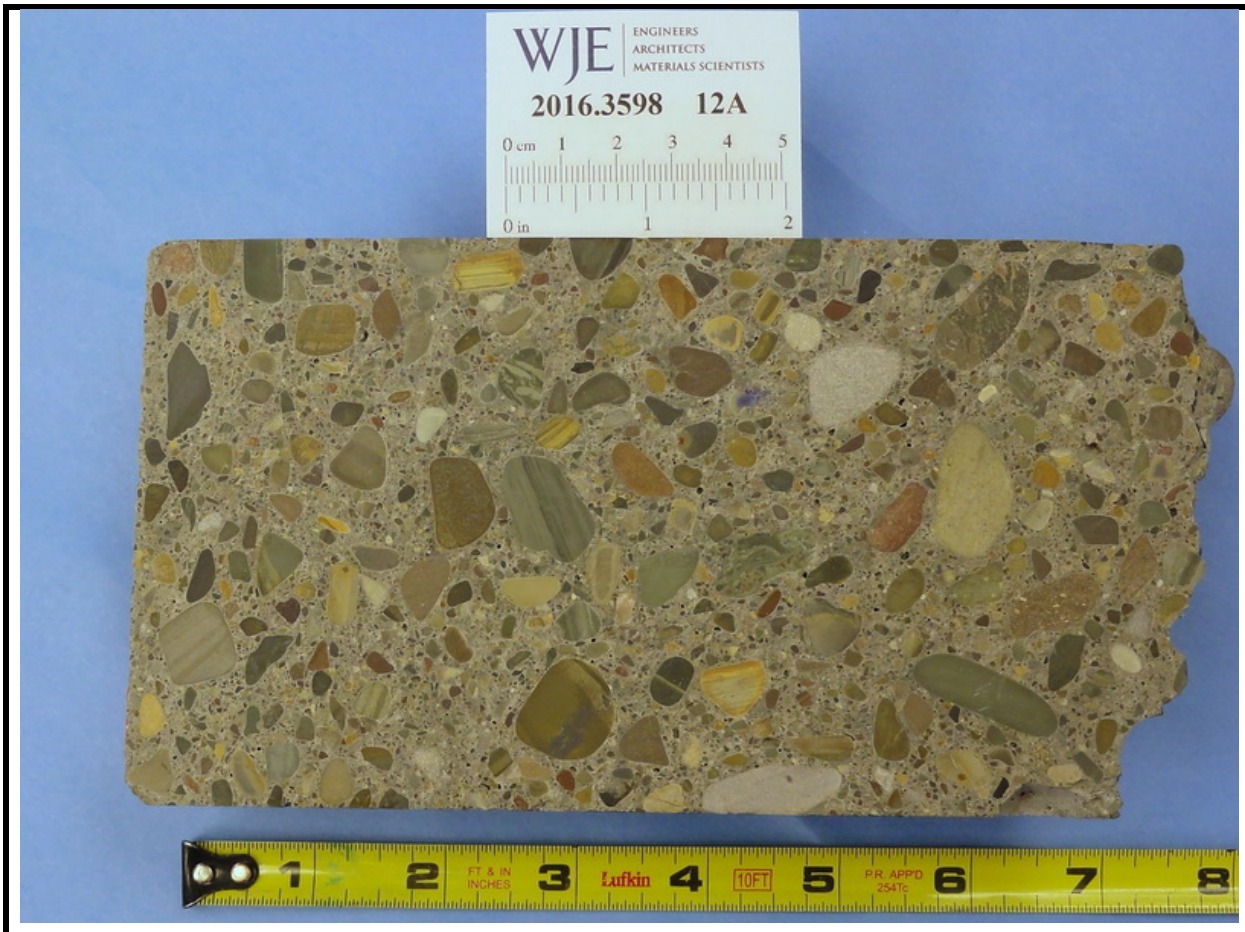

Figure 4. Lapped cross section showing the appearance and condition of the concrete. Wearing surface is on the left.

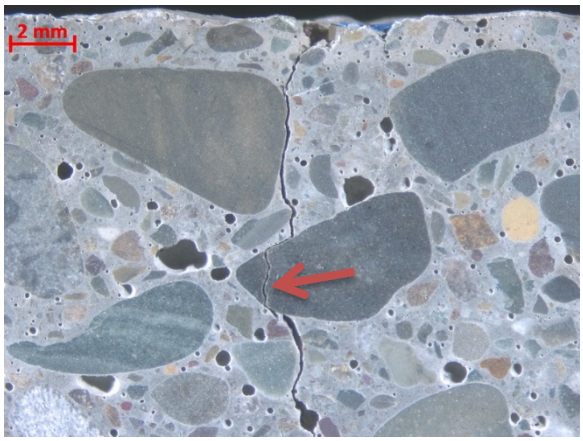

Figure 5. Close-up view of top region. Arrow shows the crack passing through an aggregate particle.

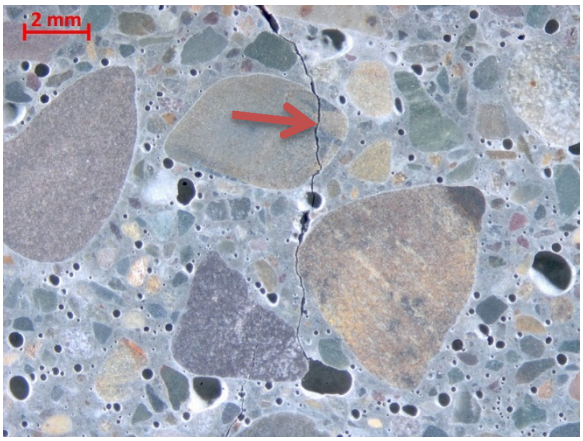

Figure 6. Close-up view at a depth approximately 1.3 inches. Arrow shows the crack passing through an aggregate particle.

APPENDIX D - MODELING

STRESS MODEL SENSITIVITY STUDY

A parameter sensitivity study was performed using the model for Bridge 1. Factors investigated include the compressive strength of the deck concrete, the thickness of the deck, the spacing of the girders, the magnitude of autogenous and drying shrinkage, a uniform temperature change in the deck and beam, and a linear temperature change through the deck. Baseline values for each parameter are provided in Table 1.

Each factor was varied independently and the resulting stresses in the top and bottom of the deck were calculated. The findings are summarized below. Unless otherwise indicated, the effects described are linear (i.e., doubling the input doubles the magnitude of the stresses generated) and have the opposite effect when the sign of the input is reversed (i.e., effects that generate tensile stresses when a factor is increased generate compressive stresses of the same magnitude when the factor is decreased).

- Uniform autogenous shrinkage (Figure 1): Autogenous shrinkage generally has a small impact on the tensile stresses developed in the deck at very early ages. At an assumed compressive strength of 1500 psi, a uniform shrinkage of 10 microstrain results in 7 psi tensile stress at the top of the deck and 8 psi tensile stress at the bottom of the deck. Autogenous shrinkage values between 0 and 40 microstrain would be anticipated at early ages for the three bridge decks investigated in this study; for Bridge 1, such strains would generate tensile stresses of up to 28 psi and 32 psi at the top and bottom of the deck, respectively.

- Uniform drying shrinkage (Figure 1): Drying shrinkage generally has a much greater impact on the tensile stresses developed in the deck at later ages due to its greater magnitude. At an assumed compressive strength of 7370 psi, a uniform 500 microstrain of drying shrinkage (typical for mature concrete) results in tensile stress of 413 psi and 477 psi at the top and bottom of the deck, respectively. As drying shrinkage is a slow process, concrete creep will reduce actual stress levels significantly. Stress due to drying shrinkage alone are likely not adequate to cause cracking of mature concrete but is a primary contributor.

- Uniform temperature change in beam (Figure 2): A 10 °F uniform increase in the temperature of the girder results in the generation of approximately 30-35 psi tensile stresses in the top and bottom of the bridge deck, for both 1500 psi and 7370 psi deck concrete. These stresses are opposite of those generated by a uniform increase in deck temperature (see discussion below).

- Uniform temperature change in deck (Figure 2): A 10 °F uniform decrease in deck temperature results in the generation of 36 psi and 40 psi tensile stresses at the top and bottom of the deck, respectively, for both 1500 psi and 7370 psi deck concrete. Significant tensile stresses may therefore develop in the deck at early ages due to cooling deck temperatures following the peak heat of hydration when the concrete strength is low.

- Linear temperature change in deck (Figure 3): A linear temperature change through the deck generates a linear strain profile, with the side of the deck experiencing the greater temperature increase (or smaller temperature decrease) experiencing greater *compressive* stresses. A temperature gradient typically generates larger stresses in the deck than a uniform temperature change, making the deck more susceptible to cracking. A 10 °F decrease in temperature at the top of the deck (and no change in temperature at the bottom of the deck) generates tensile stresses of approximately 50 psi at the top of the deck (compared to 36 psi for a uniform temperature change) and compressive stresses of

approximately 15 psi at the bottom of the deck. Note that a 10 °F change in deck surface temperature is regularly exceeded by large amounts on mountainous bridges in Montana. Further, temperature changes can be very rapid (minimizing beneficial effects of creep). A 50°F temperature change of the deck surface would result in 250 psi tensile stress of the top surface.

- Compressive strength of deck concrete (Figure 4): Increasing the compressive strength (elastic modulus) of the deck concrete has a small impact on the stresses generated in the bridge deck. Doubling the compressive strength increases stresses in the deck by approximately 20-25%.

- Deck thickness (Figure 5): Increasing the thickness of the deck generally reduces the magnitudes of the stresses that are generated. Increasing the deck thickness of Bridge 1 from 8 inches to 10 inches reduces stresses by 10-25%, while reducing it to 6 inches increases stresses by 10-20%.

- Girder spacing (Figure 6): Increasing the girder spacing also reduces the magnitudes of the stresses that are generated in the bridge deck. Increasing the spacing of the Bridge 1 girders from 9 feet to 12 feet reduces the magnitude of the stresses by 10-15%, while reducing the spacing to 6 feet generally increased the magnitude of the stresses by 15-20%. Increased girder size will likely offset some of the change in stresses.

Table 1. Inputs for Mathcad Stress Model

Input	Parameter	Bridge 1	Bridge 2	Bridge 6
Thermal and Mechanical Properties: Deck	Coefficient of Thermal Expansion	5.0×10^{-6}/°F (measured on cores)		
	Poisson's Ratio	0.20 (assumed)		
	Compressive Strength	Early-age: 1500 psi, or as indicated Mature: 7370 psi (measured on cores)	Early-age: 1500 psi, or as indicated Mature: 5090 psi (measured on cores)	Early-age: 1500 psi, or as indicated Mature: 6090 psi (measured on cores)
	Modulus of Elasticity	Early-age: $57{,}000\sqrt{f_c(psi)}$, where f_c is the compressive strength of the concrete Mature: 4450 ksi (measured on cores)	Early-age: $57{,}000\sqrt{f_c(psi)}$, where f_c is the compressive strength of the concrete Mature: 3300 ksi (measured on cores)	Early-age: $57{,}000\sqrt{f_c(psi)}$, where f_c is the compressive strength of the concrete Mature: 3950 ksi (measured on cores)
Thermal and Mechanical Properties: Beams	Coefficient of Thermal Expansion	5.0×10^{-6}/°F for concrete		
	Modulus of Elasticity	$57{,}000\sqrt{8000(psi)}$ = 5,098 ksi for concrete		
Deck Geometry	Thickness	8 in.	Spans 1-2: 7 1/4 in. Span 3: 7 3/4 in. Spans 4-5: 8 in.	7.5 in.
Beam Geometry	Depth	6 ft. 0 in.	Spans 1-2: 3 ft. 4 in. Span 3: 4 ft. 6 in. Spans 4-5: 3 ft. 4 in.	3 ft. 4 in.
	Area	886 in^2	Spans 1-2: 438 in^2 Span 3: 789 in^2 Spans 4-5: 438 in^2	438 in^2
	Moment of Inertia	636,612 in^4	Spans 1-2: 79,494 in^4 Span 3: 260,730 in^4 Spans 4-5: 79,494 in^4	79,494 in^2
	Centroid Location	32.29 in.	Spans 1-2: 17.93 in. Span 3: 24.73 in. Spans 4-5: 17.93 in.	17.93 in.
	Section Modulus	Calculated from moment of inertia and centroid location		
	Typical Spacing	9 ft. 0.5 in.	Spans 1-2: 6 ft. 7.5 in. Span 3: 8 ft. 10 in. Spans 4-5: 8 ft. 10 in.	9 ft. 5 in.
Temperature	Deck Temperature	Variable		
	Beam Temperature	Variable, Constant		
Shrinkage	Deck Shrinkage	Variable		

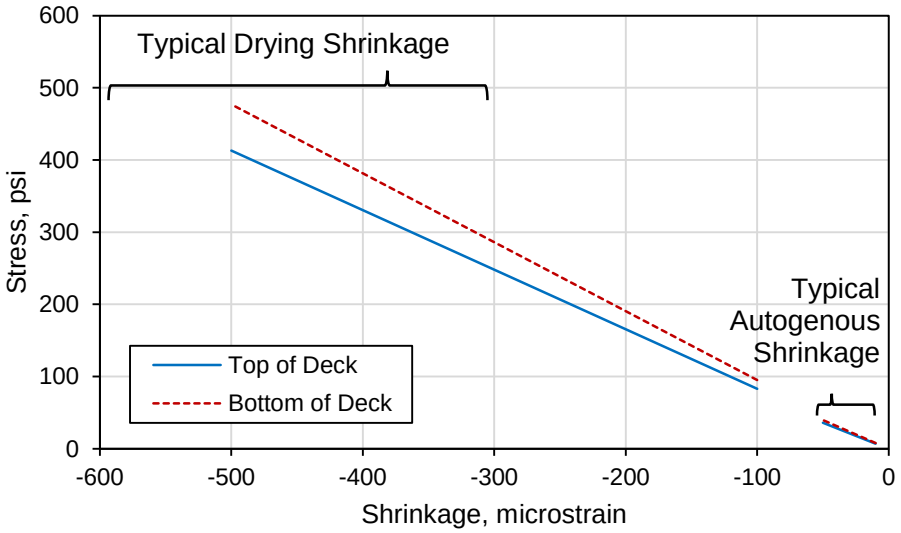

Figure 1. Modeled stresses in Bridge 1 deck due to uniform drying or autogenous shrinkage.

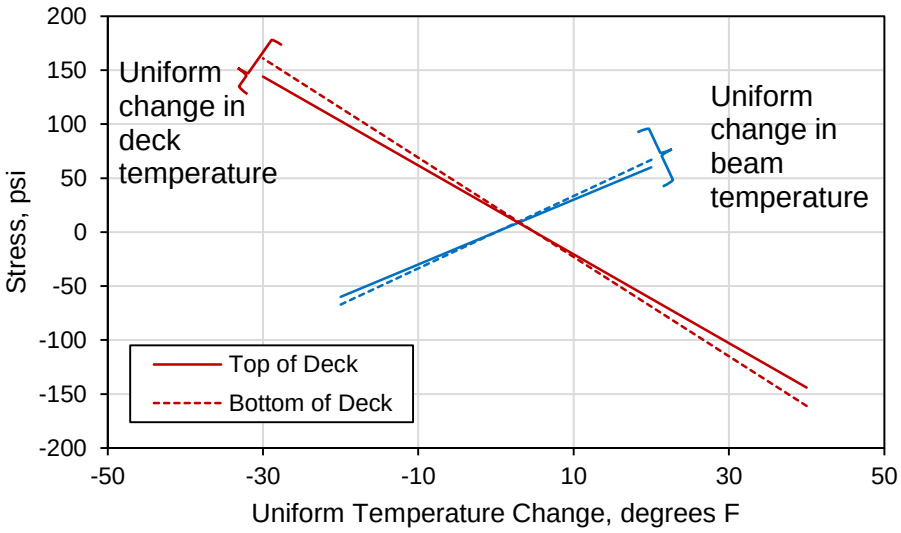

Figure 2. Modeled stresses in Bridge 1 deck due to uniform temperature changes in deck and beam.

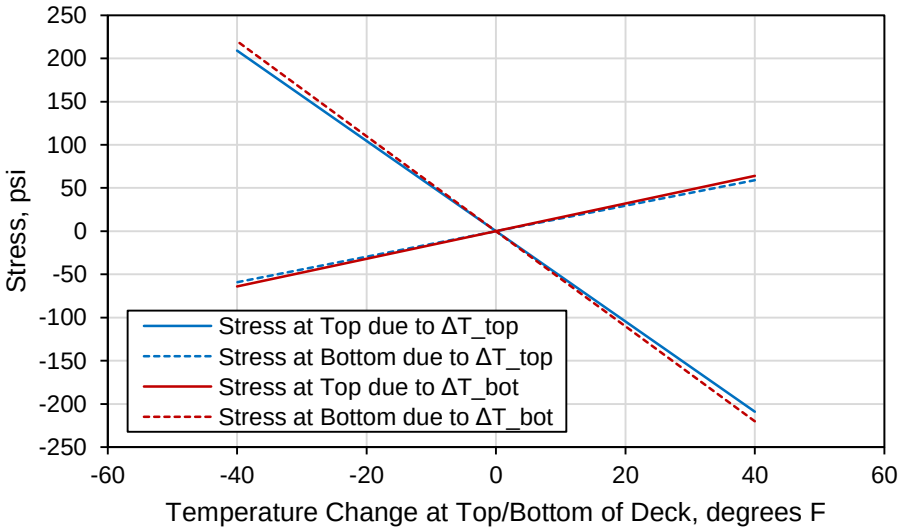

Figure 3. Modeled stresses in Bridge 1 deck due to linear temperature changes in deck. Blue lines show effect of changing only the temperature at the top of the deck (ΔT_{bot} = 0 °F); red lines show effect of changing only the temperature at the bottom of the deck (ΔT_{top} = 0 °F).

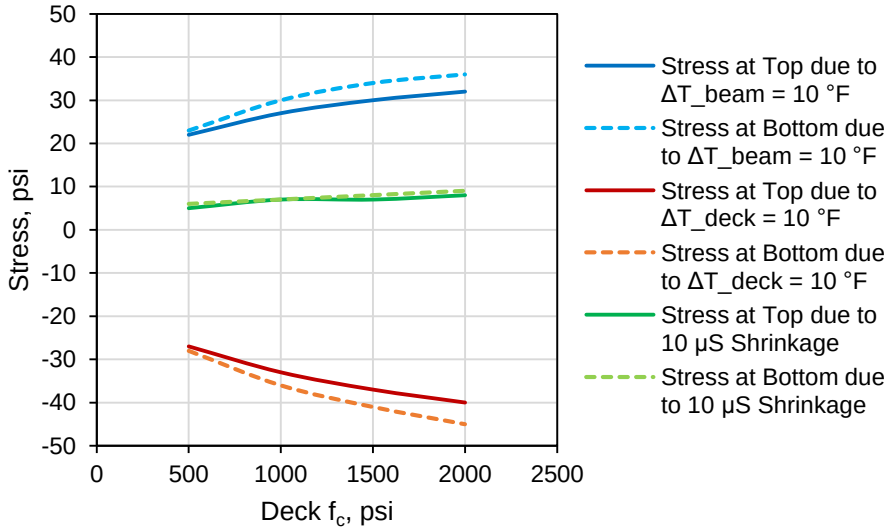

Figure 4. Modeled stresses in Bridge 1 deck due to change in compressive strength of concrete.

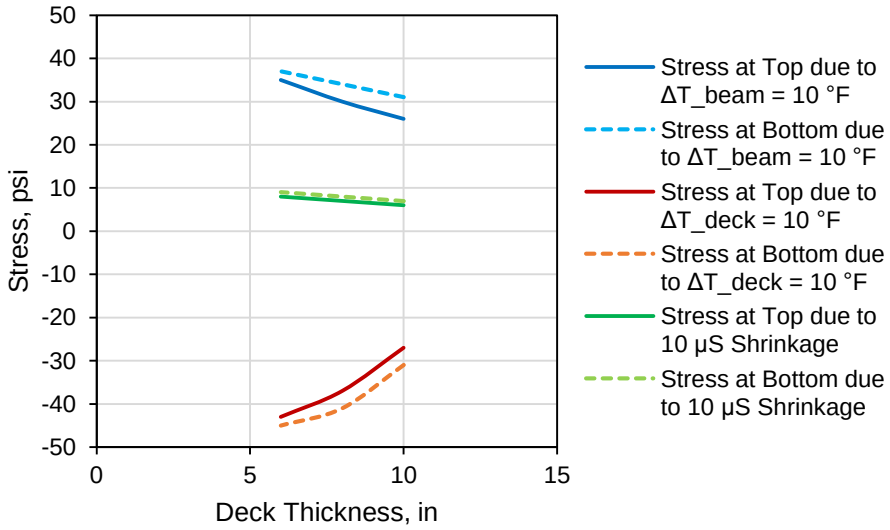

Figure 5. Modeled stresses in Bridge 1 deck due to change in deck thickness.

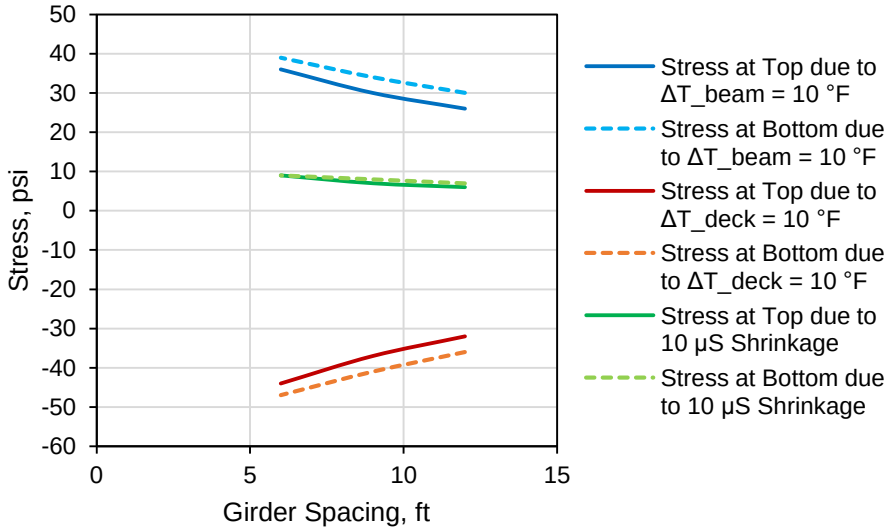

Figure 6. Modeled stresses in Bridge 1 deck due to change in girder spacing.

APPENDIX E - REFERENCES

REFERENCES

1. Aktan, Haluk, Gongkang Fu, Waseem Dekelbab, Upul Attanayaka. *Investigate Causes & Develop Methods to Minimize Early-Age Deck Cracking on Michigan Bridge Decks*. Detroit: Michigan Department of Transportation, 2003.

2. French, Catherine, Laurice Eppers, Quoc Le, Jerome Hajjar. *Transverse Cracking in Bridge Decks: Summary Report.* Minneapolis: University of Minnesota, Minnesota Department of Transportation, 1999.

3. Hadidi, Rambod and M. Ala Saadeghvaziri. *State of the Art of Early Age Transverse Cracking of Concrete Bridge Decks.* Washington DC: Transportation Research Board Annual Meeting, 2003.

4. Krauss, Paul and Ernest Rogalla. *Transverse Cracking in Newly Constructed Bridge Decks, NCHRP Report 380*. Northbrook: Wiss, Janney, Elstner Associates, Inc., 1996.

5. Neville, A.M. *Properties of Concrete,* Fourth Edition. New York: John Wiley & Sons, Inc., 1981.

6. Saadeghvaziri, M. Ala and Rambod Hadidi. *Causes and Control of Transverse Cracking in Bridge Decks, FHWA-NJ-2002-19.* Newark: Department of Civil and Environmental Engineering, New Jersey Institute of Technology, 2002.

7. Shing, P. Benson and Naser Abu-Hejleh. *Cracking in Bridge Decks: Causes and Mitigation*. Boulder: Colorado Department of Transportation, Research Branch, 1999.

8. Brown, Michael D., Greg Sellers, Kevin Folliard, David Fowler. *Restrained Shrinkage Cracking of Concrete Bridge Decks: State-of-the-Art Review*. Austin: Texas Department of Transportation, 2001.

9. Altoubat, Salah A. and David A. Lange. "Tensile Basic Creep: Measurements and Behavior at Early Age," *ACI Materials Journal*, vol. 98, no. 5 (2001): 386-393.

10. ACI Committee 207. *ACI 207.2R-07, Report on Thermal and Volume Change Effects on Cracking of Mass Concrete*. Farmington Hills, MI: American Concrete Institute, 2007.

11. ConcreteWorks, Version 2.1.3. Texas Department of Transportation. http://www.txdot.gov/inside-txdot/division/information-technology/engineering-software.html.

12. National Climatic Data Center. *Quality Controlled Local Climatological Data (QCLCD)*, https://www.ncdc.noaa.gov/qclcd/QCLCD.

13. Zuk, W. "Thermal and Shrinkage Stresses in Composite Beams," *Journal of the American Concrete Institute*, (1961): 327-340.